

Institut für Chemie
Arbeitskreis Angewandte Polymerchemie bei Prof. Dr. André Laschewsky

**THERMORESPONSIVE BLOCK COPOLYMERS
WITH UCST-BEHAVIOR AIMED AT
BIOMEDICAL ENVIRONMENTS**

D I S S E R T A T I O N

zur Erlangung des akademischen Grades
„doctor rerum naturalium“ (Dr. rer. nat.)
in der Wissenschaftsdisziplin Polymerchemie

eingereicht an der
Mathematisch-Naturwissenschaftlichen Fakultät
der Universität Potsdam

von

M.Sc. Noverra Mardhatillah Nizaro

Potsdam, 22 February 2018

“Printed and/or published with the support of the German Academic Exchange Service”

Published online at the
Institutional Repository of the University of Potsdam:
URN urn:nbn:de:kobv:517-opus4-412217
<http://nbn-resolving.de/urn:nbn:de:kobv:517-opus4-412217>

Acknowledgements

“God tasks no soul beyond its capacity.” (Q. 2:286)

First of all I would like to acknowledge my Doctoral supervisor, Prof. Dr. André Laschewsky for giving me the opportunity to work in his research group and for his support and advices during my doctoral studies. I am really inspired by his integrity, responsibility, confidence, and enthusiasm as well as his passion as a scientist. I am very grateful to him for all discussions, not only concerning polymer chemistry but also other general topics.

I especially acknowledge Deutscher Akademischer Austauschdienst (DAAD) for the funding for my Ph.D studies, so that I can continue my education in Germany as the Land of Ideas.

I would like to thank Prof. Dr. med. Hans-Peter Fink and Prof. Dr. Alexander Böker for the opportunity to work in The Fraunhofer IAP as cooperation with the university Potsdam (UP).

Also, I sincerely thank Prof. Dr. Helmut Schlaad as my Mentor for his support, including comments and suggestions during my Ph.D studies.

Many thanks to the people, who contributed directly to this work. Notably, Mrs. Marlies Walter and Mrs. Steffi Stegmann from IAP for GPC measurements, Ms. Angela Krtitschka from UP for the NMR measurements, Mr. Dirk Schanzenbach from UP for helping me organize chemicals and measurements in UP (especially for the temperature dependent NMR), Mr. Andre Gessner from IAP and Stephan Sass from UP for the fluorescence measurements, and Prof. Dr. Joachim Koetz and Jens Rumschöttel from UP for the micro-DSC measurements.

Further thanks go to all colleagues at the IAP and UP, Robert and Jean-Philippe for helping me during my first settlement at IAP, and Eric. Especially thanks to my office mate, Viet for his patience, help and advices about my lab works as well as life.

More generally, I would like to thank all my Indonesian friends, who support me with their own ways during my stay in Germany. In addition, special thanks to L’Arc~en~Ciel, whose songs always accompany me through the good and bad time, and to Berlin for entertaining me to balance my Ph.D life.

Last but not least, I am especially grateful to my family, especially to my husband, my beloved mother for her patience, support, and understanding during my stay in Germany, and to my departed father (wherever you are) without his thought and permission I would not do this whole Germany thing.

“The best of people are those that bring most benefit to the rest of mankind.” (HR.Thabrani and Daraqutni)

Scientific Publications and Awards

Manuscripts under peer-review

Noverra M. Nizardo, Dirk Schanzenbach, Eric Schönemann and André Laschewsky, “Exploring Poly(ethylene glycol)-Polyzwitterion Diblock Copolymers as Biocompatible Smart Macrosurfactants Featuring UCST-Phase Behavior in Normal Saline Solution”, *Polymers*, **2018**, 10, 325.

Poster presentations

- **N. M. Nizardo**, A. Laschewsky, “Thermoresponsive Poly(sulfobetaine)s Based Block Copolymers as Smart Materials for Controlled Delivery”, *64. SEPAWA Congress and EDC – Berlin*, **2017**.
- **N. M. Nizardo**, A. Laschewsky, “Block Copolymers of Polysulfobetaine as Smart Materials”, *Frontiers in Polymer Science 2017 – Sevilla*, **2017**.
- **N. M. Nizardo**, V. Hildebrand, E. Schönemann, A. Laschewsky, “Sulfobetaine Methacrylate Homo- and Block Copolymers as Versatile Components for Multiresponsive Systems”, *Polydays – Potsdam Golm*, **2016**.

Awards

First Poster Award, European Detergents Conference, 2017, Berlin (Germany)

Abstract

Thermoresponsive block copolymers of presumably highly biocompatible character exhibiting upper critical solution temperature (UCST) type phase behavior were developed. In particular, these polymers were designed to exhibit UCST-type cloud points (T_{cp}) in physiological saline solution (9 g/L) within the physiologically interesting window of 30-50°C. Further, their use as carrier for controlled release purposes was explored. Polyzwitterion-based block copolymers were synthesized by atom transfer radical polymerization (ATRP) via a macroinitiator approach with varied molar masses and co-monomer contents. These block copolymers can self-assemble in the amphiphilic state to form micelles, when the thermoresponsive block experiences a coil-to-globule transition upon cooling. Poly(ethylene glycol) methyl ether (mPEG) was used as the permanently hydrophilic block to stabilize the colloids formed, and polyzwitterions as the thermoresponsive block to promote the temperature-triggered assembly-disassembly of the micellar aggregates at low temperature.

Three zwitterionic monomers were used for this studies, namely 3-((2-(methacryloyloxy)ethyl)dimethylammonio)propane-1-sulfonate (SPE), 4-((2-(methacryloyloxy)ethyl)dimethylammonio)butane-1-sulfonate (SBE), and 3-((2-(methacryloyloxy)ethyl)-dimethylammonio)propane-1-sulfate) (ZPE). Their (co)polymers were characterized with respect to their molecular structure by proton nuclear magnetic resonance ($^1\text{H-NMR}$) and gel permeation chromatography (GPC). Their phase behaviors in pure water as well as in physiological saline were studied by turbidimetry and dynamic light scattering (DLS). These (co)polymers are thermoresponsive with UCST-type phase behavior in aqueous solution. Their phase transition temperatures depend strongly on the molar masses and the incorporation of co-monomers: phase transition temperatures increased with increasing molar masses and content of poorly water-soluble co-monomer. In addition, the presence of salt influenced the phase transition dramatically. The phase transition temperature decreased with increasing salt content in the solution. While the PSPE homopolymers show a phase transition only in pure water, the PZPE homopolymers are able to exhibit a phase transition only in high salinity, as in physiological saline. Although both polyzwitterions have similar chemical structures that differ only in the anionic group (sulfonate group in SPE and sulfate group in

ZPE), the water solubility is very different. Therefore, the phase transition temperatures of targeted block copolymers were modulated by using statistical copolymer of SPE and ZPE as thermoresponsive block, and varying the ratio of SPE to ZPE. Indeed, the statistical copolymers of P(SPE-*co*-ZPE) show phase transitions both in pure water as well as in physiological saline. Surprisingly, it was found that mPEG-*b*-PSBE block copolymer can display “schizophrenic” behavior in pure water, with the UCST-type cloud point occurring at lower temperature than the LCST-type one.

The block copolymer, which satisfied best the boundary conditions, is block copolymer mPEG₁₁₄-*b*-P(SPE₄₃-*co*-ZPE₃₉) with a cloud point of 45°C in physiological saline. Therefore, it was chosen for solubilization studies of several solvatochromic dyes as models of active agents, using the thermoresponsive block copolymer as “smart” carrier. The uptake and release of the dyes were explored by UV-Vis and fluorescence spectroscopy, following the shift of the wavelength of the absorbance or emission maxima at low and high temperature. These are representative for the loaded and released state, respectively. However, no UCST-transition triggered uptake and release of these dyes could be observed. Possibly, the poor affinity of the polybetaines to the dyes in aqueous environments may be related to the widely reported antifouling properties of zwitterionic polymers.

Zusammenfassung

Neue thermisch-responsive Blockcopolymere mit vermutlich hoher Biokompatibilität wurden entwickelt, die ein Phasenverhalten mit oberer kritischer Lösungstemperatur (UCST) in wässriger zeigen. Insbesondere wurden diese Polymere so gestaltet, dass sie Trübungspunkte des UCST-Übergangs (T_{cp}) in physiologischer Kochsalzlösung (9 g/l) innerhalb des physiologischen interessanten Temperaturfensters von 30-50°C zeigen. Außerdem wurde ihre Eignung als Träger für kontrollierte Freisetzungszwecke untersucht. Diese Polyzwitterionen-basierte Blockcopolymere wurden durch „Atom transfer radikal polymerisation“ (ATRP) unter Verwendung eines Makroinitiators mit verschiedenen Molmassen und Anteilen von Comonomeren dargestellt. Diese Blockcopolymere können sich im amphiphilen Zustand zu Mizellen selbstorganisieren, wenn der thermisch-responsive Block beim Abkühlen einen Übergang vom Knäulen zur Kugel erfährt. Poly (ethylenglycol) methylether (mPEG) wurde

als permanent hydrophiler Block verwendet, der die gebildeten Kolloide stabilisiert, und Polyzwitterionen als thermisch-responsiver Block, der bei niedriger Temperatur die temperaturinduzierte Bildung von Mizellen bewirkt.

Drei zwitterionische Monomere wurden für diese Untersuchungen verwendet, 3-((2-(methacryloyloxy)ethyl)dimethylammonio)propane-1-sulfonate (SPE), 4-((2-(methacryloyloxy)ethyl)dimethylammonio)butane-1-sulfonate (SBE), und 3-((2-(methacryloyloxy)ethyl)dimethylammonio)propane-1-sulfate (ZPE). Die (Co)Polymere wurden durch protonen-kernmagnetische Resonanz ($^1\text{H-NMR}$) und Gelpermeationschromatographie (GPC) charakterisiert. Ihr Phasenübergangsverhalten im Wasser sowie in physiologischer Kochsalzlösung wurde durch Trübheitsmessungen und dynamische Lichtstreuung (DLS) untersucht. Diese (Co)Polymere sind thermisch-responsiv mit einem UCST-Übergang als Phasenverhalten in wässriger Lösung. Die Übergangstemperaturen hängen stark von den Molmassen und von dem Anteil der Co-Monomeren ab: Eine Vergrößerung der Molmasse und des Anteils an schwerwasserlöslichem Comonomer führt zu einer Erhöhung der Phasenübergangstemperaturen. Des Weiteren beeinflusst ein Salzzusatz den Phasenübergang sehr stark. Während die PSPE-Homopolymere nur in Wasser einen Phasenübergang aufweisen, zeigen die PZPE-Homopolymere nur bei hohem Salzgehalt, wie in physiologischer Kochsalzlösung, einen Phasenübergang. Obwohl beide Polyzwitterionen ähnliche chemische Strukturen besitzen und sich nur in der anionischen Gruppe (Sulfonatgruppe in SPE und Sulfatgruppe in ZPE) unterscheiden, ist die Wasserlöslichkeit sehr verschieden. Daher wurden die Phasenübergangstemperaturen der Blockcopolymere durch Verwendung von statistischen Copolymeren aus SPE und ZPE als thermisch-responsivem Block mittels des Verhältnisses von SPE zu ZPE moduliert. Solche statistischen Copolymere $\text{P}(\text{SPE-co-ZPE})$ zeigen Phasenübergänge sowohl in Wasser als auch in physiologischer Kochsalzlösung. Darüber hinaus wurde überraschenderweise gefunden, dass PSBE-basierte Blockcopolymer z. T. "schizophrenes" Verhalten in Wasser besitzen, wobei der Trübungspunkt des UCST-Übergangs niedriger als der des LCST-Übergangs liegt.

Das Blockcopolymer $\text{mPEG}_{114}\text{-}b\text{-P}(\text{SPE}_{43}\text{-co-ZPE}_{39})$ erfüllte am besten die Zielsetzung mit einem Trübungspunkt von 45°C in physiologischer Kochsalzlösung. Deswegen wurde es für Solubilisierungsexperimente verschiedener solvatochromer Farbstoffe als Modelle von Wirkstoffen ausgewählt, wobei die Eignung des thermisch-responsiven Blockcopolymers als "intelligenter" Träger untersucht wurde. Die Aufnahme und Freisetzung der Farbstoffe wurden durch UV-Vis- und Fluoreszenzspektroskopie anhand der Verschiebung der

Wellenlänge der Extinktions- oder Emissionsmaxima bei niedriger und hoher Temperatur verfolgt. Diese Temperaturen entsprechen dem aggregierten bzw. gelösten Zustand des Polymeren. Jedoch wurde keine Aufnahme und Freisetzung dieser Farbstoffe durch UCST-Übergang beobachtet. Möglicherweise hängt die schwache Affinität der Polybetaine zu den Farbstoffen in wässrigen Systemen mit den bekannten Antifouling-Eigenschaften von zwitterionischen Polymeren zusammen.

List of Abbreviations and Variables

ARGET	activators regenerated by electron transfer
ATRP	atom transfer radical polymerization
BC-#	block copolymer-#
Bpy	2,2'-bipyridyl
BzAm	benzyl acrylamide
BzMA	benzyl methacrylate
Co-M	co-monomer
Conv.	conversion
CP-#	copolymer-#
[CuBr]	molar concentration of copper (I) bromide
DCM	dichloromethane
DLS	dynamic light scattering
DP_n	number average degree of polymerization
DSC	differential scanning calorimetry
EBiB	ethyl α -bromoisobutyrate
Et₃N	trimethylamine
Et₂O	diethyl ether
EtOH	ethanol
ΔG_{mix}	change of Gibbs free energy of mixing
GPC	gel permeation chromatography
HEMA	2-hydroxyethyl methacrylate
HFIP	hexafluoroisopropanol
ΔH_{mix}	change in enthalpy
HMTETA	1,1,4,7,10,10-hexamethyltriethylenetetramine
HP-#	homopolymer-#
I	initiator
[I]	molar concentration of initiator

List of Abbreviations and Variables

λ_{\max}	maximum wavelength of absorbance (UV-Vis)
$\lambda_{\max}^{\text{emission}}$	maximum wavelength of emission (fluorescence)
LCST	lower critical solution temperature
Lig	ligand
[Lig]	molar concentration of ligand
M	monomer
[M]	molar concentration of monomer
m_{co-M}	mass of co-monomer
m_{CuBr}	mass of copper (I) bromide
m_I	mass of initiator
m_{Lig}	mass of ligand
m_M	mass of monomer
m_{Red}	mass of reducing agent
MeOH	methanol
Me₆TREN	tris[2-dimethylamino)ethyl]amine
M_n	number average molar mass
M_{n(app)}	apparent molar mass calculated from GPC
M_{n(theo)}	theoretical number average molar mass
mPEG-Br	poly(ethylene glycol) methyl ether 2-bromoisobutyrate
mPEG-OH	poly(ethylene glycol) methyl ether
MW	molecular weight
NMP	nitroxide mediated polymerization
NMR	nuclear magnetic resonance
OEGMA₄₇₅	oligo(ethylene glycol) methyl ether methacrylate (M _n = 475 g/mol)
PBS	phosphate buffered saline
PDI	polymer's dispersity index
PDMAEMA	poly(2-dimethylaminoethyl methacrylate)
PEG	poly(ethylene glycol)
PHEMA	poly(2-hydroxyethyl methacrylate)
PMDETA	N,N,N',N'',N''-Pentamethyldiethylenetriamine
PMMA	poly(methyl methacrylate)
PNIPAM	poly(N-isopropylacrylamide)
POEGMA	poly(oligo(ethylene glycol) methyl ether methacrylate)
POEGMA₄₇₅	poly(oligo(ethylene glycol) methyl ether methacrylate)

PSBE	poly(4-((2-(methacryloyloxy)ethyl)dimethylammonio)butane-1-sulfonate)
PSPE	poly(3-((2-(methacryloyloxy)ethyl)dimethylammonio)propane-1-sulfonate)
PSPP	poly(3-((3-(methacrylamidopropyl)dimethylammonio)propane-1-sulfonate)
PZPE	poly(3-((2-(methacryloyloxy)ethyl)dimethylammonio)propane-1-sulfate)
RAFT	reversible addition-fragmentation chain transfer
RDRP	reversible-deactivation radical polymerization
R_h	hydrodynamic radius
r.t.	room temperature
SBE	4-((2-(methacryloyloxy)ethyl)dimethylammonio)butane-1-sulfonate
ΔS_{mix}	change in entropy
SPE	3-((2-(methacryloyloxy)ethyl)dimethylammonio)propane-1-sulfonate
SPP	3-((3-(methacrylamidopropyl)dimethylammonio)propane-1-sulfonate)
T	temperature
T_{cp}	cloud point temperature
TFA	trifluoroacetic acid
TFA-d	deuterated trifluoroacetic acid
TFE	2,2,2-trifluoroethanol
UCST	upper critical solution temperature
UV-vis	ultraviolet-visible
V	volume
ZPE	3-((2-(methacryloyloxy)ethyl)dimethylammonio)propane-1-sulfate)

Table of Contents

Acknowledgement

Scientific Publications and Awards

Abstract

List of Abbreviations and Variables

1. Introduction	1
1.1. Thermoresponsive polymers.....	3
1.2. Polyzwitterions	9
1.3. Poly(sulfobetaine)s	10
1.4. Atom transfer radical polymerization (ATRP)	11
1.5. Objectives of the thesis.....	15
2. Synthesis and Water Solubility of the Macroinitiator	18
3. PHEMA Based Copolymers: Synthesis, Characterization and Aqueous Solution Behavior	21
3.1. Synthesis and characterization.....	21
3.1.1. Statistical PHEMA copolymers	21
3.1.2. Block copolymers of PHEMA	23
3.2. Aqueous solution behavior	26
3.2.1. Statistical PHEMA copolymers	26
3.2.2. Block copolymers of PHEMA	27
4. Poly(sulfobetaine)s and Poly(sulfobetaine) Based Copolymers: Synthesis, Characterization and Aqueous Solution Behavior	29
4.1. PSPE based polymers	29
4.1.1. Synthesis and characterization	29
4.1.2. Aqueous solution behavior.....	35
4.2. PSPE with hydrophobic moieties	42
4.2.1. Synthesis and characterization	42
4.2.2. Aqueous solution behavior.....	44
4.3. PSBE based polymers.....	50
4.3.1. Synthesis and characterization	50

4.3.2. Aqueous solution behavior	52
4.4. PZPE based polymers	56
4.4.1. Synthesis and characterization	56
4.4.2. Aqueous solution behavior	65
5. Solubilization Studies of Solvatochromic Dyes as Model Active Agents by Block Copolymer BC-18	73
5.1. Reichardt's dye	74
5.2. Dansyl L-phenylalanine	76
5.3. Cyanine dyes	79
6. Conclusions	83
7. Experimental Part	86
7.1. Materials	86
7.2. Methods and calculations	88
7.3. Synthesis of mPEG-Br initiator	90
7.4. Synthesis of PHEMA based (co)polymers	91
7.4.1. Synthesis of non-ionic copolymers	91
7.4.2. Synthesis of non-ionic block copolymers	92
7.5. Synthesis of sulfobetaine and sulfobetaine based (co)polymers	93
7.5.1. Synthesis of zwitterionic homopolymers	93
7.5.2. Synthesis of zwitterionic copolymers	94
7.5.3. Synthesis of zwitterionic block copolymers	95
Appendix	101
List of Figures	118
List of Tables	122
Declaration	125
Bibliography	126

1. Introduction

In recent years, stimuli responsive polymers have received much attention for smart materials that can accommodate and deliver drugs. Their ability to change substantially key properties, notably their affinity to water, in response to environmental factors (e.g., temperature, pH, ionic strength, or electric fields) makes them potential candidates for controlled drug release systems. In particular, temperature-triggered drug delivery has been studied, and has become arguably the most interesting strategy among various responsive approaches. This includes not only the use of thermoresponsive polymers exhibiting a lower critical solution temperature (LCST), but also such that show an upper critical solution temperature (UCST), as discussed in more detail in **Chapter 1.1**. Still, most research has been focused on LCST-type polymers in aqueous media because they are easier to build chemically and to analyze compared to UCST-type polymers. Moreover, their phase transition behavior seemed to be modulated more easily by their polymer structure [1-4]. However, UCST-type polymers in aqueous media have recently started to attract more interest in the field of smart materials because the polymers become soluble upon heating, which make them suitable for many biomedical applications [5-6]. The idea to release the drug at elevated temperature, for instance due to fever or inflammation, may be accomplished by UCST-type polymers by undergoing a globule-to-coil transition. Thermoresponsive block copolymers appear particularly suitable for the controlled release of drugs, since amphiphilic block copolymers can self-assemble to form micelles. The permanently hydrophilic blocks in the micelles shall maintain the colloidal stability of the micelles so that precipitation may not occur. In the aggregated state, the less polar domain of amphiphilic block copolymers will carry poorly water-soluble drugs inside the core of micelles. Drug release is aspired upon heating via a temperature-induced transition of thermoresponsive block inducing the micelles to disassemble and become double hydrophilic block copolymer unimers in the dissolved state of polymer chains in the aqueous solutions. **Figure 1.1** describes the concept of controlled release of drug by UCST behavior.

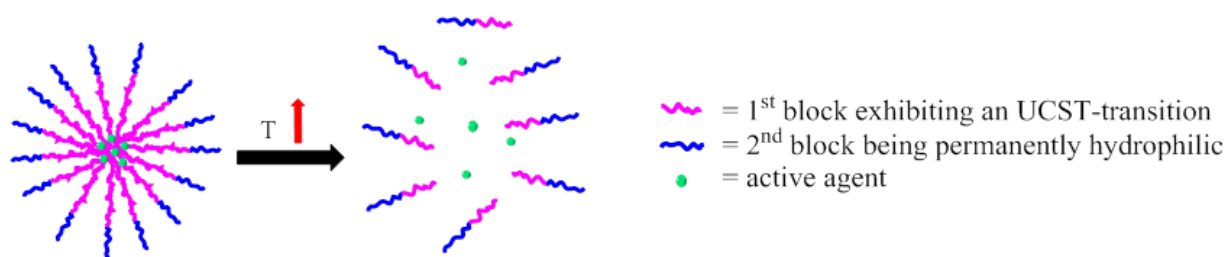


Figure 1.1. Scheme of micelle formation and disassembly of block copolymers containing an UCST-type polymer block for the controlled release of poorly water-soluble active agents (e.g., drugs) at elevated temperature.

The synthesis of block copolymers composed of at least one responsive block has been reported frequently, but studies employing UCST are exceptional. Pei *et al* studied the synthesis of thermoresponsive zwitterionic block copolymers of mPEG-*b*-PSPE-*b*-PDMAEMA via atom transfer radical polymerization, in which their temperature-sensitive properties depended on molecular compositions or solution conditions [7]. Typically, controlled radical polymerization (according to the IUPAC: reversible deactivation radical polymerization [8]) has been chosen as a preferred tool to prepare the responsive block copolymers because of its tolerance of functional groups [9-10]. The purpose is to improve control over molar mass and copolymer composition than that in conventional free radical polymerization. As the phase transition depends on the molar mass, it is preferable that the polymer chains are synthesized with good control of copolymer homogeneity. Only then, the polymer-polymer interaction as well as polymer-solvent interaction for every polymer chain will be equal. Thus, defined phase transition behavior can be achieved and precise controlled release of drugs may happen.

Reversible-addition fragmentation chain transfer (RAFT) and atom transfer radical polymerization (ATRP) are two types of controlled radical polymerization which are often used to prepare block copolymers [11-14]. On the one hand, RAFT is often used due to its convenience for not using transition metals as the catalyst, which sometimes is in conflict with the polymer structure, since transition metals can complex with functional groups of the monomer, as e.g. nitrogen-based moieties. In addition, high amounts of transition metals cannot be tolerated if the polymers will be used later in biomedical applications, thus asking for painstaking purification steps. On the other hand, RAFT has a disadvantage because of the need of particular chain transfer agents, which have to be synthesized beforehand and typically contain thiocarbonyl groups. This sulfur content in the RAFT agent is difficult to

remove and might also pose problems in biomedical applications, e.g. when liberating H₂S or COS upon hydrolysis. ATRP has the advantage for allowing to avoid the use of normal radical initiators that may cause secondary growing polymer chains. Therefore, a possible source of inhomogeneity of the polymer chains will be avoided. This approach shall result in well-defined thermoresponsive block copolymers and facilitate their perspective use for controlled release of drug. Moreover, although transition metal catalysts are needed for the ATRP reaction, the possibility of using the polymers made in biomedical applications has improved much, because less toxic transition metal, such as iron, can be used for the reaction. In addition, recent variants of ATRP, for instance Activators ReGenerated by Electron Transfer (ARGET), allow to reduce the amount of transition metal catalysts, such as copper complexes [15-16].

1.1. Thermoresponsive polymers

Thermoresponsive polymers in aqueous solutions have attracted much attention in the research in over the past few decades, in particular for applications such as drug delivery [17-18], tissue engineering [19-20], bioseparation [21-22], and bioimaging [23]. Inspired by the natural phenomena such as hot and cold weather or fever in the body, to use temperature as a trigger, this type of stimuli-responsive polymers is particular interesting because it is reversible, and can easily be applied without the need to add chemical substances, i.e., in closed systems. Many of these polymers are not toxic and are effective in a temperature range that is feasible for biomedical applications [24-26].

Depending on the region in the phase diagram where the polymer dissolves, thermoresponsive polymers can be divided into two types: polymers that dissolve in solution below a specific temperature and become insoluble above that temperature are characterized by lower critical solution temperature (LCST) behavior. This means that the polymer chains are well solvated and therefore expanded and water-soluble below a specific temperature, but the polymer chains collapse and become insoluble at higher temperature. In contrast, polymers exhibit UCST behavior when the polymers dissolve above a specific temperature, but are insoluble below [27-30]. However, the phenomenon of UCST has been rarely found in water [5]. LCST and UCST, respectively, represent the minimum and the maximum point of the binodal curve, at which the phase separation occurs. **Figure 1.2** displays schematic phase diagrams for LCST and UCST behavior.

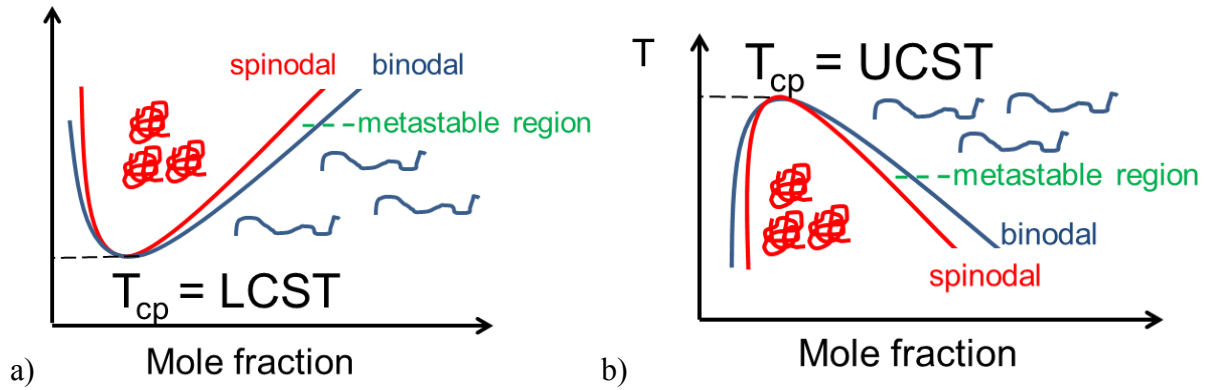


Figure 1.2. Schematic phase diagrams of polymers bearing a) LCST and b) UCST behavior (temperature v. mole fraction of polymers).

The thermodynamic reason for the solubility-insolubility of thermoresponsive polymers is based on the Gibbs free energy law, where the Gibbs free energy of mixing, ΔG_{mix} , has to be negative ($\Delta G_{mix} < 0$) to promote the solubility. In particular, the interactions of hydrophilic moieties-water and of polymer-polymer play an important role for the phase transition behavior.

$$\Delta G_{mix} = \Delta H_{mix} - T \cdot \Delta S_{mix} \quad (1.1)$$

ΔH_{mix} = change in enthalpy

T = temperature

ΔS_{mix} = change in entropy

In the classical case of LCST behavior in aqueous solution, when the temperature is low, polymers are in solution because of hydrogen bonds between the polar segments of the polymer and the water molecules [1], result not only in a loss of entropy, but also a strong negative mixing enthalpy, ΔH_{mix} . Although the mixing entropy, ΔS_{mix} , is negative and unfavorable because of the highly ordered nature of the polymer-water interactions, ΔG_{mix} is negative and makes the solubility favorable. When the temperature increases, the water molecules are more mobile than before resulting in a weakening of the hydrogen bonds between polymer and water molecules. This favors the polymer-polymer interaction and increasingly dehydrates the polymers. As consequence, the contribution of the entropy finally becomes dominant and overcomes ΔH_{mix} term resulting in a positive ΔG_{mix} , and the phase separation occurs. Therefore, the miscibility in LCST systems is driven by the mixing enthalpy.

The analogous concept can also be applied for UCST behavior in aqueous solution. At low temperature, the interaction between polymer-polymer is strong, resulting in positive ΔH_{mix} . Since the strong and positive enthalpy term surpasses the entropy term, ΔG_{mix} is positive, thus, polymers become insoluble and the phase separation takes place. At higher temperature, the system gains more mixing entropy that counterbalances the unfavorable mixing enthalpy, resulting finally in a negative ΔG_{mix} so that the polymers become soluble. In this case, the miscibility is driven by the mixing entropy [5]. Nevertheless, this explanation is an approximation to LCST and UCST phenomena. In reality, the situation is more complex because neither the mixing enthalpy nor the mixing entropy are constants as assumed in the standard case.

The quality of the solvent shifts from good to bad at the binodal line. In consequence, a coil-globule transition of the polymer chain conformation occurs. Typically, this is indicated by a change of the solution from clear to turbid due to the onset of demixing into a solvent-rich and a polymer-rich phase [5]. This phenomenon can be easily observed by turbidity measurement, e.g., when heating and cooling a polymer solution at a given concentration. The difference between the phase transition temperatures upon heating and cooling is defined as hysteresis, which indicates the metastable region between the binodal and spinodal lines of the phase diagram. Also, a hysteresis may happen if the system has not yet completely equilibrated. **Figure 1.3** shows schematically the solubility behavior of thermoresponsive polymers in aqueous media.

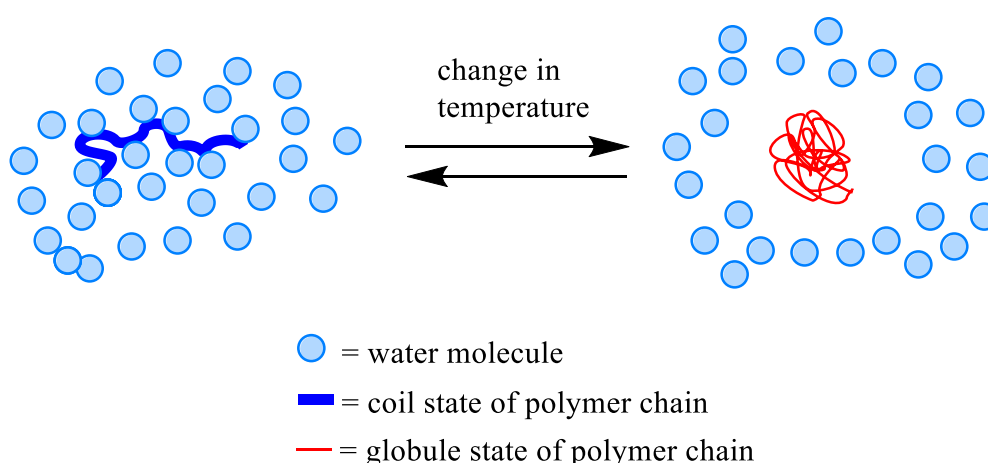
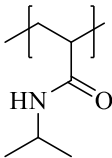
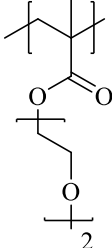
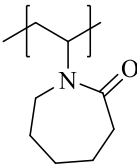
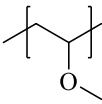


Figure 1.3. Model of the temperature triggered coil-to-globule transition of hydrated polymer chains.

1. Introduction

LCST-type polymers have stronger polymer-solvent interactions than polymer-polymer ones. Therefore, polymers show LCST behavior and become insoluble upon heating by experiencing a coil-globule transition at certain temperature, which depends not only on the precise chemical structure of the polymer (i.e., including molar mass and end groups), but also on physical parameters, such as concentration. They are well studied and known mostly for nonionic polymers in aqueous media. Poly(*N*-isopropylacrylamide) (PNIPAM) is arguably the most famous LCST-type polymer and the most intensively studied one so far. This is because PNIPAM changes its behavior from hydrophilic (because of the hydrogen bonding between the amide groups and water molecules) to hydrophobic (because of the dehydration of the polymer chains) upon heating at about 32°C in water [1, 31]. This phase transition temperature of PNIPAM makes it suitable for many applications, especially in biomedical fields [32-33]. Other thermoresponsive polymers exhibiting LCST behavior belong to the class of poly(oligo(ethylene glycol) methacrylate)s [34-37], poly(*N*-vinyl amide)s [26, 33], and poly(vinyl ether)s [1, 38]. The structure and LCST of some polymers is given in **Table 1.1**.

Table 1.1. Examples of polymers with LCST behavior.

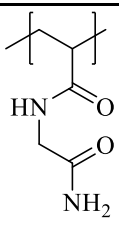
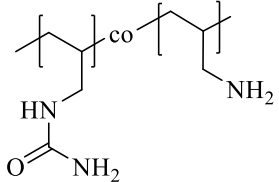
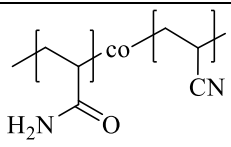
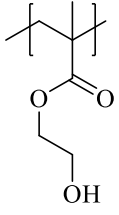
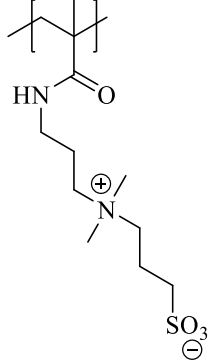
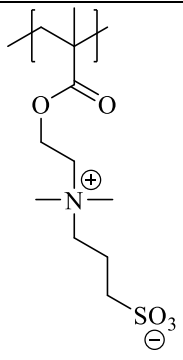
Polymer	Structure	LCST ^a	Ref.
Poly(<i>N</i>-isopropylacrylamide) (PNIPAM)		32°C	[31, 39]
Poly(oligo(ethylene glycol) methyl ether methacrylate) (POEGMA)		26°C	[37, 40]
Poly(<i>N</i>-vinyl-ε-caprolactam) (PNVCL)		31°C	[41-42]
Poly(methyl vinyl ether) (PMVE)		36°C	[43-44]

^a Estimated values; moreover, value may depend on the molar mass, tacticity, end groups, and added salt

In the case of UCST behavior, the polymers become soluble upon heating. Due to, e.g., Coulomb interactions and hydrogen bonds between the chains, the interaction between polymer-polymer is stronger than polymer-solvent interaction at low temperature. Nevertheless, this polymer-polymer interaction can be easily disturbed by applying heat [29, 45]. Thus, UCST-type polymers dissolve at increasing temperature. UCST behavior is usually observed in organic solvents or in water-organic solvent mixtures [30, 46] but rarely found in water. However, the research interest of UCST polymers in aqueous solution is increasing recently. For instance, Agarwal *et al* and Ohnishi *et al* studied UCST-type nonionic polymers in aqueous solution, especially in the class of poly(*N*-acryloylglycinamide) (PNAGA) [5, 45, 47-48]. Other examples of nonionic polymers with UCST behavior are ureido-derivatized polymers [30, 49-50], poly(acrylamide-*co*-acrylonitrile) [6, 51-52], and possibly poly(2-hydroxyethyl methacrylate) (PHEMA) [53]. Besides nonionic polymers, certain zwitterionic polymers also exhibit UCST behavior, particularly from the class of polysulfobetaines [7, 54-57]. A list of UCST-type polymer structures is given in **Table 1.2**.

1. Introduction

Table 1.2. Examples of polymers with UCST behavior.

Polymer	Structure	UCST ^a	Ref.
Poly(<i>N</i>-acryloylglycinamide) (PNAGA)		17-30°C	[45, 47]
Poly(allylamine-<i>co</i>-allylurea)		8-65°C	[49]
Poly(acrylamide-<i>co</i>-acrylonitrile)		6-60°C	[6]
Poly(2-hydroxyethylmethacrylate) (PHEMA)		> 90°C ^b	[5, 53]
Poly(3-((3-(methacrylamidopropyl)dimethyl ammonio)propane-1-sulfonate) (PSPP)		9-27°C	[57]
Poly(3-((2-(methacryloyloxy)ethyl)dimethylammonio)propane-1-sulfonate) (PSPE)		41-71°C	[56]

^a Value depends on the molar mass, tacticity, and copolymer composition

^b Conflicting data

1.2. Polyzwitterions

A polyzwitterion is defined as a polymer, which carries pairwise negative and positive charges in the same side chain, so that the overall charge is zero (neutral) [58-61]. The numerous charged groups cause strong intra- and intermolecular electrostatic interactions within the polymers (**Figure 1.4**), thus counteracting solubility, at least at lower temperatures [62-63]. For this reason, many polyzwitterions exhibit an UCST in solution, with a coil-globule transition upon cooling.

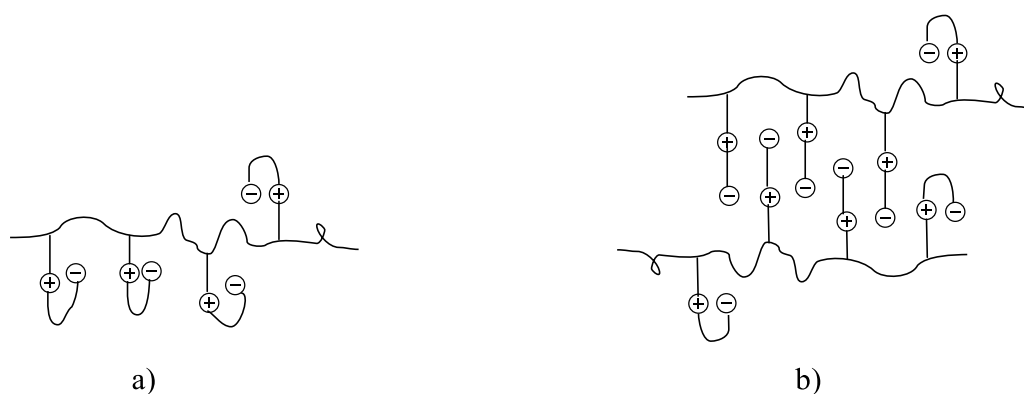


Figure 1.4. Schematic illustration of a) intra- and b) intermolecular electrostatic interactions within zwitterionic polymers causing UCST behavior.

Low molar mass zwitterions are often found in nature. One example of natural zwitterionic compounds are phosphatidyl cholines, which carry a phosphobetaine group and form a major group of lipids, the lecithins. The structure of lecithins is given in **Figure 1.5**.

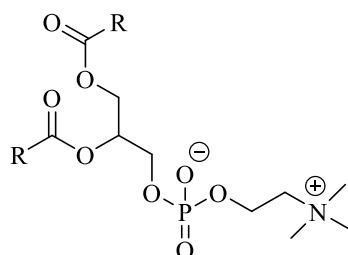


Figure 1.5. The general chemical structure of phosphatidyl choline lipids (lecithins).

The three most widespread classes of polyzwitterions are poly(phosphobetaine)s, poly(carboxybetaine)s, and poly(sulfobetaine)s (**Figure 1.6**) [59-61, 64-66]. The similarity of their chemical structure to biological compounds such as phospholipids, their high prevention

1. Introduction

of protein adsorption, and their high biocompatibility make them receive great attention in the field of biomaterials [67-69].

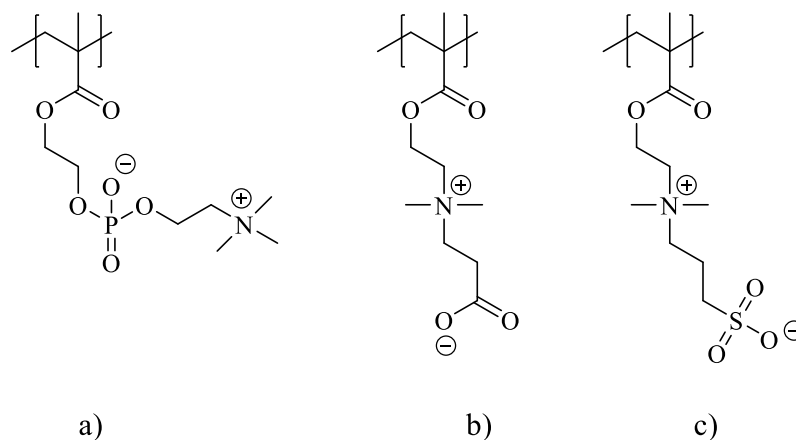


Figure 1.6. Exemplary chemical structures of a) poly(phosphobetaine)s, b) poly(carboxybetaine)s, and c) poly(sulfobetaine)s derived from poly(methacrylate)s.

1.3. Poly(sulfobetaine)s

Poly(sulfobetaine)s are one class of polyelectrolytes that has been widely studied. They are capable to bind water molecules using their positively and negatively charged ions, creating a strong hydration layer, which prevents, e.g., protein adsorption. Therefore, poly(sulfobetaine)s are favorably used to reduce “fouling” of surfaces [7, 57, 67, 70-71].

Many poly(sulfobetaine)s display UCST behavior in aqueous solution, which in detail is sensitive to molar mass, and salt concentration [7, 28, 55-57, 59, 69, 72-73]. Poly(sulfobetaine)s show anti-polyelectrolyte effect in aqueous salt solution, in which the addition of salts makes the opposing charges shield from the charges in the side chain of the polymers [60]. This charge shield reduces the interaction between the polymer bound charges, thus changing the conformation of the polymer chains to coil-like (as the solubility of the polymers increases), and decreasing the UCST.

Only few monomers for the synthesis of poly(sulfobetaine)s are commercially available. 3-((2-(methacryloyloxy)ethyl)di-methylammonio)propane-1-sulfonate (SPE) and 3-((3-(methacrylamidopropyl)dimethylammonio)propane-1-sulfonate (SPP) are the most well-studied sulfobetaine monomers, which can be bought currently. Most other monomers have to be synthesized beforehand [54, 56-57, 61, 68]. The most common preferred method to

synthesize sulfobetaine monomers is via ring opening alkylation of dialkyl amino-functional monomers by sultones to produce simultaneously quarternary ammonium and sulfonate moieties in the side chain, as can be seen in **Figure 1.7**. [59, 61].

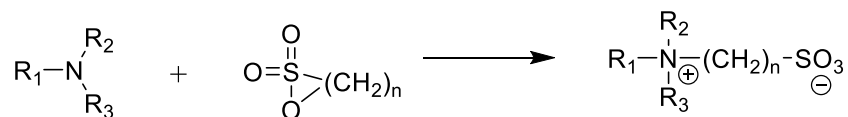


Figure 1.7. The reaction scheme of the typical sulfobetaine monomer synthesis (mostly $n=3$ or 4).

Very recently, people have tried to extend the chemical structure of poly(sulfobetaine)s also in making poly(sulfobetaine)s [74-77], which have a similarity to the lecithins because the spacer between the cationic and anionic groups can be hydrolyzed easily. These compounds have been rarely studied as it has been found that they are less water soluble than their poly(sulfobetaine) analogs [76, 78].

The strong intra- and intermolecular electrostatic interaction within the polymer chains makes the synthesis of poly(sulfobetaine)s challenging, since the monomers and even more the polymers are insoluble in nonpolar organic solvents. They generally require polar protic solvent, such as trifluoroethanol (TFE) and hexafluoroisopropanol, or aqueous solutions or brine to conduct the reaction in a homogeneous system during polymerization [54, 61, 69, 79]. Taking this and the marked hygroscopy into account, the choice to synthesize poly(sulfobetaine)s is by free radical polymerization. Free radicals are mostly chemically inert toward nucleophiles and electrophiles, in this respect from the monomer itself, which may interfere with the polymerization reaction. Also, much research has been done recently in preparing poly(sulfobetaine)s via reversible-deactivation radical polymerization (RDRP), previously known as “controlled radical polymerization” methods [7, 56-57, 79-81].

1.4. Atom transfer radical polymerization (ATRP)

RDRP allows for synthesizing polymers with good control of the molar mass and the molar mass distribution (low polydispersity), as well as of the polymer architecture, such as block or graft copolymers, hyperbranched, and star polymers. These features cannot be provided by conventional free radical polymerization. In RDRP, the reaction is controlled by fast initiation

1. Introduction

in the system and adding reversible deactivation by deactivating the growing polymer chains into a inactive state called “dormant”. This dormant species is activated when the dynamic equilibrium between dormant and the growing polymer chains is reached, as illustrated in **Figure 1.8**. In general, the requirements to achieve controlled system of RDRP are [82]:

- negligible termination
- fast initiation compared to propagation
- the exchange between the active and dormant species is faster than the propagation
- a homogeneous system
- large amount of control agent compared to initiator

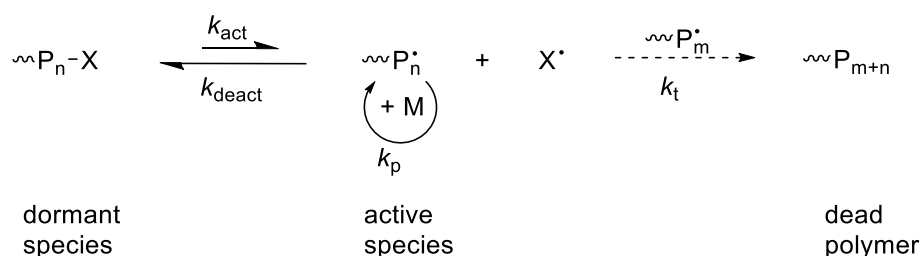


Figure 1.8. General reaction mechanism as one major principle of reversible-deactivation radical polymerization (RDRP).

RDRP is divided into three major techniques: reversible addition-fragmentation chain transfer polymerization (RAFT), nitroxide mediated polymerization (NMP), and atom transfer radical polymerization (ATRP). Among these techniques, RAFT and ATRP have been used most often to prepare poly(sulfobetaine)s [61].

ATRP was established in 1995 simultaneously by Matyjaszewski and Sawamoto [13-14]. It is one of the most successful free radical polymerization techniques that enables effective control of the polymerization, in particular for styrenes, (meth)acrylates, and some other monomers [83]. ATRP has been used to prepare well-defined polymer structures, for instance block, brush, star, and end-functional ones [10, 84], including polymers for the field of biomedical applications, in particularly of drug delivery [85-86]. As typical RDPD technique, ATRP was introduced to control the reaction by creating a fast initiation via dynamic transfer between the active species, in this case the growing polymer chains, and the dormant species. In order to promote those requirements, ATRP uses transition metal complexes, often formed in situ from, e.g., copper (I) bromide, along with specific ligands that act as activators of the

dormant species, and copper (II) bromide, as deactivator of the growing polymer chains in the reaction via redox reaction. The reversibly deactivated polymers in form of dormant chains keep the stationary radical concentration during the reaction low (the number of the dormant is greater than of the growing polymer chains). The dormant species makes the number of dead polymer chains caused by irreversible termination become relatively small, when the exchange rate between the active and dormant species is faster than the propagation rate. This allows most polymer chains that started in the early stage of the polymerization, to grow in parallel. Therefore, a narrow molar mass distribution can be achieved. **Figure 1.9** shows the general mechanism of ATRP

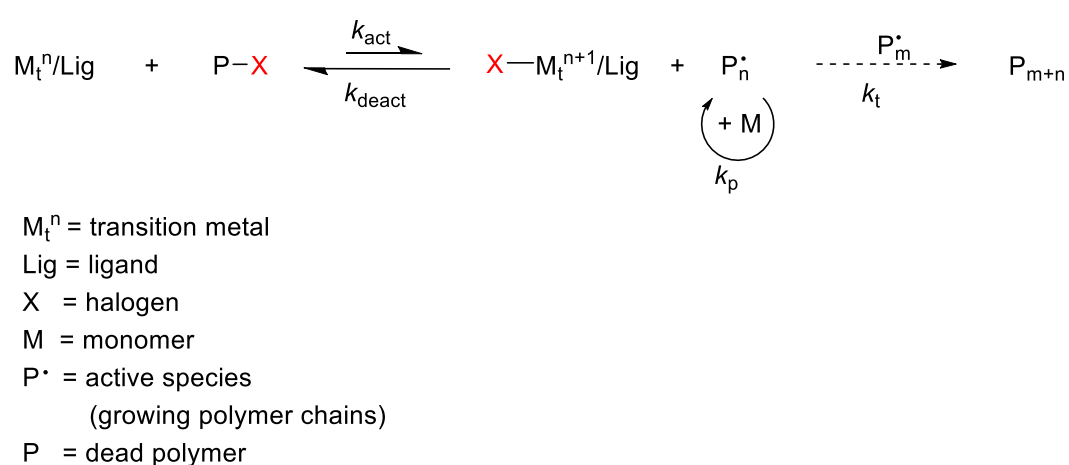


Figure 1.9. General mechanism of atom transfer radical polymerization (ATRP) [13].

The reversible deactivation step in ATRP consists of an oxidative addition of the growing polymer radical onto a transition metal complex (“catalyst”). Thus, an ATRP system consists of monomer, (pseudo)halogen initiator, catalyst, and solvent. It has been successfully used to polymerize different classes of monomers such as styrenes, (meth)acrylates, (meth)acrylamides, and acrylonitrile [13, 83-84, 87-89]. However, hydrophilic monomers are more challenging to be polymerized via ATRP since side reactions, such as a complexation between monomers and transition metals, may occur and reduce the control of the reaction.

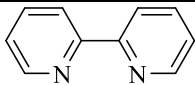
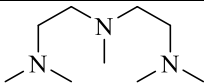
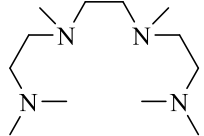
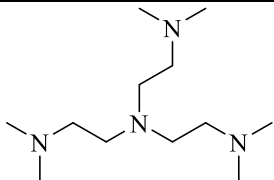
As in the conventional free radical polymerization, an initiator is essential to initiate the reaction and to produce the growing polymer chains. Initiators should promote a fast initiation to give the growing polymer chains in the early stage of the polymerization, in order to yield narrow molar mass distributions. Typical ATRP initiators are from the class of activated alkyl

1. Introduction

halides, for example benzylic halides, α -haloesters, α -haloketones, α -halonitriles, and sulfonyl halides [13, 84].

ATRP uses a catalyst to manage the exchange between dormant and the active species. The transition metal used must have at least two oxidation states and have good affinity to the halogen. The classical examples of transition metals used in ATRP are copper, ruthenium, and to a lesser extent, iron. ATRP catalysts use specific ligands to complex the metal, especially to dissolve the metal salt in the organic phase, and to tune the redox potential of the metal for the exchange process. The most common ligands used in ATRP for copper catalysts contain nitrogen, such as 2,2'-bipyridyl (bpy), pentamethyldiethylenetriamine (PMDETA), 1,1,4,7,10,10-hexamethyltriethylenetetramine (HMTETA), and tris[2-(dimethylamino)ethyl]amine (Me_6TREN) [13, 84].

Table 1.3. Examples of ligands for copper catalyst in ATRP.

Name of the ligand	Structure
2,2'-bipyridyl (bpy)	
Pentamethyldiethylenetriamine (PMDETA)	
1,1,4,7,10,10-Hexamethyltriethylenetetramine (HMTETA)	
Tris[2-(dimethylamino)ethyl]amine (Me_6TREN)	

ATRP has been performed in many nonpolar and polar solvents, not only in homogeneous but also in heterogeneous systems. The important part in choosing the right solvent for ATRP is that the solvent should have a better interaction with the catalyst to tune the redox potential and does not compete with the ligands for the metal. Moreover, the solvent has to minimize side reactions via chain transfer to the solvent [13, 84].

The ATRP of zwitterionic monomers, such as poly(sulfobetaine)s, is complicated due to the low solubility of the monomers and the polymers. As mentioned before, zwitterionic monomers and polymers require polar protic solvent to dissolve them. Such protic solvents may promote bad control of the reaction, for instance by displacing halide ligands from the catalysts and deactivating the catalyst and/ or the propagation site [89]. Nonetheless, some examples of well-controlled poly(sulfobetaine)-based materials via ATRP, which can be used for further applications, have been reported. Kobayashi *et al.* prepared poly(sulfobetaine)s brushes via ATRP in TFE-ionic liquid mixtures as solvent and studied the effect of the solvent mixture on the polymerization of the sulfobetaines. They found that the addition of a small amount of ionic liquid can improve the control on the polymerization of polymer brushes and linear polymers to favor high molar mass and narrow molar mass distribution [79, 90]. Song *et al.* also synthesized poly(sulfobetaine)s, namely PSPE, brushes in TFE as well as in a TFE-ionic liquid mixtures, and also obtained well-defined PSPE [91]. Zhao *et al.* reported that hydrophilic polyzwitterions, such as PSPE, could be synthesized via ATRP combined with click chemistry, resulting in high conversion and producing polymers that could be used as antifouling membranes [62]. Yao *et al.* showed that graft copolymers of polyamidoamine dendrimers and PSPE can be prepared by ATRP, which due to their micellar structure could act as nanocarriers [81]. Pei *et al.* synthesized thermoresponsive block copolymers of poly(ethylene glycol), PSPE, and poly(2-(dimethylamino)ethyl methacrylate) (PDMAEMA) [7].

1.5. Objectives of the thesis

Until now, the research of thermoresponsive polymers for drug delivery applications has been mostly based on polymers featuring LCST behavior. However, it seems that thermoresponsive systems with UCST-behavior would cover the more realistic scenario for temperature-triggered drug delivery in practice. Hence, smart UCST-based systems present an interesting concept to be investigated. Up to now, only very few examples have been reported. Therefore, the aim of this thesis was to prepare UCST-type block copolymers as smart materials and to explore the possibility of their use for controlled release of poorly water-soluble active agents. Only during the duration of this thesis, few other groups also have addressed this alternative concept and published first results [6, 92-93]. In particular, the thermal response should be realized under meaningful conditions, namely in a physiologically useful temperature window as well as salinity.

1. Introduction

In order to explore options for such smart delivery, thermoresponsive micellar systems are in the focus of the thesis. The idea is that such polymers are designed to form micelles that exist at low temperature [94-95], but decompose at high temperature. Thus, at low temperature, the system can accommodate and transport the active agents, whereas at the moment where the phase transition temperature is reached, the polymeric micelles will liberate the solubilized active agents. In this respect, the polymeric micelles act as carriers to transport the active agents, e.g., a drug, while the temperature is used as the trigger to release the active agents upon heating by the disassembling the micelles. In order to implement this concept, UCST-type block copolymers are chosen. They are expected to behave as amphiphiles at low temperature; when increasing the temperature, they shall become double hydrophilic compounds so that the micelles will disassemble. The best way to start for this purpose is to take the polymer architecture of block copolymers, in which the first block contains the less water soluble and thermoresponsive polymer (namely polymers with UCST behavior) and acts as the core of the micelles and is sensitive to the occurring of the phase transition. The second block consists of a permanently hydrophilic polymer, to guarantee the colloidal stability of the micelles in the aqueous phase and to assume the role of the shell of the micelles (see **Figure 1.10**). Taking into account future applications of such smart materials, for instance to be suited for medical uses, the polymers should have the potential for good biocompatibility. Therefore, the choice of the responsive polymers as starting point was based on PHEMA on the one hand, and on the other hand on polyzwitterions, such as poly(sulfobetaine)s (in this case PSPE). PHEMA has been reported to be highly biocompatible [96]. It has been used in several applications which have contact with body, such as for implants. In addition, reports suggest that transitions similar to UCST behavior can occur if the molar mass of PHEMA is not too high [53]. Poly(sulfobetaine)s are well-known for showing UCST behavior in aqueous media and also to be biocompatible [97-98]. Considering biocompatibility of the permanently hydrophilic block, poly(ethylene glycol) is chosen [99-100].

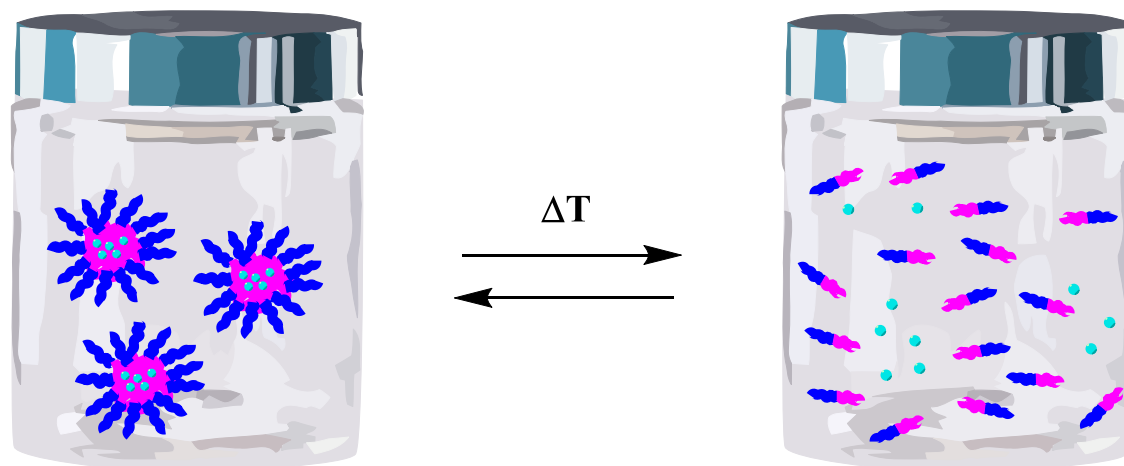


Figure 1.10. Schematic illustration of active agents release via polymer micelle formation-disassembly using a globule-to-coil phase transition in a physiological relevant temperature range.

The target temperature for the controlled release of the active agents is aspired to be in the range of physiological temperature, which is around 37°C for human beings. Notably, the medium for the responsive system and the release is also a factor to keep in mind for its design. The system should be investigated to which extent it is able to switch under relatively realistic conditions. In this respect, physiological saline solution was considered to be a good model system for a biological fluid environment rather than pure water.

This study is organized as the following:

- 1) First, synthesizing PHEMA-based copolymers which had been claimed to have UCST-type phase behavior, and which would be particularly convenient to use for biomedical applications. Their molecular structure and phase transition behavior is studied.
- 2) Second, preparing zwitterionic homo- and block (co)polymers with UCST-type behavior, along with the characterization of their molecular structure as well as their phase transition behavior. The study comprises the use of the co-monomers to tune the phase transition temperature of the zwitterionic block in physiological saline solution.
- 3) Third, exploring the possibility of using the polymers, which have the desired phase transition profile, for controlled release of models for drugs.

2. Synthesis and Water Solubility of the Macroinitiator

The macroinitiator was synthesized by esterification of a monofunctional PEG, in this case of poly(ethylene glycol) monomethyl ether (mPEG-OH) with molar mass of 5000 g/mol, and 2-bromo isobutyryl bromide resulting in poly(ethylene glycol) methyl ether 2-bromoisobutyrate (mPEG-Br). The reaction scheme is shown on **Figure 2.1**.

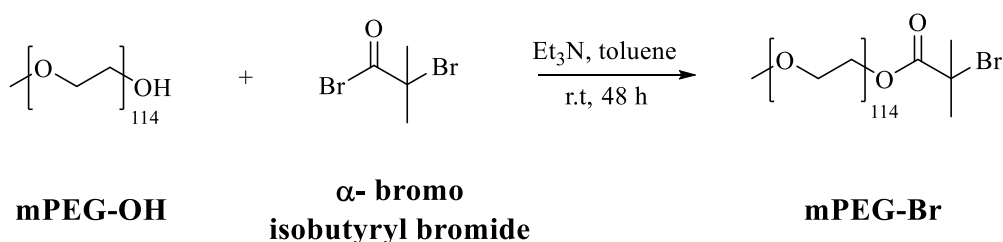


Figure 2.1. Reaction scheme of macroinitiator, mPEG-Br, synthesis.

This macroinitiator approach via esterification on one hand has some disadvantages. First, since it relies on the commercially available monofunctional PEG polymers, its molecular structure, such as the range of molar mass and α -functionalities, is limited. Second, the use of an ester linkage may be problematic because it might be hydrolyzed in aqueous media, in particular at low or high pH values [36]. On the other hand, the reaction of an acid halogenide with an alcohol in the presence of a tertiary amine is highly effective and has a good chance to go to completion [101], minimizing the residual mPEG-OH at the end of the reaction. Moreover, mPEG-OH and α -bromo isobutyryl bromide as starting materials are commercially available and well-priced. Furthermore, the successful use of similar ATRP macroinitiators has been reported [7, 86].

The reaction was conducted for 48 h at room temperature, since the poly(ethylene glycol) monomethyl ether of molar mass 5000 g/mol did not dissolve completely in toluene at low temperature. The reaction was nevertheless carried out at room temperature because the acid bromide is highly reactive and tends to undergo side reactions. As higher the temperature is, the more side reactions might occur. Toluene was used because it was necessary to dry mPEG-OH beforehand, and toluene is a good solvent for azeotropic drying since the boiling point is still decent in toluene, while the temperature difference between the azeotrope and the

pure solvent is high (boiling point of toluene is 110°C, while the boiling point of azeotropic toluene/water mixture is 84°C). In addition, toluene is nearly inert in the radical polymerization of methacrylates, so that traces of toluene in the further ATRP reaction will not cause side reactions. Triethylamine (Et₃N) was used to remove the acid as the byproduct of this reaction.

After the reaction was finished, toluene was diluted with dichloromethane (DCM). The product was extracted with DCM in water, in which the ester preferred to partition compared to the aqueous phase. The reason for that is because the product of mPEG-Br is soluble in toluene, DCM, and water. However, the solubility follows the order of DCM > water > toluene. The aqueous phase was extracted with 3 x 50 mL of DCM. The organic phases were collected and the solvent was removed by evaporation. The crude DCM extract was precipitated into a 20 fold excess of diethyl ether, and the macroinitiator was isolated as colorless powder by filtration.

The NMR spectra (**Figure 2.2**) proved that the ester bond was formed, which can be seen from the new peak at 4.3 – 4.4 ppm attributed to the α -CH₂ group next to the ester moiety. In addition, the comparison of the integrated intensities of peaks **a**, **e**, and **f**, which gives a ratio of approximately 2: 3: 6, proved that at least 95% purity was achieved. In addition, end group analysis from this NMR spectrum gives the number of repeat units in the poly(ethylene glycol) of 114, which resulted in the number average molar mass of about 5000 g/mol by multiplying it with 44 (molar mass of ethoxy group repeat unit). This end group analysis was calculated as follows:

$$DP_n = \frac{Integrals(a,b,c,d)/4H}{Integrals(e)/3H} \quad (2.1)$$

$$DP_n = \frac{(2.00 + 2.56 + 3.30 + 428.07 + 3.01)/4H}{2.88/3H}$$

$$DP_n = 114$$

$$M_n(mPEG-OH) = 15 + (114 \times 44) + 17 = 5048 \text{ g/mol} \quad (2.2)$$

$$M_n(mPEG-Br) = 15 + (114 \times 44) + 166 = 5197 \text{ g/mol} \quad (2.3)$$

2. Synthesis and Water Solubility of the Macroinitiator

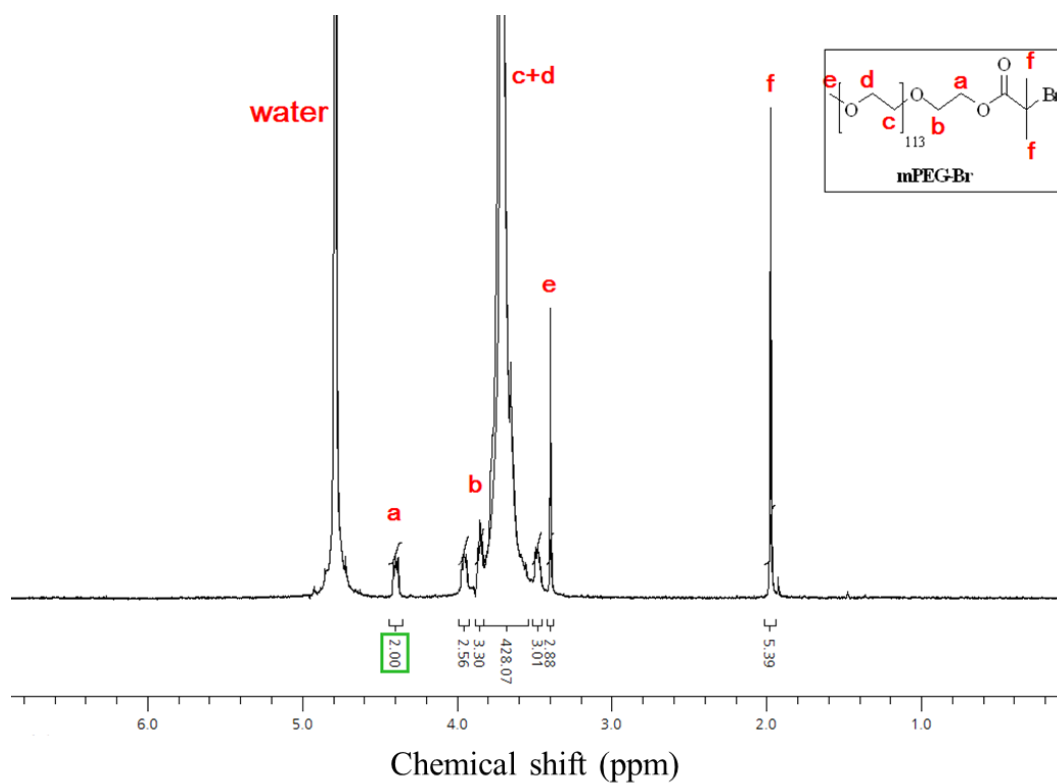


Figure 2.2. $^1\text{H-NMR}$ spectra of poly[(ethylene glycol) methyl ether 2-bromoisobutyrate] (mPEG-Br) macroinitiator in D_2O .

In order to verify the permanently hydrophilic character, the temperature dependent solubility of mPEG-Br macroinitiator was investigated. A solution of mPEG-Br with concentration of 30 g/L in ultra-pure water and PBS buffer was prepared, and the turbidity of the solution was followed during heating from 25°C to 90°C. The macroinitiator dissolved completely in ultra-pure water as well as in PBS at all studied temperatures and no clouding indicating a phase transition was observed.

3. PHEMA Based Copolymers: Synthesis, Characterization and Aqueous Solution Behavior

3.1. Synthesis and characterization

3.1.1. Statistical PHEMA copolymers

A copolymer of P(HEMA-*co*-OEGMA₄₇₅) was prepared in order to get knowledge about its phase behavior in aqueous solution. PHEMA, possibly, exhibits an UCST-type transition, with the phase transition proposed to occur above 90°C [53]. OEGMA₄₇₅ is used as co-monomer to tune the phase transition temperature of the copolymers since OEGMA₄₇₅ is known to have a high hydrophilicity. Thus, it was reasoned that, by incorporating OEGMA₄₇₅ into PHEMA, the additional hydrophilicity of OEGMA₄₇₅ residues would decrease the putative phase transition temperature of PHEMA, and to reach the desired window for a phase transition temperature, i.e. in the temperature range of 30 - 50°C, preferentially in the physiological most interesting window of 37 - 40°C. In addition, both PHEMA and POEGMA₄₇₅ have shown good biocompatibility [37, 96]. Hence, such a copolymer might be suitable for controlled release purposes.

The synthesis of P(HEMA-*co*-OEGMA₄₇₅) copolymers was carried out via ATRP using EBiB as initiator in ethanol as with 95 mol% of HEMA and 5 mol% of OEGMA₄₇₅ in the monomer feed. The obtained copolymers were characterized at the molecular level to learn their chemical structure and molar mass. The results are summarized in **Table 3.1**. NMR analysis for the copolymers was performed to verify the incorporation of OEGMA₄₇₅ into PHEMA (**Figure 3.1**).

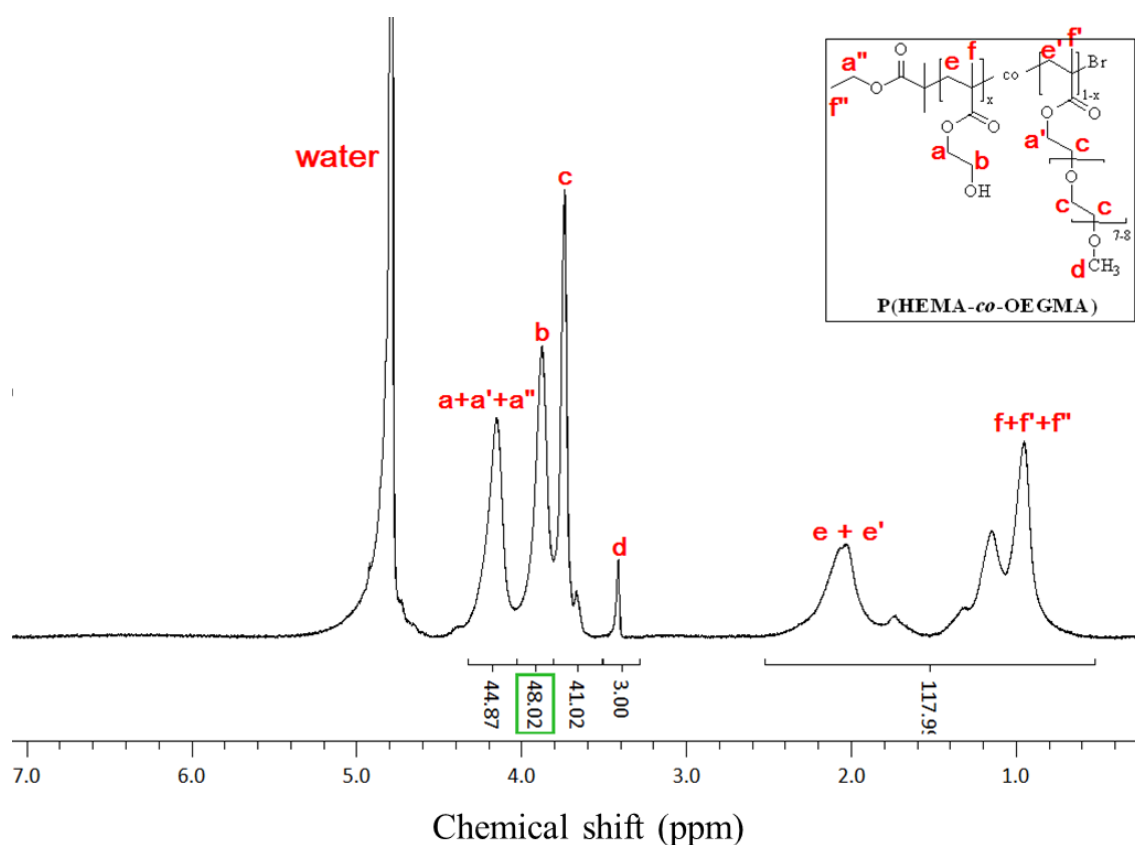


Figure 3.1. $^1\text{H-NMR}$ spectrum of P(HEMA-*co*-OEGMA₄₇₅) copolymer (**CP-1**) in D_2O .

The NMR spectrum shows that P(HEMA-*co*-OEGMA₄₇₅) copolymers (**CP-1**) were formed, which is indicated by the presence of a peak at 3.4 ppm, which is attributed to the $-\text{O-CH}_3$ of OEGMA₄₇₅, and a peak between 3.8 – 4 ppm, which belongs to the $-\text{CH}_2\text{-OH}$ of PHEMA. No peak of vinylidene groups between 5 – 7 ppm was observed, which implied that no monomer contaminates the copolymers. **CP-1** was obtained in the quite high yield of 70%, with a copolymer composition of 96 mol% for PHEMA and 4 mol% of POEGMA₄₇₅. Although both monomers have the same methacrylate structure, their reactivities seem to differ slightly, which is possibly due to the sterical hindrance by the size of OEGMA₄₇₅, which is much bigger than HEMA. Hence, the incorporation of OEGMA₄₇₅ to PHEMA became slower and in the end, the copolymer contains more HEMA versus OEGMA₄₇₅ than the monomer feed does. GPC analysis shows that the molar mass distribution was broad (high PDI of 2.5) and bimodal. This might indicate that the exchange between the active species and the dormant one was not fast enough, leading to unequal growth of polymers as well as molar mass. Another possible explanation is that HEMA tends to induce a slight branching of polymers by transesterification via its OH groups [102]. Branching increases the polymer's dispersity index (PDI), and may also result in a bimodal molar mass distribution.

Table 3.1. Analytical data of the P(HEMA-*co*-OEGMA₄₇₅) copolymer.

Sample	Monomer feed ratio HEMA:OEGMA ₄₇₅	Yield [%]	HEMA:OEGMA ₄₇₅ ^b content in the copolymer	M _{n(theo)} ^c [g/mol]	M _{n(app)} ^d [g/mol]	PDI
CP-1 ^a	95 : 5	71	0.96 : 0.04	10600	10200	2.5

^a Ratio of [M] : [I] was always 100 : 1

^b Calculated from the relative signal intensities of signal groups at 3.4 and 3.6 – 4.5 ppm

^c Calculated from the yield and the feed composition, assuming that the incorporation ratio is the same as the feed ratio

^d Measured by the GPC using DMF as eluent and polystyrene as calibration standards

3.1.2. Block copolymers of PHEMA

mPEG-*b*-PHEMA and mPEG-*b*-P(HEMA-*co*-OEGMA₄₇₅) block copolymers were prepared via the macroinitiator approach by ATRP in ethanol. The macroinitiator mPEG-Br (see **Figure 2.1**) was used, and HEMA and eventually, OEGMA₄₇₅ were added onto the macroinitiator to form block copolymers. In order to explore the influence of OEGMA₄₇₅ as co-monomer on the phase transition behavior, mPEG-*b*-P(HEMA-*co*-OEGMA₄₇₅) block copolymers with different monomer feed ratios were prepared.

¹H-NMR spectroscopy showed that the polymerization happened because of the presence of broad peaks. Moreover, the absence of peaks characteristic for double bonds at 5.8 and 6.2 ppm indicated that the polymers are free from monomers. In the polymer spectra, peaks appeared, which are typical for mPEG, HEMA, and OEGMA₄₇₅ derived polymers. Those characteristic peaks are a peak between 3.6 – 3.8 ppm, which is attributed to –CH₂-CH₂-O- of mPEG, a peak between 3.8 – 4 ppm, which is attributed to –CH₂-OH on PHEMA, and a peak at 3.4 ppm, which is attributed to –O-CH₃ on OEGMA₄₇₅ (**Figure 3.2** and **Figure 3.3**). Since no other initiator besides the macroinitiator had been used for these reactions, a mixture of macroinitiator (mPEG-Br), PHEMA, and POEGMA₄₇₅ could not occur, and therefore, the block copolymerization was successful. Yet from the NMR spectrum, it is not possible to distinguish whether all mPEG-Br had been incorporated into block copolymers, or if a mixture of mPEG-Br and mPEG-*b*-PHEMA or mPEG-*b*-P(HEMA-*co*-OEGMA₄₇₅) block copolymers is present. But the GPC elugram shows a monomodal molar mass distribution with shorter elution times than for mPEG-Br, which means that the macroinitiator was consumed and fixed in the copolymers. Thus, successful chain extension and purification from residual monomers was achieved.

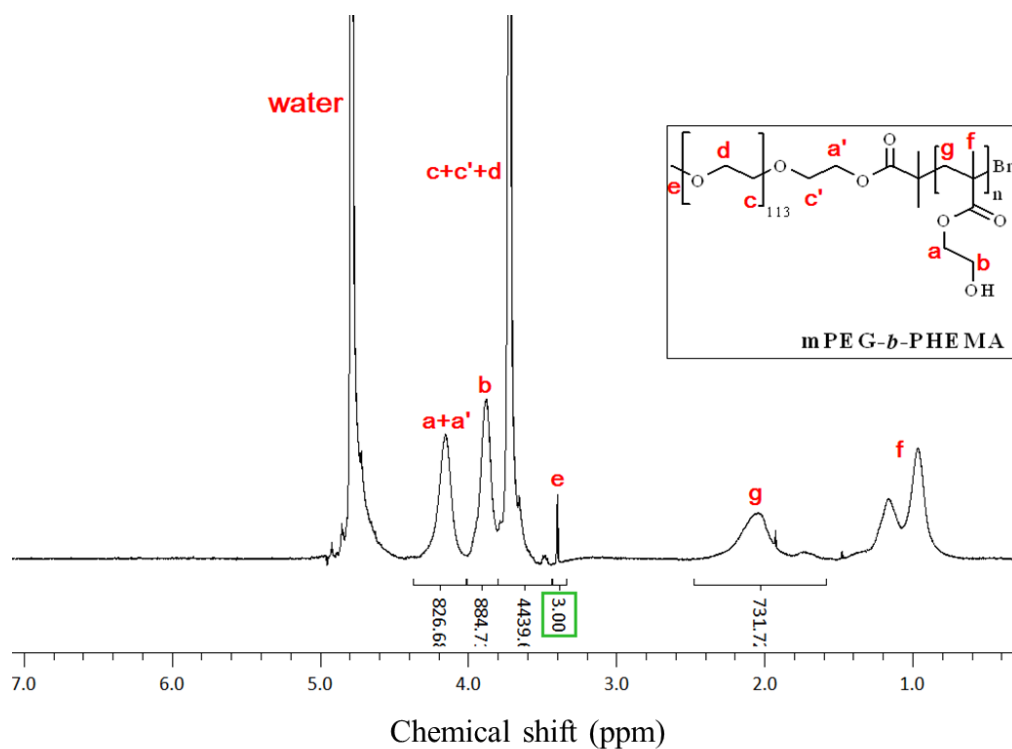


Figure 3.2. ¹H-NMR spectrum of mPEG-*b*-PHEMA copolymer (BC-1) in D₂O.

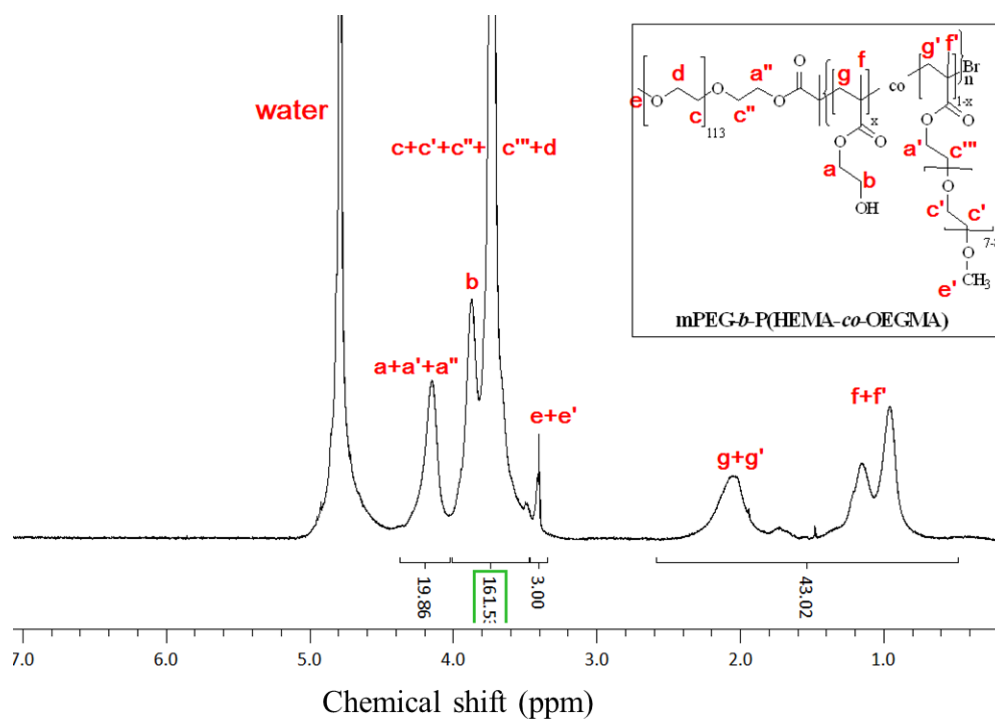


Figure 3.3. ¹H-NMR spectrum of mPEG-*b*-P(HEMA-co-OEGMA₄₇₅) copolymer (BC-3) in D₂O.

However, it is difficult to quantify the presence of POEGMA₄₇₅ in the copolymer. The NMR spectrum is no more resolved enough to enable the calculation of the copolymer compositions because the peaks are so similar for the components. However, it is reasonable to assume that the copolymerization using the macroinitiator behaves similar to the low molar mass initiator, for which it was proven that the co-monomer incorporation was close to the monomer feed composition. Still, in detail one has to assume that the OEGMA₄₇₅ content is slightly lower than in the feed.

Table 3.2. Analytical data of the mPEG-*b*-P(HEMA-*co*-OEGMA₄₇₅) block copolymers.

Sample ^a	Monomer feed ratio HEMA : OEGMA ₄₇₅	Yield [%]	M _{n(theo)} ^b [g/mol]	M _{n(app)} ^c [g/mol]	PDI
BC-1	100 : 0	66	13500	20700	1.3
BC-2	98 : 2	59	13000	19700	1.2
BC-3	95 : 5	50	12300	18600	1.2
BC-4	85 : 15	36	11500	40000	1.4

^a Ratio of [M] : [I] was always 100 : 1

^b Calculated from the yield and the feed composition, assuming that the incorporation ratio is the same as the feed ratio

^c Obtained from the GPC measurement using DMF as eluent and polystyrene as calibration standards

The results of block copolymerization are summarized in **Table 3.2**. It can be seen that the yields for these syntheses were 35 – 67%. However, unlike **CP-1**, the PDI was low and a rather narrow molar mass distribution was obtained, which means that the molar masses of the polymer chains were similar. The finding of a much smaller PDI for the block copolymers compared to the copolymer of **CP-1** is striking. A possible explanation might be branch formation in **CP-1**, which is sterically hindered by the presence of the PEG block in the block copolymers.

3.2. Aqueous solution behavior

3.2.1. Statistical PHEMA copolymers

Table 3.3 and **Figure 3.4** show the phase transition behavior of **CP-1** in ultra-pure water. A cloud point indicating a soluble-insoluble phase transition of **CP-1** was observed at 30°C with a very sharp transition, in which the system changed from transparent to opaque. After prolonged heating, the solution stayed cloudy and no precipitation was observed. However, it turned out that the phase transition behavior of P(HEMA-*co*-OEGMA₄₇₅) copolymers is of the LCST-type, not of the UCST-type as should be expected when following the data interpretation by Stöver *et al* [53]. Nevertheless, it was interesting to study also the phase transition behavior of the mPEG-*b*-P(HEMA-*co*-OEGMA₄₇₅) block copolymers.

Table 3.3. LCST-type phase transition temperature of 3 g/L aqueous solutions of the P(HEMA-*co*-OEGMA₄₇₅) copolymer in H₂O. Temperature measurement between 25 – 60°C (heating run).

Sample	Monomer feed ratio HEMA : OEGMA ₄₇₅	H ₂ O [°C]
CP-1	95 : 5	30

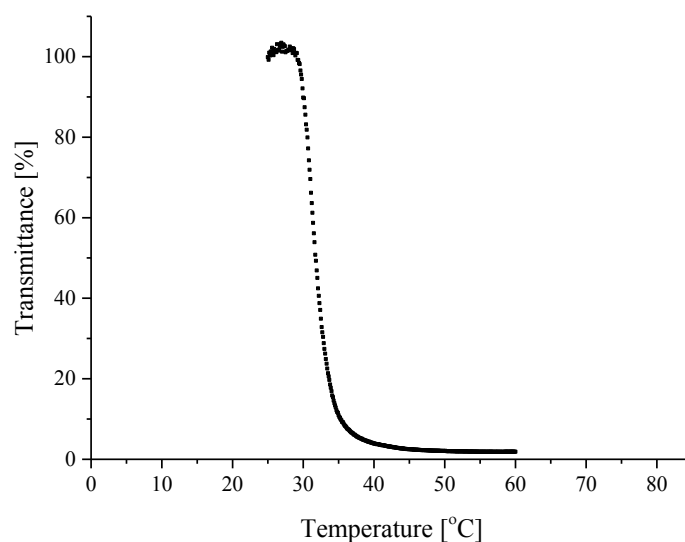


Figure 3.4. Temperature dependent turbidity (heating run) of 3 g/L aqueous solutions of **CP-1** in H₂O.

3.2.2. Block copolymers of PHEMA

Table 3.4 summarizes the phase transition behavior of mPEG-*b*-P(HEMA-*co*-OEGMA₄₇₅) block copolymers in pure water. Just like **CP-1**, mPEG-*b*-P(HEMA-*co*-OEGMA₄₇₅) block copolymers display LCST-type phase transition behavior but not UCST-type behavior (**Figure 3.5**). By adding more hydrophilic component, such as OEGMA₄₇₅, to the PHEMA block, the overall system becomes more hydrophilic and the phase transition goes up. Hence, the block copolymers behaved as expected for LCST-type polymers, in which the phase transition temperature increases with increasing hydrophilic content of OEGMA₄₇₅ within the polymer chains (phase transition temperature of **BC-1** < **BC-2** < **BC-3** < **BC-4**). The more OEGMA₄₇₅ is incorporated, the higher is the phase transition.

Table 3.4. LCST-type cloud point of 3 g/L aqueous solutions of mPEG-*b*-P(HEMA-*co*-OEGMA₄₇₅) block copolymers in H₂O. Temperature measurement between 40 – 95°C (heating run).

Sample	Monomer feed ratio HEMA : OEGMA ₄₇₅	Phase transition temperature in H ₂ O [°C]
BC-1	100 : 0	60
BC-2	98 : 2	65
BC-3	95 : 5	75
BC-4	85 : 15	82

It is also notable that for the block copolymer with the same feed ratio of 5 mol% OEGMA₄₇₅ (**BC-3**), which corresponds to **CP-1**, a much higher cloud point was obtained than for **CP-1**. This implies that the hydrophilic block influences the overall hydrophilicity of the system and phase transition. This behavior is not self-evident and has to be kept in mind when designing smart amphiphilic polymers, since the optimization of one block needs not necessarily be relevant for the case of block copolymers.

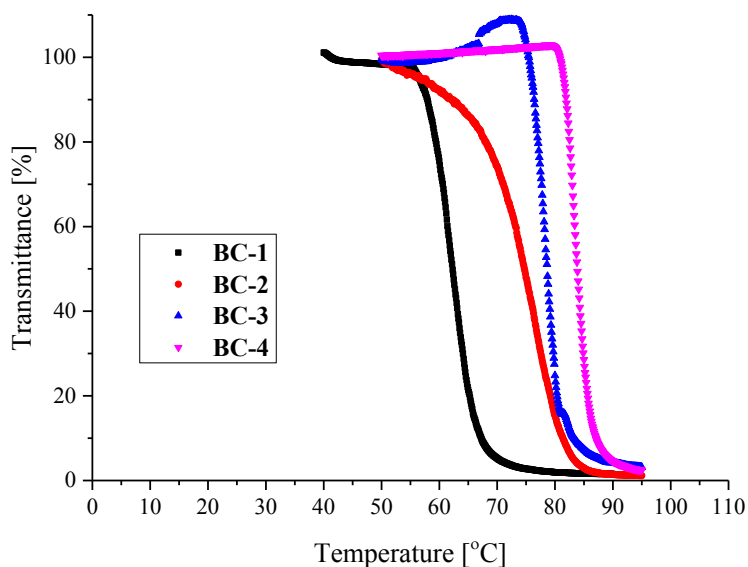


Figure 3.5. Temperature dependent turbidity (heating run) of 3 g/L aqueous solutions of mPEG-*b*-P(HEMA-*co*-OEGMA₄₇₅) block copolymers.

Since the phase transition behavior found for mPEG-*b*-P(HEMA-*co*-OEGMA₄₇₅) block copolymers was not of the UCST-type, as suggested by the report of Stöver *et al* [53], the block copolymer synthesis was shifted to the use of other monomers, for which the polymers indeed exhibit UCST-type phase transition behavior, and which also offer good biocompatibility, namely to zwitterionic poly(sulfobetaine)s.

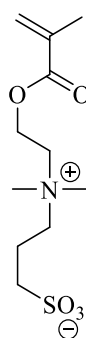
4. Poly(sulfobetaine)s and Poly(sulfobetaine) Based Copolymers: Synthesis, Characterization and Aqueous Solution Behavior

4.1. PSPE based polymers

4.1.1. Synthesis and characterization

4.1.1.1. Homopolymer of PSPE

There is not much research dealing with ATRP polymerization of sulfobetaine monomers, especially in homogeneous reaction systems [79, 90]. This is presumably because of the poor solubility of poly(sulfobetaine)s in most solvents. Therefore, as mentioned in the first chapter, homogeneous polymerization of sulfobetaine monomers requires particular polar protic solvents, such as TFE, to maintain the solubility of poly(sulfobetaine)s formed during the polymerization. According to that, the first step was to carry out homopolymerization of the commercially available sulfobetaine methacrylate SPE via ATRP with EBiB as the ATRP initiator in TFE. By analyzing the polymers obtained, the phase transition behavior of PSPE can be studied. The SPE monomer was chosen because its polymer has a good biocompatibility and thermoresponsiveness with UCST-type phase transition behavior [97-98]. In fact, several groups have reported the UCST-type phase transition of PSPE [54, 56, 80].



SPE

Figure 4.1. Chemical structure of monomer SPE.

4. Poly(sulfobetaine)s and Poly(sulfobetaine) Based Copolymers

The polymerization was performed via ATRP in order to maintain the general architecture of a mPEG-*b*-UCST block structure. ATRP is an established technique, which normally works smoothly for methacrylates [13, 82-84, 103]. Nevertheless, it has to be kept in mind that the need of using TFE, which is rarely used as solvent, for this system might cause some difficulties. TFE is chemically aggressive, and it might compromise the in situ formation of the copper catalyst. Since TFE is a rather acidic alcohol, it might, moreover, attack the ester group, in particular in the presence of a Lewis acid like copper salts. Another point is that TFE might interfere with the preservation of the bromide end group leading to substitution or elimination reactions.

The choice of nitrogen ligands to complex with the copper catalyst is essential for the success of ATRP [13, 15, 82, 84]. Each ligand contributes differently to the ATRP reaction, as the activity depends on features such as the number of coordinating sites, the number of carbon atoms between the nitrogen atoms, as well as branching. Thus, at first, different ligands were explored for the ATRP of SPE, to know which one gives best yields and molar mass distributions for PSPE. The ligands chosen are bipyridyl (bpy), PMDETA, and HMTETA, which have different reactivities toward copper complex [84]. Bpy has the standard ligand activity on the copper catalyst, but PMDETA and HMTETA are much more active. In order not to lose control over the polymerization, a good balance to make the ATRP run and to make the reaction not too rapid is necessary. The molar ratio for the reaction, [M]:[I]:[CuBr]:[Lig], was kept to be 100:1:1:2 with the target degree of polymerization (DP_n) of 100.

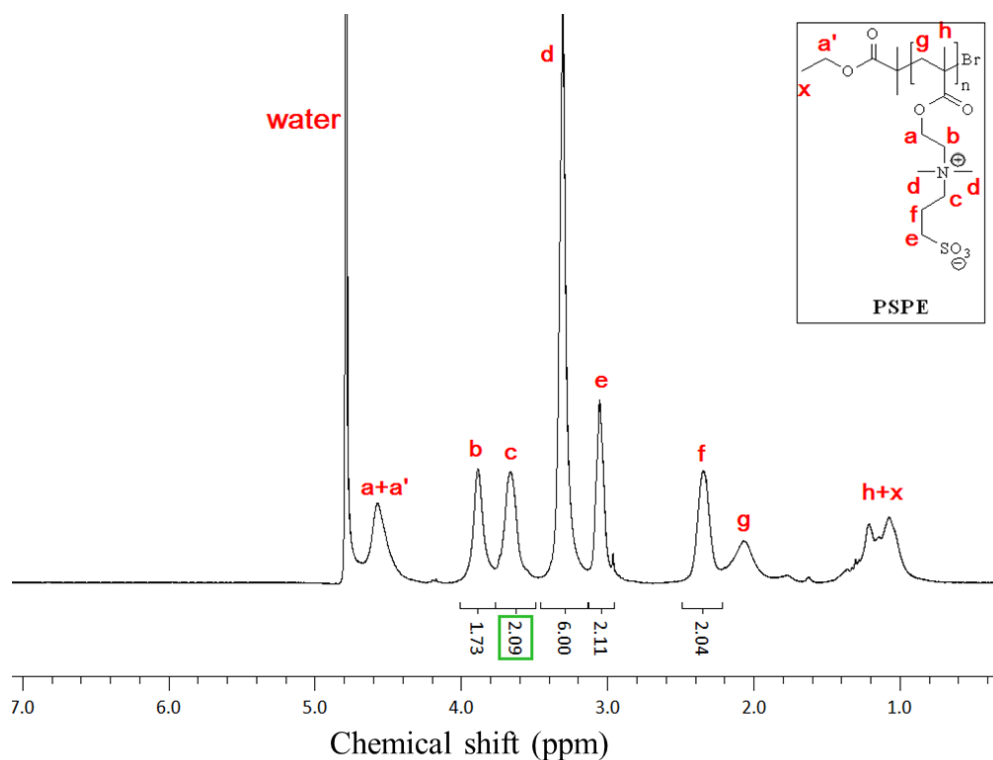


Figure 4.2. ¹H-NMR spectrum of PSPE homopolymer (HP-2) in D₂O with 0.5 M NaCl.

NMR analysis shows that the polymer PSPE was formed since signals are broad, and the olefinic peaks of the monomer vanished (**Figure 4.2**). PSPE is characterized by the peak between 3 – 3.2 ppm which belongs to methylene nears the sulfonate (–SO₃) group. The signals of the methacrylate group in the backbone at 0.8 – 2.2 ppm are broader than the signals of the protons in the side chain. Often, the degree of polymerization can be determined by end group analysis from the NMR spectrum. However, due to the high molar mass obtained and low amount of ATRP initiator that was used, the end groups, which come from ATRP initiator, EBiB, could not be resolved in the NMR spectrum.

Notably, it is also possible from the NMR spectra to estimate roughly the tacticity within the methacrylate backbone [104]. According to the shape of the signal group **h** from the right to the left, the majority of the triads is syndiotactic, a substantial part is atactic, and only a small fraction is isotactic. This result is in agreement with the results reported by Hildebrand *et al* that polymerization of sulfobetaine methacrylate by RAFT method in the fluorinated solvent, TFE, does not enhance the general tendency favoring syndiotacticity [56]. Therefore, it may be concluded that compared with RAFT-made PSPE, ATRP-made PSPE had at best marginal difference in tacticity, as the spectra look a priori the same.

4. Poly(sulfobetaine)s and Poly(sulfobetaine) Based Copolymers

Table 4.1 summarizes the results of the homopolymerization of SPE. The conversion tells that the molar mass increase with increasing the reactivity of the ligands. In addition, GPC data also show that clearly chain extension occurred. Thus, homogeneous polymerization in TFE was successfully carried out yielding PSPE. This indicates that the catalysts were active and the ATRP reaction took place. By using PMDETA and HMTETA as ligands instead of bpy, homopolymerization of SPE results in higher conversions. The activity of ligands increases with increasing number of coordinating sites, in this case the number of nitrogen atoms. Bidentate ligands, such as bpy, have lower activity to complex with copper than tridentate ligands, in this respect PMDETA and HMTETA [84]. Therefore, at the same polymerization time, the conversion increases when using PMDETA and HMTETA.

Table 4.1. Analytical data of the PSPE homopolymers made by ATRP using EBiB as initiator and CuBr as catalyst precursor in TFE at 60°C for 24 h.

Sample ^a	Ligand	Conv. [%]	Yield [%]	M _{n(theo)} ^b [g/mol]	M _{n(app)} ^c [g/mol]	PDI
HP-1	bpy	60	43	16000	26000	1.6
HP-2	PMDETA	96	72	20000	41000	1.6
HP-3	HMTETA	96	72	20000	32000	1.5

^a Ratio of [M] : [I] was always 100 : 1

^b Calculated from the yield and the feed composition

^c Obtained from the GPC measurement using HFIP as eluent and PMMA as calibration standards

There is a difference between the theoretical molar mass and the molar mass obtained from GPC measurements, in which GPC gives much higher molar masses than the theoretical values. This might be attributed to the imperfect match of the calibration standard used, which in this case is PMMA. Apart from this general problem, GPC gave higher molar mass for **HP-2** than for **HP-3** although theoretically, similar molar masses were expected. Similar dispersity indexes were obtained for the use of bpy, PMDETA, and HMTETA, meaning that these ligands produce similar molar mass distributions. However, the PDI values were relatively high. This indicates that the reaction had not perfect control, which might be attributed to the fact that TFE is chemically aggressive and this, to a certain extent, endangered the ATRP process.

4.1.1.2. Block copolymers of mPEG₁₁₄-*b*-PSPE_{*n*}

The next step was to prepare PSPE based block copolymers. The block copolymers consist of a permanently hydrophilic block, in this case mPEG, and a thermoresponsive block, in this case PSPE. As mentioned before, ATRP is a powerful method to synthesize block copolymers [13]. Therefore, the block copolymers were synthesized via ATRP using the macroinitiator approach, in which the mPEG-Br macroinitiator that was synthesized as explained in **Chapter 2.1** was employed. The macroinitiator was used to initiate the ATRP using CuBr/ligand as catalyst. The synthesis of the block copolymers of mPEG₁₁₄-*b*-PSPE_{*n*} was carried out in two solvents, i.e., in TFE and in a H₂O/MeOH mixture (3/2 v/v).

¹H-NMR spectra show that chain extension was successful, and SPE added onto the mPEG macroinitiator. This is indicated by the appearance of a peak between 3 – 3.2 ppm, which is characteristic for PSPE (CH₂ next to the SO₃ group), and the peak at about 3.8 ppm, which is attributed to mPEG (CH₂) (**Figure 4.3**). The absence of an olefinic peak between 5.6 – 6.2 ppm also indicates that the polymers obtained were free from the monomer. The number average degree of polymerization, DP_{*n*} was also determined via NMR analysis, by comparing the integrals of the peak from mPEG with the ones of the peaks from PSPE. By knowing DP_{*n*} of PSPE, the influence of PSPE chain length on the phase transition temperature of the block copolymers can be analyzed.

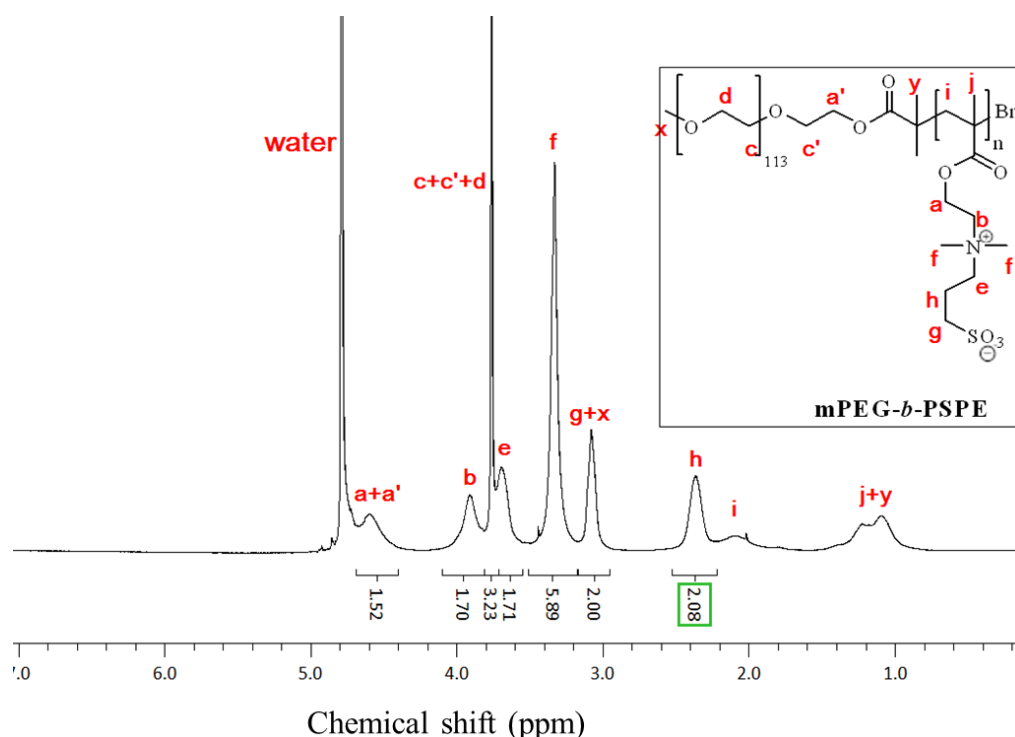


Figure 4.3. ¹H-NMR spectrum of mPEG-*b*-PSPE block copolymer (**BC-10**) in D₂O with 0.5 M NaCl.

4. Poly(sulfobetaine)s and Poly(sulfobetaine) Based Copolymers

Table 4.2. Analytical data of the mPEG₁₁₄-*b*-PSPE_n block copolymers. Unless indicated, the ratio of [M] : [I] was 100 : 1.

Sample	Ligand	Solvent	Conv. [%]	Yield [%]	DP _n	M _{n(theo)} ^b [g/mol]	M _{n(app)} ^c [g/mol]	PDI
BC-5	bpy	TFE	83	85	84	28200	45000	1.3
BC-6	HMTETA	TFE	86	74	74	28900	35000	1.7
BC-7^a	bpy	H ₂ O/MeOH	quantitative	70	22	12500	20000	1.4
BC-8^a	bpy	H ₂ O/MeOH	quantitative	80	38	16100	19000	1.6
BC-9	bpy	H ₂ O/MeOH	quantitative	83	81	28100	30000	1.7
BC-10^a	bpy	H ₂ O/MeOH	quantitative	73	137	45700	36000	2.1

^a Ratio of [M]:[I] was 30:1 for **BC-7**, 50:1 for **BC-8**, and 200:1 for **BC-10**

^b Calculated from the yield and the feed composition, assuming that the incorporation ratio is the same as the feed ratio

^c Obtained from the GPC measurement using HFIP as eluent and PMMA as calibration standards

Table 4.2 gives the results of the chain extension to give the block copolymerization of PSPE (from **BC-5** to **BC-10**). The reaction proceeded smoothly and resulted in 70 - 85% yields with moderate dispersities. It can be seen that the use of bpy or HMTETA results in equally high monomer conversions and similar yields of the block copolymers. However, the dispersity index obtained in TFE with HMTETA was higher than with bpy (compare **BC-5** with **BC-6**). It is seen in the GPC elugram (Appendix **Figures A.20** and **A.21**) that a shoulder appeared and the peak is broad for **BC-6** when using HMTETA as ligand. This suggests that bpy provides better control over the catalysis in this ATRP reaction. Thus, bpy was used for all further ATRP reactions.

Block copolymers of mPEG₁₁₄-*b*-PSPE_n were also prepared in a H₂O/MeOH mixture (3/2 v/v) as adapted from Pei *et al* [7]. The results are shown in **Table 4.2** with sample names **BC-7**, **BC-8**, **BC-9**, and **BC-10**. It is seen that ATRP reaction in H₂O/MeOH mixture resulted also in high yield (between 70 and 83%). Since it was hard to determine the olefinic peak in the NMR spectra of reaction mixture in the end of polymerization, nearly complete conversion was achieved. It is also interesting to see that the longer chain of PSPE block is, the higher the dispersity index obtained. This might be attributed the unequal growth of polymer chains, because of growing polymer chains already reached high molar mass (long chain length). Thus, the reaction control is increasingly lost and the molar mass distribution becomes broad. Moreover, the polymerization in the H₂O/MeOH mixture (3/2 v/v) was not completely

homogeneous over the entire reaction time. At the beginning, monomer and macroinitiator dissolved completely in the H₂O/MeOH mixture (3/2 v/v). But as longer the polymer chains formed are, as more viscous the reaction solution becomes. In the end, the reaction mixtures formed a turbid gel. The high viscosity in the reaction mixture may promote uncontrolled polymerization since the growing polymer chains are less mobile, and thus, it makes the addition of monomers into the growing polymer chains difficult. It is also possible that H₂O and MeOH might interfere to a certain extent with the catalyst formation, leading to uncontrolled polymerization [87].

4.1.2. Aqueous solution behavior

4.1.2.1. Homopolymer of PSPE

The aqueous phase behavior of PSPE in H₂O was studied as shown in **Figure 4.4**. Cloud point measurements were performed by cooling the sample solutions, which have concentrations of 30 g/L (3 wt%).

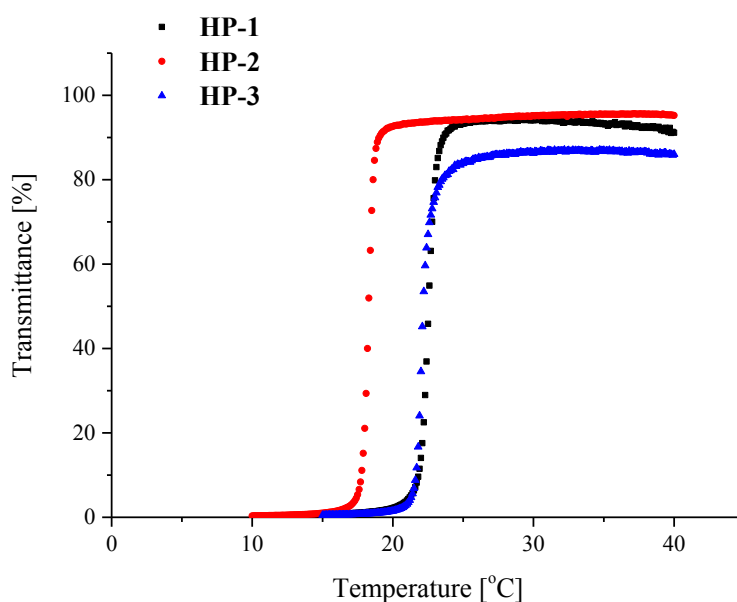


Figure 4.4. Temperature dependent turbidity (cooling run) of 30 g/L aqueous solutions of PSPE homopolymers synthesized using different ligands in H₂O: bpy (black squares), PMDETA (red circles), HMTETA (blue triangles).

4. Poly(sulfobetaine)s and Poly(sulfobetaine) Based Copolymers

As explained in **Chapter 1**, poly(sulfobetaine)s can exhibit UCST behavior in aqueous solution because of the strong intra- and interpolymer electrostatic interactions in the polymer chains. The PSPE samples obtained by the ATRP reactions have a cloud point at about 20°C. This value is lower than the one that had been reported by Hildebrand *et al* for PSPE samples made by the RAFT polymerization method, with similar degrees of polymerization (samples of $DP_n = 85$ as the case of PMDETA and HMTETA) [56]. Although the polymer concentration that had been used in the experiments by Hildebrand *et al* was 50 g/L, according to their report, the effect of polymer concentration on the cloud point is not significant enough at the studied concentrations to justify the differences observed. A plausible explanation for the low cloud points of the PSPE samples obtained by ATRP is that the polymers contain traces of salt from the catalyst (copper bromide), which give a salting-in effect, i.e. they increase the solubility of the polymers and bring the phase transition temperature down. Efficient salting-in by various salts has been frequently reported for PSPE [56]. O'Reilly *et al* reported similar results, in which the homopolymer of PSPE has a low phase transition temperature when salt was present during the polymerization [105]. While salt was absent in the RAFT polymerization experiments, the phase transition temperature of PSPE of comparable DP_n in H₂O can reach 41°C [56].

Table 4.3. UCST-type cloud point of 30 g/L aqueous solutions of PSPE homopolymers in H₂O and physiological saline. Temperature measurement between 10 - 40°C (cooling run). Concentration of sodium chloride in physiological saline is 9 g/L or 0.154 M.

Sample	Cloud Point	
	H ₂ O [°C]	Physiological saline [°C]
HP-1	23	soluble
HP-2	18	soluble
HP-3	22	soluble

It is also interesting to note that the more active ligands, in this respect PMDETA (for **HP-2**) and HMTETA (for **HP-3**), result in a lower phase transition temperature, although monomer conversion is higher (resulting in a higher degree of polymerization and higher molar mass) than that in the case of bpy (**HP-1**), whereas usually the opposite effect happens (higher molar masses increasing T_{cp} in the UCST behavior). It seems that PMDETA and HMTETA form strong complexes with the catalyst and interact stronger with the polymers. This might result

in a different affinity of the copper catalyst for the polymers according to the ligand chosen. The explanation that the copper complexes of PMDETA and HMTETA bound more strongly to the polymers than in the case of bpy, and thus, at the end, the residual amount of salt in the polymers is higher, which is supported by the difficulties encountered to get colourless polymers in the case of PMDETA and HMTETA. As consequence, the salt, presumably copper bromide (the halogen counter ion), sticking to the polymers gave rise to a strong reduction of T_{cp} . This effect is well documented in the work of Hildebrand *et al*, in which the effect of salts on PSPE solubility was explored [56].

The high sensitivity of the phase transition temperature of poly(sulfobetaine)s to salt was also shown in investigations in physiological saline solution. Physiological saline solution has a concentration of sodium chloride of 9.0 g/L (0.154 M). As the polymers dissolve easier in physiological saline solution than in pure water, it proves a marked salting-in effect. Studies of the phase transition behavior of PSPE in physiological saline solution revealed, that PSPE is soluble in the entire temperature window studied (5 - 75°C). Added salts shield the intra- and interpolymer Coulomb interactions within the polymer chains and thus, the attractive interactions decrease so that the phase transition temperature is lowered.

4.1.2.2. Block copolymers of mPEG₁₁₄-*b*-PSPE_n

The phase transition behavior of mPEG₁₁₄-*b*-PSPE_n block copolymers was investigated as summarized in **Table 4.4**. The cloud points were investigated for the polymer concentration of 30 g/L in water and in physiological saline. In pure water, all block copolymers **BC-5** – **BC-10** showed a cloud point upon cooling. In order to learn about the UCST behavior of mPEG₁₁₄-*b*-PSPE_n, the cloud point of the block copolymers was analyzed with respect to the degree of polymerization (DP_n) of PSPE. The cloud points increase with increasing DP_n of SPE. Cloud points increase from 39°C to 65°C with increasing DP_n of PSPE (**BC-7**, **BC-8**, **BC-9**) in pure water (**Figure 4.5 and 4.6**). The plausible reason for this behavior is that with increasing degree of polymerization, the entropic contribution to dissolution decreases. Therefore, the phase transition temperature increases. The same tendency of results was reported by Pei *et al* and Morimoto *et al*, although they used a different chain length of mPEG [7, 92].

4. Poly(sulfobetaine)s and Poly(sulfobetaine) Based Copolymers

However, when the DP_n of PSPE is higher than DP_n of mPEG, the phase transition temperature decreases. This can be seen from the sample **BC-10**, which has a phase transition temperature of 50°C, about 15°C lower than for **BC-9**, while normally, the opposite effect would happen. This behavior is not well understood. A possible explanation behind that could be due to a higher amount of residual salt from the copper bromide complex. Nevertheless, as **BC-9** and **BC-10** had the same purification treatment, this possibility was unlikely. Another plausible explanation could be that partial hydrolysis of the methacrylate ester group becomes more prone to occur for **BC-10** because it has the higher molar mass. If hydrolysis occurred, the total net charge within the PSPE side chain would not be zero anymore increasing the solubility of the polymers and decreasing the cloud point.

Table 4.4. UCST-type cloud point of 30 g/L aqueous solutions of mPEG₁₁₄-*b*-PSPE_n block copolymers in H₂O and physiological saline. Temperature measurement between 5 - 75°C (cooling run). Concentration of sodium chloride in physiological saline is 9 g/L or 0.154 M.

Sample	Polymers	Cloud Point	
		H ₂ O [°C]	Physiological saline [°C]
BC-5^a	mPEG ₁₁₄ - <i>b</i> -PSPE ₈₄	54	soluble
BC-6^{a,b}	mPEG ₁₁₄ - <i>b</i> -PSPE ₇₄	48	soluble
BC-7^c	mPEG ₁₁₄ - <i>b</i> -PSPE ₂₂	39	soluble
BC-8^c	mPEG ₁₁₄ - <i>b</i> -PSPE ₃₈	45	soluble
BC-9^c	mPEG ₁₁₄ - <i>b</i> -PSPE ₈₁	65	soluble
BC-10^c	mPEG ₁₁₄ - <i>b</i> -PSPE ₁₃₇	50	soluble

^a Using TFE as solvent

^b Using HMTETA as ligand

^c Using H₂O/MeOH (3/2 v/v)

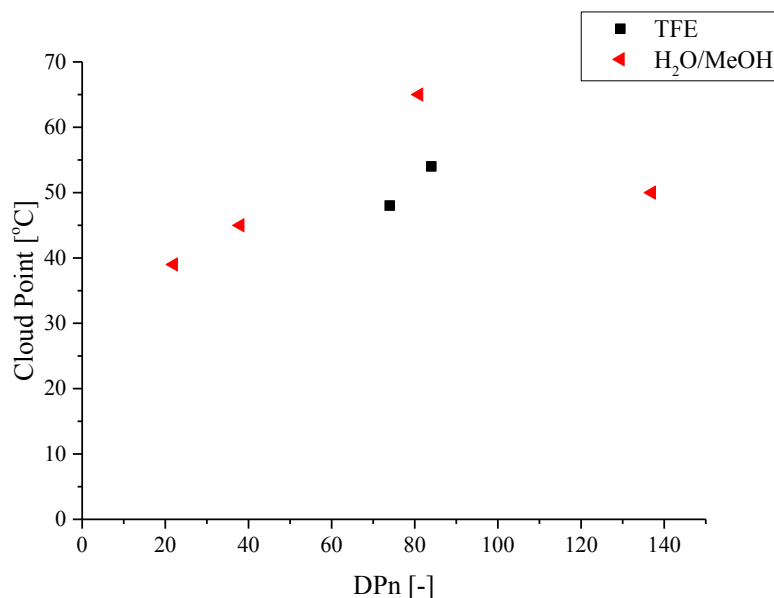


Figure 4.5. Cloud points versus degree of polymerization (DP_n) of mPEG₁₁₄-b-PSPE_n in H₂O: polymers synthesized in TFE (black squares), and in H₂O/MeOH 3/2 v/v (red triangles).

Block copolymers, which were prepared using different ligands (**BC-5** for using bpy and **BC-6** for using HMTETA) give results of cloud points of about 50°C in pure water. However, **BC-6** shows a slightly lower cloud point, which might be explained as the previous explanation that the different ligand, which complexes with the copper catalyst, may have a different affinity toward the polymers. The copper complexes of HMTETA seem to have a higher affinity toward the polymer than the complex of bpy, so that the residual amount of salt in the polymer is relatively high. This implies a decrease of T_{cp}.

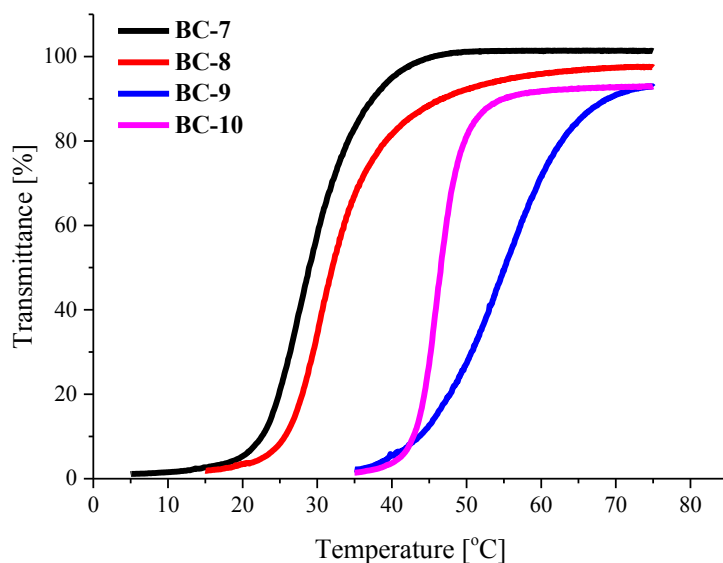


Figure 4.6. Temperature dependent turbidity (cooling run) of 30 g/L aqueous solutions of mPEG₁₁₄-*b*-PSPE_n with different degrees of polymerization in H₂O.

Another interesting feature is that the block copolymers of mPEG₁₁₃-*b*-PSPE_n prepared in the H₂O/MeOH mixture, as **BC-9**, have higher phase transition temperatures than that made by using TFE, **BC-5**, as reaction solvent. For instance, **BC-5** (using TFE) has a by about 11°C lower cloud point than **BC-9** (using H₂O/MeOH mixture) despite their similar DP_n values of around 80. The possible reason would be that some hydrolysis had taken place in TFE, when it is not completely dry, resulting in increasing solubility of the polymer, and thus, the cloud point decreases.

Comparing with homopolymers of PSPE (**HP-1**), which had DP_n of 60, and using the same ligand as **BC-5**, **BC-7**, **BC-8**, **BC-9**, and **BC-10**, all block copolymers of mPEG₁₁₄-*b*-PSPE_n exhibit higher cloud points (the cloud point of **HP-1** is 23°C). Even in comparison with the PSPE homopolymer of Hildebrand *et al*, whose system was free from salts, the block copolymers of mPEG₁₁₄-*b*-PSPE_n exhibit higher cloud points [56]. It seems that the addition of poly(ethylene glycol) block affected the phase transition temperature of mPEG₁₁₄-*b*-PSPE_n. This might occur because of an attractive interaction between the mPEG block and the betaine block. Such an interaction might reduce the solubility of the polymers, resulting in increasing phase transition temperatures. This explanation is proven by the result that when the macroinitiator mPEG-Br was mixed physically with PSPE homopolymer, the phase transition became about 10°C higher than of PSPE homopolymer itself, as shown in **Figure 4.7**.

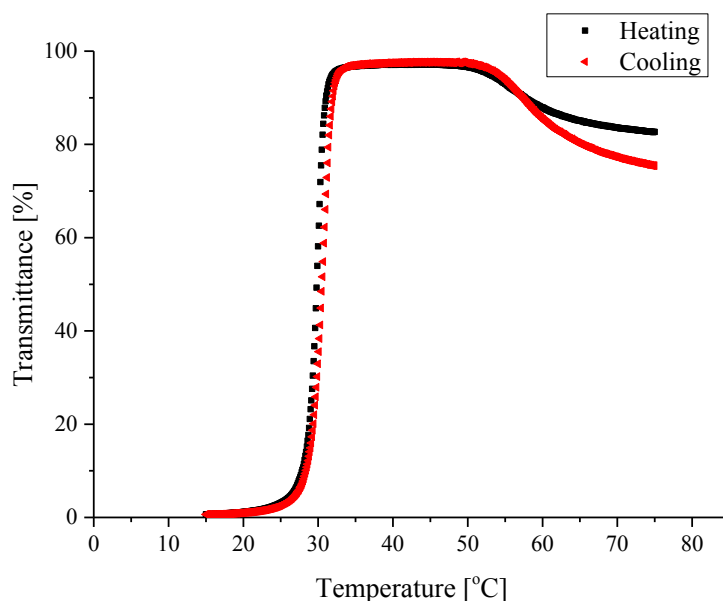


Figure 4.7. Temperature dependent turbidity of 30 g/L aqueous solutions of physical mixing of mPEG-Br with PSPE (**HP-2**) in H₂O.

The phase transition behavior of the series mPEG₁₁₄-*b*-PSPE_{*n*} was also investigated in physiological saline solution, which has a NaCl concentration of 9 g/L (0.154 M). This experiment is important to mimic the physiological condition. The cloud points obtained are expected to be precise, as the presence of a substantial amount of NaCl should cover any residual small amounts of catalysts possibly present. As listed in **Table 4.4**, no clouding transition occurred for all mPEG₁₁₄-*b*-PSPE_{*n*} samples. The block copolymers were soluble in the entire temperature range from 5°C to 75°C. Thus, the presence of this rather high amount of salt strongly reduces the phase transition temperature of the PSPE polymers, including the block copolymers, and such with high DP_{*n*} (**BC-10**). This finding is in agreement with the work of Hildebrand *et al* [56]. The phase transition temperature of homopolymers PSPE with DP_{*n*} up to 575 were measured for with varying NaCl concentrations, revealing that above 0.1 M of added salt, the phase transition temperature drops below freezing point due to the salting-in effect. Thus, the polymers become soluble in the entire temperature range studied. Analogous results were obtained by Morimoto *et al* [92]. They studied the effect of added NaCl on the phase transition temperature of mPEG₂₃-*b*-PSPE₇₄ block copolymers and observed that the phase transition temperature decreased with increasing amounts of added salt. A phase transition occurred only until a concentration of added salt of 60 mM, and was absent for salt concentrations higher than 80 mM. This concentration range is still below the

concentration of physiological saline. Thus, the missing clouding transition of mPEG₁₁₄-*b*-PSPE_{*n*} in physiological saline is not unexpected. Therefore, in order to bring the phase transition up into physiologically relevant temperature range in physiological saline solution, another strategy had to be chosen.

4.2. PSPE with hydrophobic moieties

4.2.1. Synthesis and characterization

The phase transition temperature obtained for the polymers explored in the previous chapters is not high enough to occur in physiological saline. One strategy to increase the phase transition temperature is to make the polymer less water soluble, for instance to copolymerize it with hydrophobic co-monomers [73], such as benzyl methacrylate (BzMA), which carries an aromatic group. The homopolymer is completely water-insoluble. Therefore, it was expected by using benzyl methacrylate as co-monomer, the phase transition temperature might be tuned, as with increasing hydrophobic content in polymers which exhibit UCST-type behavior, the phase transition temperature would also increase. However, copolymerization of non-polar monomers with zwitterionic monomers is complicated. It is most likely that the copolymerization reactivity ratios of SPE and BzMA are different from 1, which could lead to gradient copolymers by ATRP, so that the copolymer composition becomes function of conversion. Such a behavior is very complicated to handle. In order to avoid this problem, the choice of a co-monomer pair with identical polymerizable group, i.e., a methacrylate ester, is preferable, in order to render the reactivity ratios nearly the same ($r \approx 1$). Nevertheless, it is known that copolymerization of zwitterionic monomer, SPE with non charged monomers, such as butyl methacrylate works poorly [106]. This was explained by the low compatibility of the monomers, so that the local concentration of monomer around the growing radical center differs from its average concentration in the reaction solution. It was hoped that this incompatibility could be reduced by introducing a benzyl group, which is more polar than the butyl residual due to the π -system. An additional advantage of using BzMA is that it facilitates the analysis of the copolymers by ¹H-NMR, as aromatic protons are well separated from the mPEG- and SPE-derived signals. Moreover, the addition of hydrophobic monomers might help to encapsulate hydrophobic active agents, and therefore may be useful in future applications of controlled release.

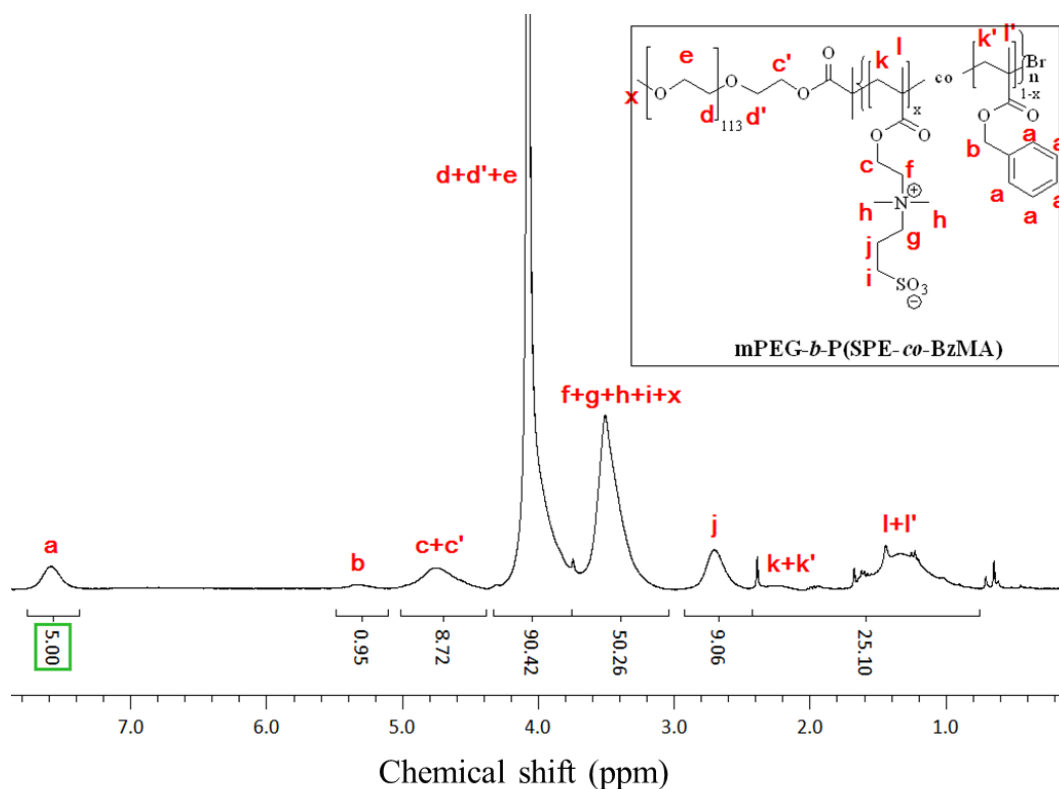


Figure 4.8. ¹H-NMR spectrum of mPEG-*b*-P(SPE-*co*-BzMA) block copolymer (BC-12) in TFA-d.

Similar to previous studies, ATRP with macroinitiator approach was used to prepare mPEG₁₁₄-*b*-P(SPE_{*x*}-*co*-BzMA_{*y*}) block copolymers. The NMR spectrum (**Figure 4.8**) shows that benzyl methacrylate was incorporated into the zwitterionic block creating mPEG₁₁₄-*b*-P(SPE_{*x*}-*co*-BzMA_{*y*}), which is indicated by the presence of a peak between 3.4 – 3.6 ppm which is attributed to the SPE repeat units, and a signal characteristic for aromatic protons between 7.4 – 7.6 ppm which is attributed to the BzMA repeat unit, as well as the peak at about 4 ppm, which is attributed to mPEG, as should be expected (**Figure 4.8**). These block copolymers were free from monomer since there is no sharp signal from olefinic groups. Due to the incorporation of the hydrophobic co-monomer, TFA-d was used as solvent for ¹H-NMR spectra, since the signal of the benzyl group could not be seen in D₂O, probably due to hydrophobic association.

4. Poly(sulfobetaine)s and Poly(sulfobetaine) Based Copolymers

Table 4.5. Analytical data of the mPEG₁₁₄-*b*-P(SPE_{*x*}-*co*-BzMA_{*y*}) block copolymers.

Sample	BzMA feed	Yield	DP _n ^b	M _{n(theo)} ^c	M _{n(app)} ^d	PDI
	[mol%]		PSPE:PBzMA	[g/mol]	[g/mol]	
BC-11 ^a	2	57	50 : 8	20300	18000	1.4
BC-12 ^a	5	74	55 : 9	25300	19000	1.3
BC-13 ^a	10	55	36 : 14	19700	23000	1.3

^a Ratio of [M]:[I] was 100:1

^b Calculated from end group analysis of mPEG

^c Calculated from the yield and the feed composition, assuming that the incorporation ratio is the same as the feed ratio

^d Obtained from the GPC measurement using HFIP as eluent and PMMA as calibration standards

Table 4.5 shows the results of mPEG₁₁₄-*b*-P(SPE_{*x*}-*co*-BzMA_{*y*}) synthesis. The increasing molar mass shows that chain extension had happened, although the yield of the block copolymers was moderate only, with about 50 – 74 %. Comparing the BzMA content in the feed and in the copolymer, it is noted that BzMA is preferentially incorporated. In addition, this gives not only a problem of compositional drift, but also gradient copolymer in the system. A possible reason might be preferred solvation of TFE as solvent in SPE growing polymer chains, which hindered the radical in the SPE growing polymer chains to attack the SPE monomers. The GPC elugrams show monomodal distributions. Although there is a difference between the theoretical and the molar mass from GPC, which might be due to the imperfect calibration standard, the PDI values obtained for these three block copolymers were relatively small (about 1.3). This means the chains were able to grow in parallel in similar time, and not many late initiations occurred during the reaction, and good control of the polymerization was achieved.

4.2.2. Aqueous solution behavior

Turbidity measurements were also performed in order to study the phase transition behavior of mPEG₁₁₄-*b*-P(SPE_{*x*}-*co*-BzMA_{*y*}) block copolymers. For this purpose, 30 g/L sample solutions of **BC-11**, **BC-12**, and **BC-13** were prepared. In general, the cloud point increased along with the BzMA content within the polymer chains (**Table 4.6**). This result is similar to that of Roth *et al*, who used benzylacrylamide (BzAm) in the copolymerization with poly[(3-((3-acrylamidopropyl)dimethylammonio)propane-1-sulfonate)] (PADPS) [73]. However, the phase transition behavior was not obvious for the case of mPEG₁₁₄-*b*-P(SPE_{*x*}-*co*-BzMA_{*y*})

since the two transition (a big and a small one) appeared in the turbidity curves for **BC-11** (at 17 and 45°C) and **BC-12** (at 21 and 45°C), while only one, small transition (at 39°C) was seen for **BC-13** (**Figure 4.9**).

Table 4.6. UCST-type cloud point of 30 g/L aqueous solutions of mPEG₁₁₄-*b*-P(SPE_{*x*}-*co*-BzMA_{*y*}) block copolymers in H₂O and physiological saline.

Sample	Polymers	Cloud Point			
		H ₂ O		Physiological saline	
		[°C]		[°C]	
		Major	Minor	Major	Minor
BC-11	mPEG ₁₁₄ - <i>b</i> -P(SPE ₅₀ - <i>co</i> -BzMA ₈)	17	45	45	-
BC-12	mPEG ₁₁₄ - <i>b</i> -P(SPE ₅₅ - <i>co</i> -BzMA ₉)	21	45	45	-
BC-13	mPEG ₁₁₄ - <i>b</i> -P(SPE ₃₆ - <i>co</i> -BzMA ₁₄)	< 5	39	41	-

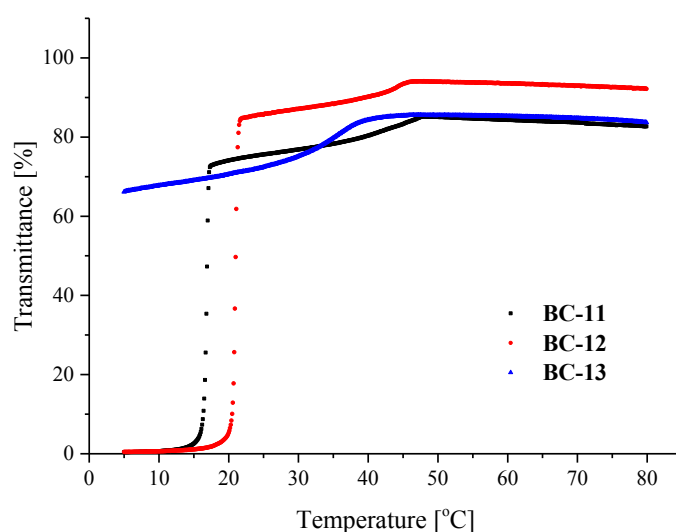


Figure 4.9. Temperature dependent turbidity (cooling run) of 30 g/L aqueous solutions of mPEG₁₁₄-*b*-P(SPE_{*x*}-*co*-BzMA_{*y*}) block copolymers in H₂O.

DLS studies were performed to analyze further, whether the weak transition, shown by **BC-13**, was real. As can be seen on **Figure 4.10**, there was a transition happening since bigger particles began to form at 39°C upon cooling.

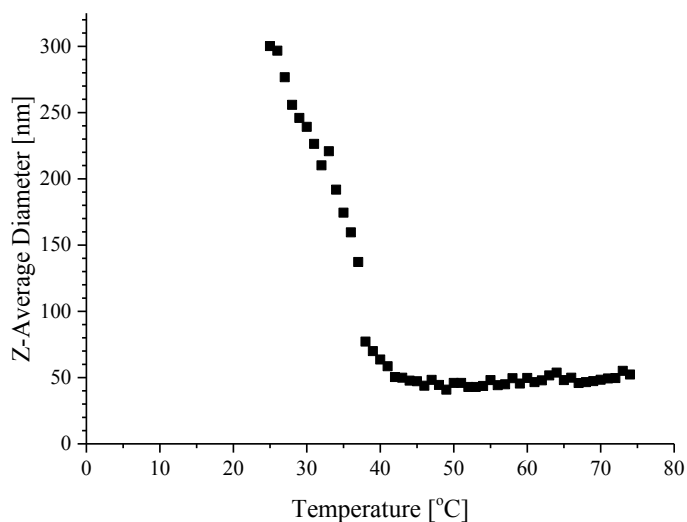


Figure 4.10. Temperature dependent DLS measurement (cooling run) of 30 g/L aqueous solutions of **BC-13** in H₂O.

Also, the phase transition behavior in physiological saline was studied. As listed in **Table 4.6**, all three samples show apparently the same weak cloud point. Yet, unlike the phase transition behavior of other poly(sulfobetaine) polymers in physiological saline, this cloud point in physiological saline was higher than in pure water. Because of this surprising behavior and the weakness of the transitions seen (**Figure 4.11**), the effect of salt concentration on the small turbidity transitions of mPEG₁₁₄-*b*-P(SPE_{*x*}-*co*-BzMA_{*y*}) was investigated in more detail. For this purpose, **BC-12** was used, because **BC-12** had better yield and PDI than **BC-11** and **BC-13**, while all had similar DP_{*n*} values.

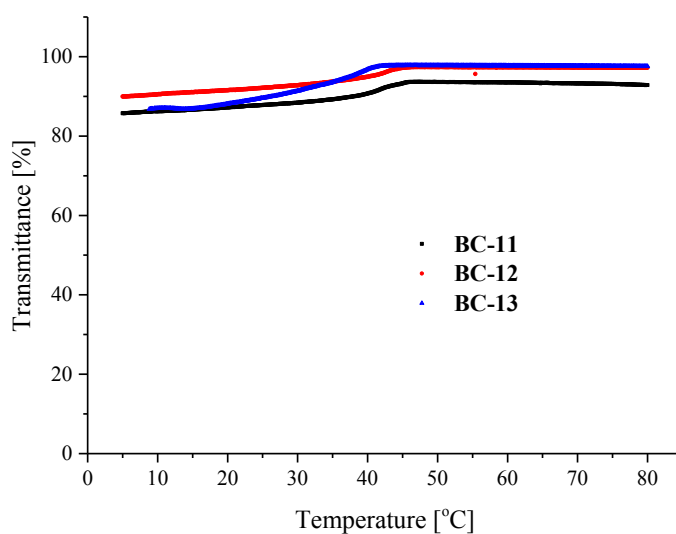


Figure 4.11. Temperature dependent turbidity (cooling run) of 30 g/L aqueous solutions of mPEG₁₁₄-*b*-P(SPE_{*x*}-*co*-BzMA_{*y*}) block copolymers in physiological saline.

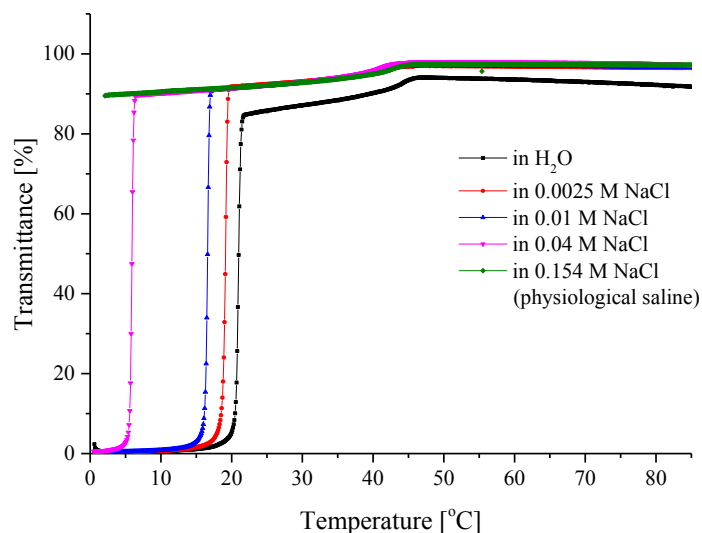


Figure 4.12. Temperature dependent turbidity (cooling run) of 30 g/L aqueous solutions of **BC-12** with different salt concentration.

Figure 4.12 displays the effect of added salt on the phase transition behavior of **BC-12**. As found in pure water, two transitions occurred, while only the big transition was salt dependent. The more salt was added into the solution, the lower is the cloud point of the big transition. This means that the big transition corresponds to the thermoresponsive behavior of the poly(sulfobetaine)s because of the salting-in effect, by which the solubility of poly(sulfobetaine)s increases with the addition of salts. In any case, the addition of small amounts of benzyl methacrylate was not sufficient to bring the cloud point up in physiological saline solution. As reported by Roth *et al*, more than 35% of benzylacrylamide (BzAm) was needed to achieve a high cloud point of copolymers P(ADPS-*co*-BzAm) in pure water, while in physiological saline solution, copolymers were still soluble [73]. In analogy, it is most probable that this also happens for mPEG₁₁₄-*b*-P(SPE_x-*co*-BzMA_y) block copolymers. Nevertheless, the appearance of the small turbidity transition was still unclear.

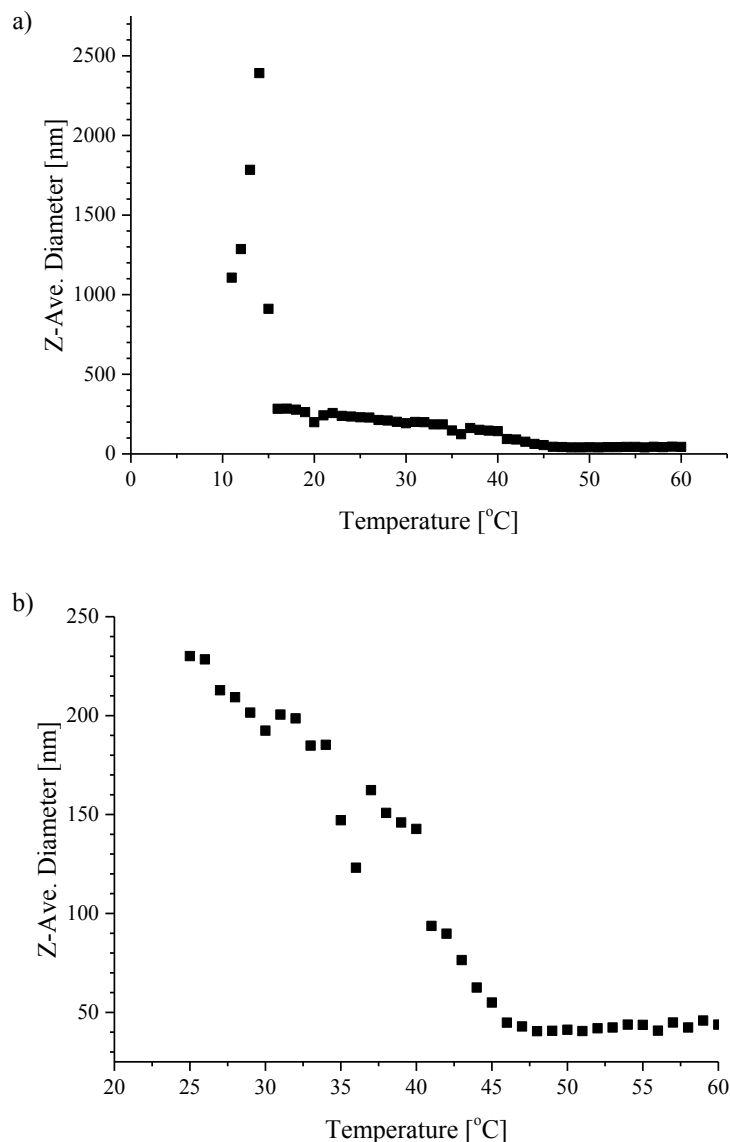


Figure 4.13. Temperature dependent DLS measurement (cooling run) of 30 g/L aqueous solutions of **BC-12** in H₂O a) from 10 to 60°C and b) zoom-in from 25 to 60°C.

In order to learn more about the small transition of mPEG₁₁₄-*b*-P(SPE_{*x*}-*co*-BzMA_{*y*}) block copolymers, the temperature dependent size in solution was followed by DLS. A solution of **BC-12** in pure water was taken for this purpose, and the change of sizes was recorded while cooling the sample. **Figure 4.13** displays the Z-average diameter of **BC-12** polymers. A big rise of the size of the polymers was observed at about 15°C. Still, if the graph is zoomed-in, a small but notable increase of size occurs also at about 40°C (**Figure 4.13b**). From these graphs, one may conclude that both transitions are real.

To get more insight in the nature of the minor transition, a micro DSC experiment of **BC-12** solution in pure water was also performed. The heat flow of a semi dilute solution of **BC-12** was measured and compared with the turbidity studies. Interestingly, an endothermic peak occurred in the similar temperature range as the small turbidity transition, but not for the major transition (**Figure 4.14**). Nevertheless, a detailed explanation remains unresolved.

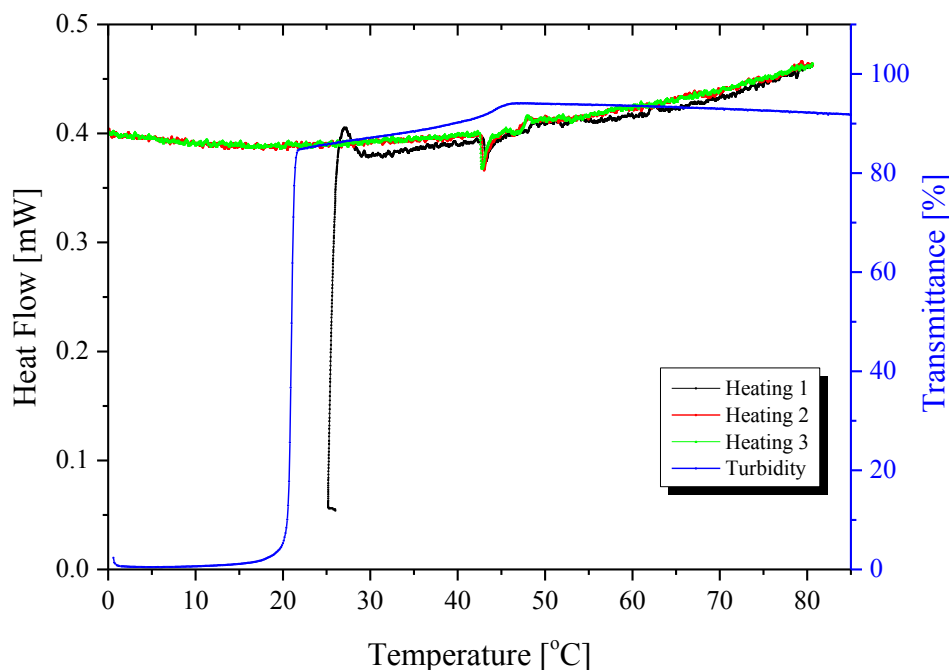


Figure 4.14. Turbidity (cooling runs) and micro DSC measurements (heating run) of 30 g/L solutions of **BC-12** in H₂O.

Accordingly to all the measurements that were performed, the appearance of two transitions, although the origin is not clear, seems real. It could be related to the gradient structure, which mPEG₁₁₄-*b*-P(SPE_{*x*}-*co*-BzMA_{*y*}) block copolymers might have. Since this system is complicated and cannot provide the aspired transition suited for a model study, another approach was followed, by trying to make the betaine monomer unit itself less water-soluble, which will be discussed in more detail in the next chapter.

4.3. PSBE based polymers

4.3.1. Synthesis and characterization

In order to increase the phase transition temperature of the block copolymers, the poly(sulfobetaine) blocks can be made less water-soluble. The studies of Hildebrand *et al* revealed that the simple assumption that the solubility of polybetaines in water is governed by the sum of the incremental hydrophilicities or hydrophobicities of the various molecular fragments contained is not true [56]. In fact, the effect of changing the various substituents cannot be rationalized at present. The only parameter, which seems reliably to increase the phase transition temperature, is increasing the spacer between the positively and negatively charged groups from C3 to C4. By making the alkyl spacer between ammonium and sulfonate groups longer, e.g., four carbon atoms instead of three like in the SPE (**Figure 4.15**), the cloud point increases significantly. This monomer is 3-((2-(methacryloyloxy)-ethyl)dimethylammonio)-butane-1-sulfonate (SBE). Its homopolymer phase transition temperatures have been investigated occasionally [54, 56, 107]. According to the report of Hildebrand *et al*, the phase transition temperature of PSBE is higher than 100°C starting for DP_n of 80, which is much higher than that of PSPE with the same DP_n . This monomer showed a cloud point even in quite high amounts of NaCl, which in the aspired context might be good enough. In addition, it was shown for SPE, that the block copolymer gives higher cloud point than its homopolymer (see **Chapter 4.1**). Thus, it was hoped that by using SBE, the phase transition in physiological saline would be more prone to happen.

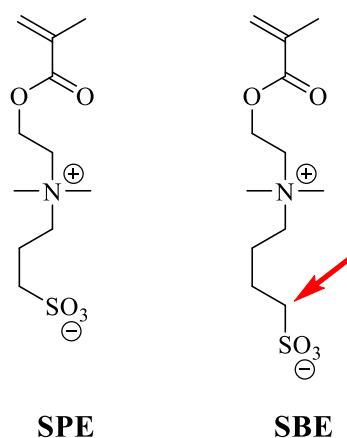


Figure 4.15. Chemical structure difference between SPE and SBE.

Sulfobetaine monomer SBE is not commercially available. Therefore, it had to be synthesized beforehand, which was done via ring opening alkylation of 2-(dimethyl amino) ethyl methacrylate by 1,4-butane sultone in acetonitrile [54, 56].

In analogy to the polymers of SPE, block copolymers of mPEG₁₁₄-*b*-PSBE_{*n*} were also successfully prepared via ATRP with the macroinitiator approach (**Table 4.7**). The NMR spectrum shows that the PSBE has been incorporated to mPEG blocks, which is indicated by the appearance of a peak at about 3 ppm which is characteristic for PSBE, and the peak at about 3.8 ppm which is attributed to mPEG (**Figure 4.16**). Since the synthesis used only the macroinitiator but no low molar mass ATRP initiator (such as EBiB), no homopolymer of PSBE could be formed. Moreover, the block copolymers were not contaminated by residual monomer since no peaks of anolefinic group in the range 5.5 – 6.5 ppm were observed. It is also noteworthy that the peaks, which are attributed to the polymer backbone, such as **k**, are broader than those attributed to the side chain, such as **g**. This is explained by the higher mobility of the latter.

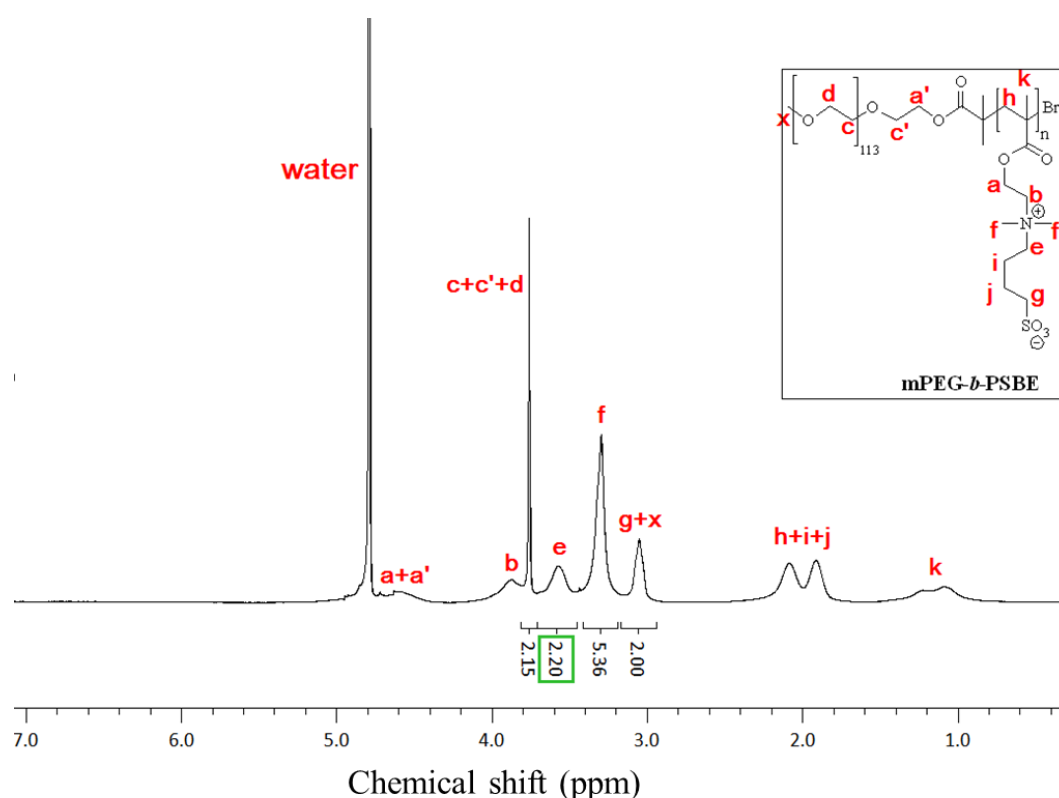


Figure 4.16. ¹H-NMR spectrum of mPEG-*b*-PSBE block copolymer (**BC-15**) in D₂O with 0.5 M NaCl.

4. Poly(sulfobetaine)s and Poly(sulfobetaine) Based Copolymers

Table 4.7. Analytical data of the mPEG₁₁₄-*b*-PSBE_n block copolymers made by ATRP using mPEG-Br as macroinitiator, CuBr/ bipyridyl as complex catalyst in TFE at 60°C for 24 h.

Sample	Conv. [%]	Yield [%]	DP _n	M _{n(theo)} ^b [g/mol]	M _{n(app)} ^c [g/mol]	PDI
BC-14 ^a	73	70	70	25500	42000	1.4
BC-15 ^a	quantitative	91	183	58300	71000	1.3

^a Ratio of [M]:[I] was 100:1 for **BC-14**, and 200:1 for **BC-15**

^b Calculated from the yield and the feed composition, assuming that the incorporation ratio is the same as the feed ratio

^c Obtained from the GPC measurement using HFIP as eluent and PMMA as calibration standards

Two block copolymer samples with different DP_n of SBE were prepared, i.e., **BC-14** with a DP_n of 70 and **BC-15** with a DP_n of 183. As can be seen from **Table 4.7**, both of them are obtained in high yields (70% for **BC-14** and 91% for **BC-15**). The high yield and rise of molar mass indicates also that chain extension occurred and block copolymers mPEG₁₁₄-*b*-PSBE_n were formed. According to the very low intensity of the signal of olefinic peaks in the reaction mixture of **BC-15** after polymerization, nearly complete conversion was reached.

The GPC data show monomodal distributions for both samples. However, a small shoulder was noticed for **BC-14**, which could explain the higher PDI obtained. Notably, the shift of the elution time between macroinitiator and both samples indicates successful block copolymerization. The GPC data also show higher molar masses than theoretically expected. As explained before, this may be due to the use of PMMA as calibration standard in the GPC measurements, which might be not a good match for poly(sulfobetaine)s. However, relatively narrow molar mass distributions were obtained for these block copolymers (PDI about 1.3 – 1.4), meaning that good control was achieved in their synthesis.

4.3.2. Aqueous solution behavior

The phase transitions of mPEG₁₁₄-*b*-PSBE_n were also investigated by turbidimetry. Sample solutions with concentration of 30 g/L were prepared in pure water and in physiological saline. The results summarized in **Table 4.8** are somewhat surprising. Although the turbidity transitions were rather broad, **BC-14** showed not only an UCST but also apparently an LCST-type phase transition. It seems that the mPEG block brings a LCST transition into the overall

phase behavior of mPEG₁₁₄-*b*-PSBE_{*n*}. Interestingly, as the DP_{*n*} of PSBE block becomes longer, the LCST-type transition disappeared (**BC-15**), and block copolymer **BC-15** showed only a UCST-type cloud point above 75°C (**Figure 4.17a**). This result contrasts with the behavior of the more water-soluble sulfobetaine block copolymers mPEG₁₁₄-*b*-PSPE_{*n*} such as **BC-6** having similar DP_{*n*} of the betaine block, which exhibit only one phase transition with UCST-type behavior. PEG itself is known to show LCST-type phase transition behavior [108-109]. Therefore, it is possible that mPEG affects the phase transition behavior of **BC-14** since the length of the poorly water-soluble PSBE block is less than the length of the water-soluble mPEG block. Yet, because of the longer PSBE block in **BC-15**, the contribution of the mPEG block to the phase transition behavior disappears. Still, comparing the UCST-type phase transition temperatures for **BC-14** and **BC-15**, it is noted that the cloud point increased with increasing degree of polymerization, as expected from theory.

Table 4.8. Cloud point of 30 g/L aqueous solutions of mPEG₁₁₄-*b*-PSBE_{*n*} block copolymers in H₂O and physiological saline. Temperature measurement between 5 - 75°C (cooling run). Concentration of sodium chloride in physiological saline is 9 g/L or 0.154 M.

Sample	Polymers	Cloud Point	
		H ₂ O [°C]	Physiological saline [°C]
BC-14	mPEG ₁₁₄ - <i>b</i> -PSBE ₇₀	30 (UCST-type) 45 (LCST-type)	20 (LCST-type)
BC-15	mPEG ₁₁₄ - <i>b</i> -PSBE ₁₈₃	> 75	soluble

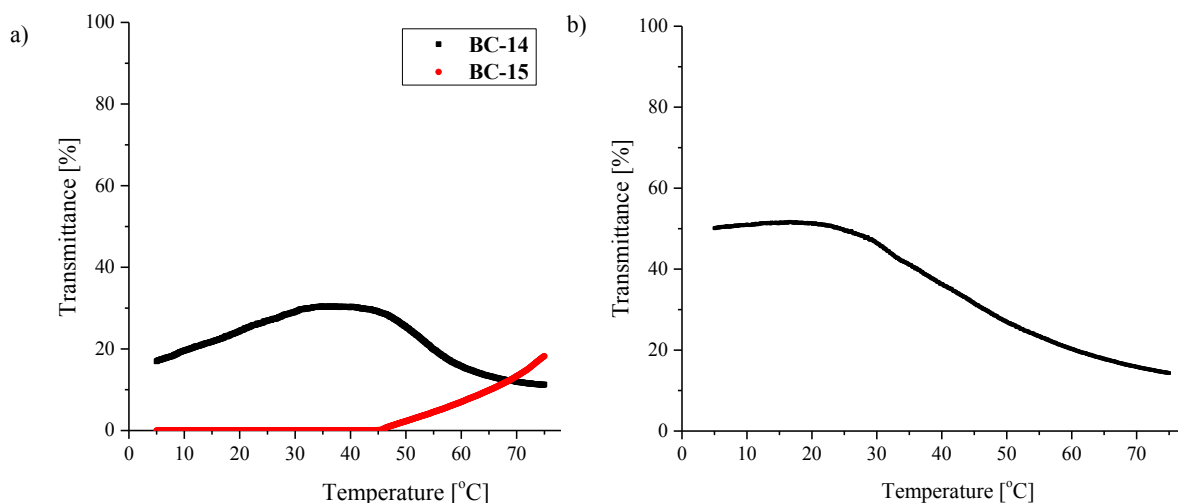


Figure 4.17. Temperature dependent turbidity (cooling run) of 30 g/L aqueous solutions of mPEG₁₁₄-*b*-PSBE_{*n*} block copolymers in a) H₂O, b) physiological saline solution (9 g/L NaCl). Black is **BC-14**, red is **BC-15**.

Temperature dependent ¹H-NMR was performed to study the phase transition of **BC-14** in water and the result is shown in **Figure 4.18**. It is noticed that the characteristic peak of PSBE, for instance between 2.8 – 3 ppm (pointed by red arrow), becomes sharper and gathers more intensity within the temperature higher than 35°C, which indicates the increasing of hydration of PSBE. Meanwhile, there is no significant change, with respect to shape and intensity, from the characteristic peak of mPEG (pointed by blue arrow) which suggests that the mPEG block is well-hydrated in the entire temperature measurement, even in the temperature higher than LCST-type cloud point.

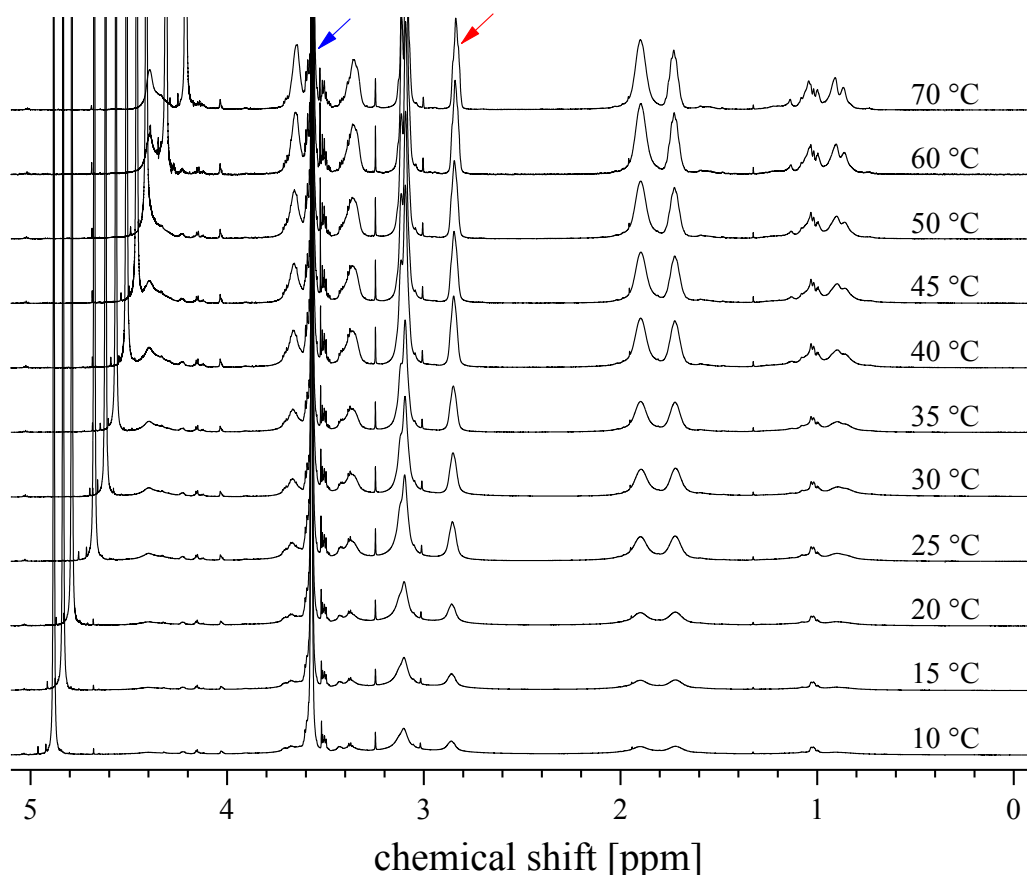


Figure 4.18. Temperature dependent $^1\text{H-NMR}$ (heating run) of 30 g/L aqueous solutions of **BC-14** in D_2O

The study of the aqueous solubility behavior was extended to studying the phase transitions of **BC-14** and **BC-15** in physiological saline solutions (**Figure 4.17b**). Both SBE based block copolymers **BC-14** and **BC-15** did not show anymore a UCST-type cloud point in the temperature range of 5 - 75°C. This most probably happened because the added salt influenced strongly the poly(sulfobetaine) blocks, in this case the PSBE blocks, promoting a salting-in effect. Thus, the PSBE blocks become soluble over the full temperature range and the UCST-type phase transition vanished. In the case of **BC-15**, the block copolymer becomes fully soluble in physiological saline solution. In contrast, in the case of **BC-14**, the LCST-type cloud point is preserved but it is lower than in H_2O . This behavior is just as expected for mPEG block copolymers, because the addition of salt results in a salting-out effect that lowers the LCST-type cloud point. The decrease of cloud point of mPEG₁₁₄-*b*-PSBE_{*n*} block copolymers matches to the work of Gao *et al* and Hildebrand *et al*, in which the UCST-type phase transition temperature of homopolymers of PSBE alone decreased with increasing NaCl concentration [56, 107].

Interestingly, as mentioned before, **BC-14** had a system, which shows in one molecule not only a UCST-type but also a LCST-type phase transition. Even if this system is not well understood at the moment, one can only assume that the mPEG block affects the overall phase transition and that the UCST-type cloud point in physiological saline is very much reduced because of the interaction between the betaine and salt. This also makes this structure interesting in the context of "schizophrenic" diblock copolymers that can self-assemble in aqueous solution and are able to form two micellar structures by inverting the core and the shell of micelles by the respective blocks as a response of changing pH, temperature or ionic strength [110-112].

4.4. PZPE based polymers

4.4.1. Synthesis and characterization

4.4.1.1. Homopolymer of ZPE

Another attempt to increase the phase transition temperature in physiological saline was done by using other zwitterionic monomers from the class of sulfobetaines instead of sulfobetaines. Sulfobetaines have a similar chemical structure as sulfobetaines, but differ in the anion group, carrying a sulfate instead of a sulfonate moiety. The sulfobetaine analogue of SPE is called in the following ZPE (**Figure 4.19**).

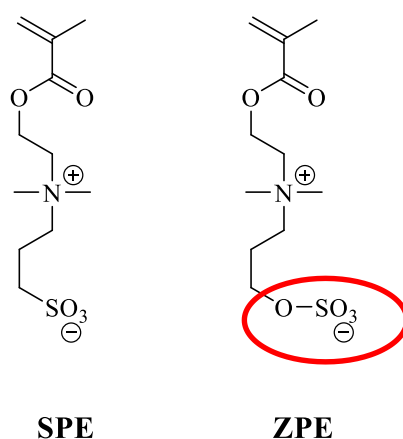


Figure 4.19. Chemical structure difference of SPE and ZPE.

Like most sulfobetaines, sulfobetaine monomers are not commercially available, and have to be synthesized beforehand. In particular, ZPE is prepared by reacting a cyclic sulfate with methacrylates bearing a tertiary amine moiety. The homopolymers of PZPE exhibit also

UCST behavior, but are considerably less water soluble than PSPE. In fact, Vasantha *et al* reported that PZPE is insoluble in pure water, whereas it shows a phase transition in concentrated aqueous NaCl at higher than physiological saline concentration [76]. Because of that, ZPE was considered to be suitable for this research project.

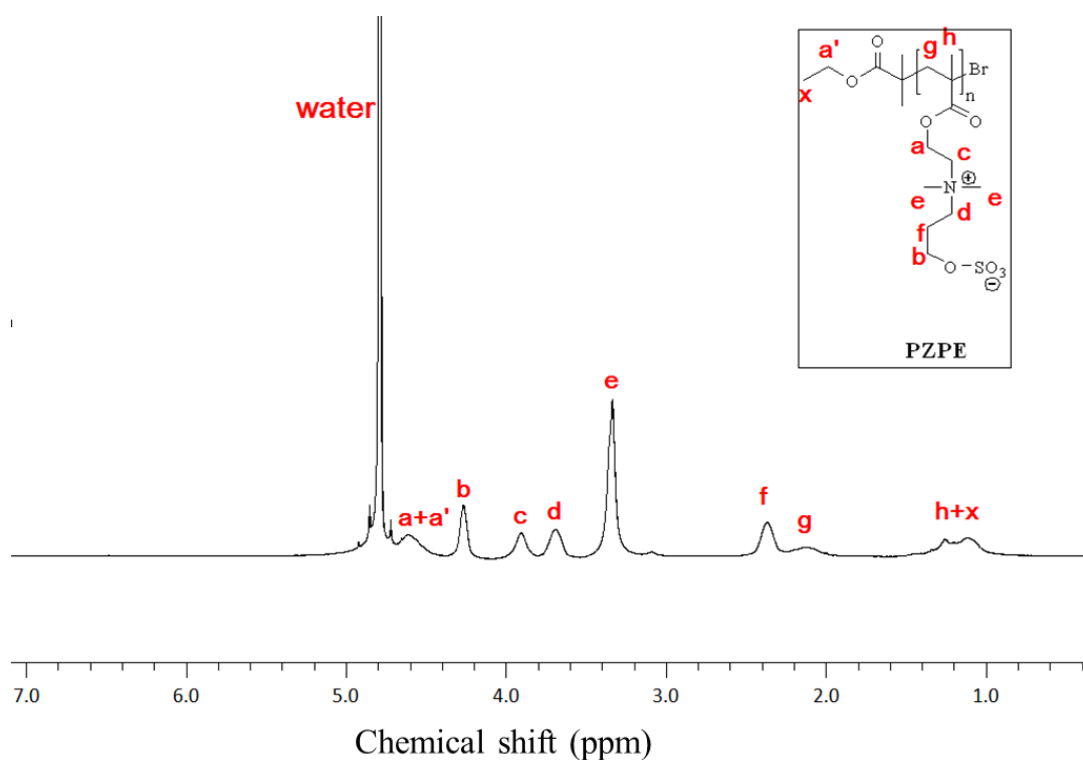


Figure 4.20. ¹H-NMR spectrum of PZPE homopolymer (HP-4) in D₂O with 0.5 M of NaCl.

In order to get more information about the behavior of this sulfobetaine polymer, a series of PZPE homopolymers with different DP_n (target DP_n of 50, 100, and 200) was synthesized via ATRP in TFE. NMR analysis shows that PZPE was formed. The sulfobetaine motif is characterized by the peak between 4.2 – 4.4 ppm that is attributed to the –CH₂-O-SO₃⁻ groups (**Figure 4.20**). Notably, the signals of the methacrylate group incorporated in the backbone (signal **g** and **h**) are broader than the ones of the side chain. No olefinic peak was observed indicating no contamination by residual monomer, which means that the purification method resulted in pure polymers.

Table 4.9. Analytical data of the PZPE homopolymers made by ATRP using EBiB as initiator, CuBr/ bipyridyl as complex catalyst in TFE at 60°C for 24 h.

Sample	Conv. [%]	Yield [%]	DP _n ^b	M _{n(theo)} ^c [g/mol]	M _{n(app)} ^d [g/mol]	PDI
HP-4 ^a	80	84	40	12500	19000	1.3
HP-5 ^a	60	78	60	26100	28000	1.4
HP-6 ^a	97	88	194	46200	77000	1.9

^a Ratio of [M]:[I] was 50:1 for **HP-4**, 100:1 for **HP-5**, and 200:1 for **HP-6**

^b Calculated from the conversion and monomer to initiator ratio

^c Calculated from the yield and the feed composition

^d Obtained from the GPC measurement using HFIP as eluent and PMMA as calibration standards

Table 4.9 summarizes the results of homopolymerization of ZPE. It shows that the homopolymerization proceeded quite well and, in general, gives relatively high monomer conversions with yields of about 80%. Relatively high molar masses could be obtained (**HP-6**). However, the apparent molar masses from GPC were different from the calculated molar masses. The possible reason for that is that the GPC used PMMA as calibration standards, which is not suitable for the poly(sulfobetaine).

Analogously to the results of mPEG₁₁₄-*b*-PSPE_n with different DP_n of PSPE (**BC-7**, **BC-8**, **BC-9**, **BC-10**), homopolymers of PZPE also show increasing dispersity index with increasing DP_n (PDI of **HP-4** < **HP-5** < **HP-6**) meaning that although GPC elugrams gave monomodal distributions for all three samples, rather broad molar mass distribution occurred for **HP-6**, which had the target DP_n of 200. This might be due to a low exchange rate between the active species and the dormant one, resulting in unequal growth of the polymers as well as of molar masses. It might also be due to the use of TFE, which is chemically aggressive and prone to induce side reactions in ATRP. This suggests that the polymerization is no more well-controlled, and may also explain the pronounced mismatch between theoretical M_n and apparent M_n from GPC.

4.4.1.2. Statistical copolymers of SPE and ZPE

The previous studies in this work show that PSPE was soluble in physiological saline solution (see **Chapter 4.1.2.1**). Therefore, copolymerization of SPE with ZPE was carried out. It was expected that copolymers exhibit an intermediate phase transition behavior, and that the phase

transition temperature could be tuned by modulating the ratio of SPE to ZPE in the copolymer. The close similarity of the chemical structures of SPE and ZPE (both of them are zwitterionic methacrylates and bear the same ammonium groups) seemed advantageous for the copolymerization, since their reactivities were assumed to be nearly identical.

Copolymers with different monomer feeds of SPE and ZPE (**CP-2** had the highest amount of SPE in the monomer feed, while **CP-4** had the lowest) were prepared via ATRP in TFE. Both monomers were copolymerized successfully, which is indicated from the appearance of peaks between 3 – 3.2 ppm and 4 – 4.4 ppm in the NMR spectrum. These are characteristic for the methylene protons near the sulfonate group in PSPE and the methylene protons near the sulfate group in PZPE, respectively (**Figure 4.21**). The absence of olefinic peaks between 5.6 – 6.2 ppm tells that no monomer is present, and pure copolymers were obtained. NMR analysis also provides the compositions of the statistical copolymers. As expected, **CP-4** had the lowest PSPE portion within the P(SPE-*co*-ZPE) copolymers (**Table 4.10**).

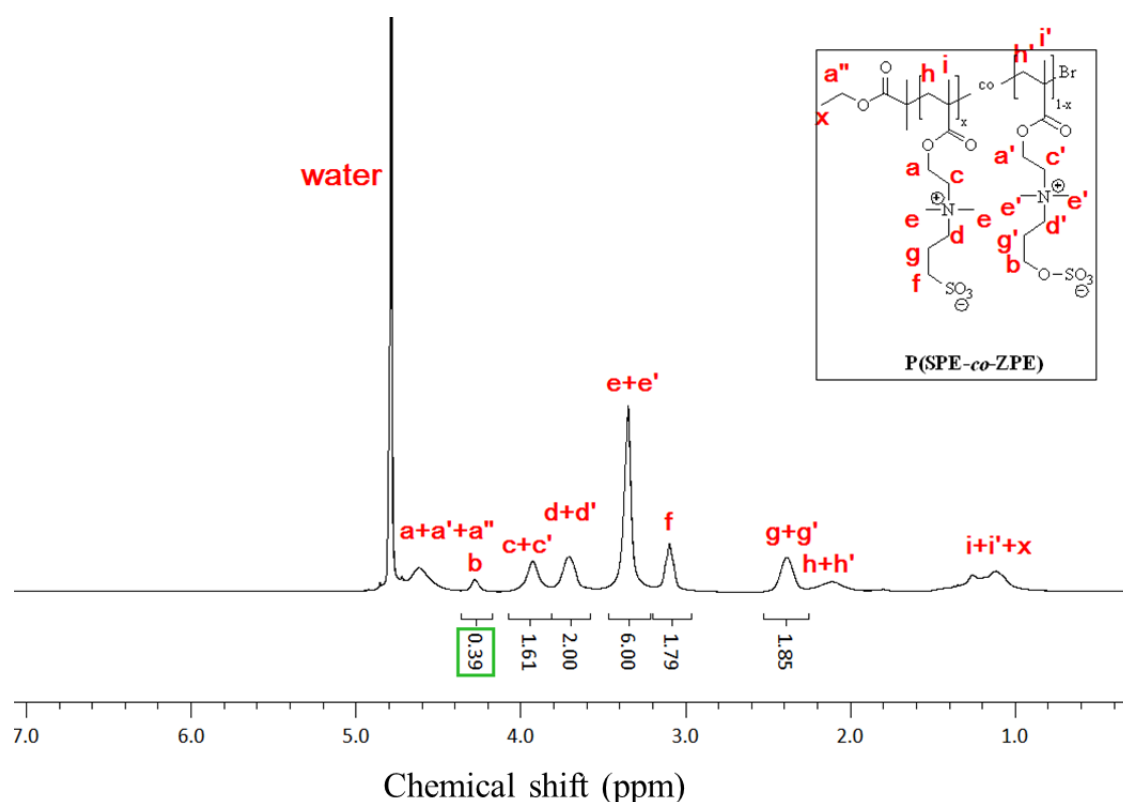


Figure 4.21. $^1\text{H-NMR}$ spectrum of P(SPE-*co*-ZPE) copolymer (**CP-2**) in D_2O with 0.5 M NaCl.

4. Poly(sulfobetaine)s and Poly(sulfabetaine) Based Copolymers

Table 4.10. Analytical data of the P(SPE-*co*-ZPE)_n copolymers made by ATRP using EBiB as initiator, CuBr/ bipyridyl as complex catalyst in TFE at 60°C for 24 h.

Sample	ZPE feed [mol%]	Conv.	Yield [%]	SPE:ZPE ^b Content in the copolymer	M _{n(theo)} ^c [g/mol]	M _{n(app)} ^d [g/mol]	PDI
CP-2 ^a	20	85	80	0.82 : 0.18	21200	18000	1.4
CP-3 ^a	50	90	88	0.52 : 0.48	25400	23000	1.5
CP-4 ^a	80	95	88	0.24 : 0.76	25800	25000	1.5

^a Ratio of [M]:[I] was 100:1

^b Calculated from integration ratio peaks of **f** and **b**

^c Calculated from the yield and the feed composition, assuming that the incorporation ratio is the same as feed ratio

^d Obtained from the GPC measurement using HFIP as eluent and PMMA as calibration standards

In general, copolymerization of SPE and ZPE proceeded very well, as can be seen from the high yields (about 80%) and the increasing molar masses up to 25000 g/mol. In general, all three copolymers had compositions which correspond within the analytical precision to the monomer feed ratios. Thus, it can be concluded that copolymers were formed, and assumed that both monomers SPE and ZPE have indeed a similar reactivity in their copolymerization behavior. The GPC data gave only slightly different apparent molar masses, M_{n(GPC)}, than theoretical molar masses, M_{n(theo)}. The reason for that could be the difference of chemical structure between the calibrations standards used in GPC (using PMMA) and the copolymers obtained. The copolymerization also produced relatively narrow molar mass distributions. This is shown by the rather low PDI values obtained (about 1.5). This means that the copolymerization proceeded relatively smoothly, and each polymer chain grew for a similar time. Thus, reasonable control on the polymerization could be maintained during the reaction.

4.4.1.3. Block copolymers of ZPE

Having demonstrated the successful homopolymerization and statistical copolymerization of ZPE, it was also interesting to study the behavior of PZPE based block copolymers. In analogy to the previous block copolymer systems, mPEG₁₁₄-*b*-PZPE_n block copolymers were prepared via ATRP using the macroinitiator approach in TFE as solvent, with the target DP_n of 100.

The $^1\text{H-NMR}$ spectrum of the copolymerization product shows that ZPE was added to the mPEG-block, forming mPEG₁₁₄-*b*-PZPE_{*n*} block copolymers (**Figure 4.22**). This is seen from the occurrence of the peak between 3.2 – 3.4 ppm which is attributed to PZPE, and the peak at about 3.8 ppm which is attributed to mPEG. The absence of an olefinic peak between 5.6 – 6.2 ppm demonstrates that the polymers were free from monomer.

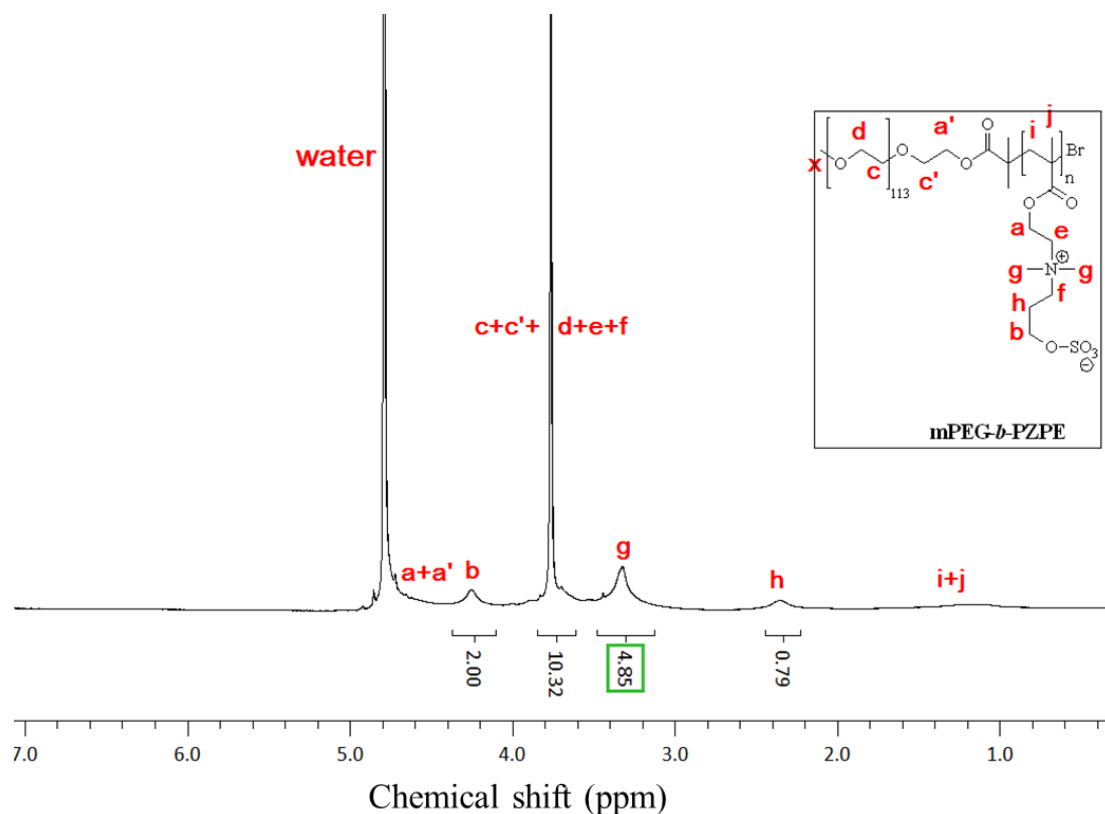


Figure 4.22. $^1\text{H-NMR}$ spectrum of mPEG-*b*-PZPE block copolymer (**BC-16**) in D_2O with 0.5 M NaCl.

The reaction yield was only moderate with 64%, DP_n reaching 58 (**Table 4.11**). In addition, the PDI value obtained was quite high (PDI of 1.7). In fact, the GPC elugram shows a bimodal distribution. A probable explanation for this finding is that once the ZPE has added onto the mPEG, the growing sulfobetaine polymer chains suffered from decreasing hydrophilicity. The monomer ZPE is soluble in water. However, PZPE has low water solubility, so that the higher DP_n of PZPE block is, the lower the water solubility becomes. PZPE has different properties from mPEG, which has high water solubility. Therefore, it is possible that after initiation, the ZPE monomer prefers to react with the active site on the growing PZPE blocks (propagation was faster than initiation), until it saturated enough and became less water soluble. This creates a gap of hydrophilicity between monomer ZPE and

4. Poly(sulfobetaine)s and Poly(sulfabetaine) Based Copolymers

the growing polymer chains, which make the new ZPE monomers preferentially react with the macroinitiator creating new growing polymer chains. Hence, low yield and diverse molar mass occurred, and a broad molar mass distribution was obtained.

Table 4.11. Analytical data of the mPEG₁₁₄-*b*-PZPE_{*n*} block copolymers made by ATRP using mPEG-Br as macroinitiator, CuBr/ bipyridyl as complex catalyst in TFE at 60°C for 24 h.

Sample	Yield	DP _n ^b	M _{n(theo)} ^c	M _{n(app)} ^d	PDI
	[%]		[g/mol]	[g/mol]	
BC-16 ^a	64	58	23200	53000	1.7

^a Ratio of [M]:[I] was 100:1

^b Calculated from the conversion and monomer to initiator ratio

^c Calculated from the yield and monomer feed, assuming that the incorporation ratio is the same as feed ratio

^d Obtained from the GPC measurement using HFIP as eluent and PMMA as calibration standards

4.4.1.4. Statistical block copolymers with SPE and ZPE

The studies continued by adding P(SPE-*co*-ZPE) copolymers onto the mPEG block. As for the previous block copolymers, the macroinitiator approach was used to make such block copolymers via ATRP. Monomers SPE and ZPE were added to the reaction mixture, to react with the macroinitiator, mPEG-Br. Thus, block copolymers containing a statistical copolymer of PSPE and PZPE as switchable block should be formed. The block copolymerization employing SPE and ZPE was carried out in a H₂O/MeOH mixture (3/2 v/v).

Two block copolymers with different monomer feed ratios of SPE and ZPE were prepared. The first had a higher amount of monomer SPE than ZPE in the monomer feed, while the other contained equal amounts of SPE and ZPE.

The analysis of the reaction products showed that both PSPE and PZPE were added onto the mPEG macroinitiator. This is shown in the ¹H-NMR spectra by the appearance of the peaks between 3 – 3.2 ppm and 4.2 – 4.4 ppm, which are characteristic for PSPE and PZPE, respectively (see **Chapter 4.4.1.2**), and of the peak at about 3.8 ppm, which is characteristic for mPEG (**Figure 4.23**). In addition, the absence of olefinic peaks at 5.8 and 6.2 ppm indicated that after work up, the polymers are free of monomers. A mixture of macroinitiator (mPEG-Br), PSPE, and PZPE could not occur, since no other initiator besides the macroinitiator was used for these reactions. Thus, the block copolymerization was successful. However, it is not possible to distinguish whether all mPEG-Br was incorporated into block

copolymers, or if a mixture of mPEG-Br and mPEG-*b*-PSPE or mPEG-*b*-PZPE or mPEG-*b*-P(SPE-*co*-ZPE) block copolymers is present by looking at the NMR spectra. Nevertheless, the GPC data show a monomodal distribution (with a small shoulder), and the peak of the block copolymers is shifted compared to the peak of mPEG-Br. Thus, it is concluded that chain extension and purification from residual monomers had successfully occurred.

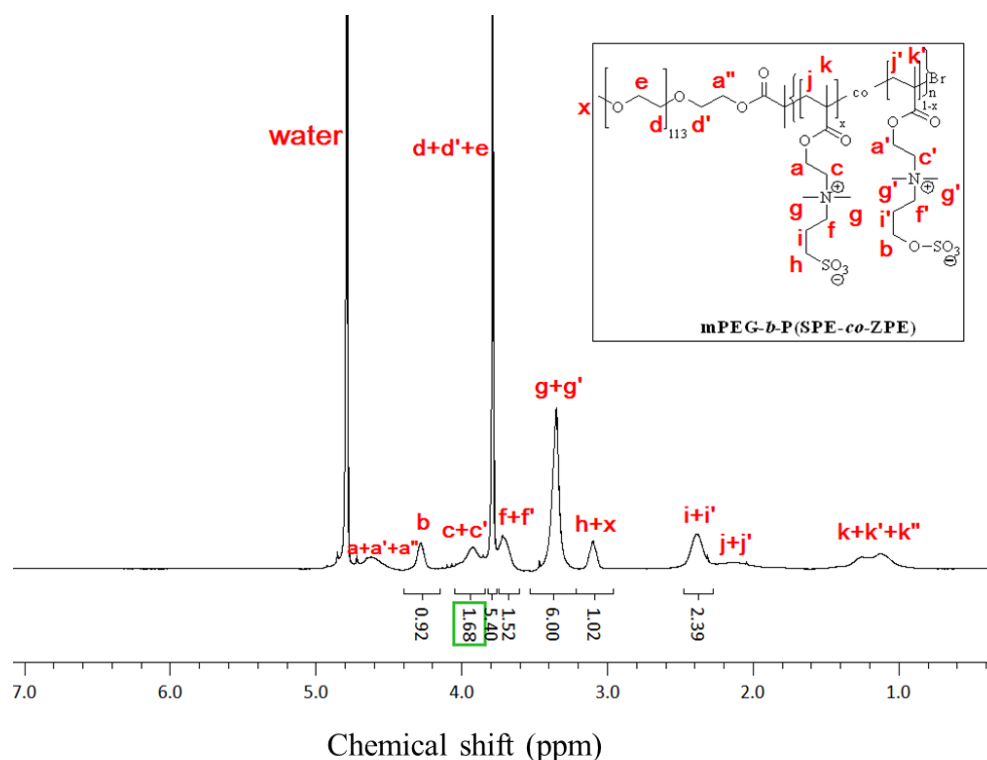


Figure 4.23. ^1H -NMR spectrum of mPEG-*b*-P(SPE-*co*-ZPE) block copolymer (**BC-18**) in D_2O with 0.5 M NaCl.

Table 4.12. Analytical data of the mPEG₁₁₄-*b*-P(SPE_{*x*}-*co*-ZPE_{*y*}) block copolymers made by ATRP using mPEG-Br as macroinitiator, CuBr/ bipyridyl as complex catalyst in $\text{H}_2\text{O}/\text{MeOH}$ (3/2 v/v) at r.t for 5 h.

Sample	ZPE feed [mol%]	Conv.	Yield [%]	SPE:ZPE ^b content in the copolymer	$M_{n(\text{theo})}$ ^c [g/mol]	$M_{n(\text{app})}$ ^d [g/mol]	PDI
BC-17 ^a	20	quantitative	84	0.82 : 0.18	28700	30000	1.8
BC-18 ^a	50	quantitative	90	0.52 : 0.48	30800	35000	2.5

^a Ratio of [M]:[I] was 100:1

^b Calculated from integration ratio peaks of **h** and **b**

^c Calculated from the yield and the feed composition, assuming that the incorporation ratio is the same as the feed ratio

^d Obtained from the GPC measurement using HFIP as eluent and PMMA as calibration standards

4. Poly(sulfobetaine)s and Poly(sulfobetaine) Based Copolymers

The results of $m\text{PEG}_{114}\text{-}b\text{-P}(\text{SPE}_x\text{-}co\text{-ZPE}_y)$ synthesis are summarized in **Table 4.12**. The polymerizations have high yields of more than 80%. As shown in the synthesis of $\text{P}(\text{SPE}\text{-}co\text{-ZPE})$, the copolymerization of SPE and ZPE proceeded well, which may be due to the similar reactivities of SPE and ZPE, that come from their closely similar chemical structures. Increasing molar masses indicate also that chain extension took place. The small difference between the calculated molar masses and the apparent molar masses from the GPC measurements might be due to the different calibration standards used for the GPC analysis (using PMMA as standards).

Nevertheless, both **BC-17** and **BC-18** had high polymer's dispersity indexes. This means, they had broad molar mass distributions. The GPC elugrams show that monomodal distributions with small shoulders were obtained. One plausible explanation for this phenomenon is the use of a $\text{H}_2\text{O}/\text{MeOH}$ mixture as reaction medium, which might interact partially with the catalyst and deactivate the catalyst [87].

We also note that, for the case of **BC-17** and **BC-18**, PDI rose with increasing amounts of PZPE. Although the data base is too small for allowing more than speculations, this might be caused by the property of PZPE being less water-soluble than PSPE, leading to the local solubility problem. Different hydrophilicities of mPEG and PZPE might cause that the initiation of monomer ZPE by mPEG-Br in the beginning was difficult. Since **BC-18** has the same amount of SPE and ZPE in the monomer feed, mPEG-Br might prefer to initiate SPE, which could solvate the mPEG-Br better than ZPE. This growing chain prefers to react further with SPE rather than ZPE, until it reaches certain length and the reaction accelerated with the addition of ZPE since now, the solubility properties of the SPE and ZPE is similar and amount of SPE in the monomer feed became less than ZPE. This might result in an unequal rate of initiation. This situation makes the reaction lose its control and increase PDI. Therefore, the more PZPE is in the system, the more uncontrolled reaction became. This could lead to broadened molar mass distributions with high PDI values. This explanation is supported by the results for sample **BC-16** ($m\text{PEG}_{113}\text{-}b\text{-PZPE}_n$), which showed a relatively high PDI value and rather low yield (only 64%).

4.4.2. Aqueous solution behavior

4.4.2.1. Homopolymer of ZPE

Table 4.13 gives information about phase transition temperature of PZPE homopolymers. Cloud points were determined by turbidimetry. Because PZPE is poorly water-soluble, the concentration was reduced to 3 g/L in these measurements. As can be seen, all three homopolymers did not dissolve in pure water in the entire temperature window investigated (from 20°C to 75°C). Accordingly, the intra- as well as interchains electrostatic interactions between the betaine groups were stronger than the polymer-water interactions. Although heating was applied to make them dissolve in pure water, they showed only swelling but did not dissolve completely.

Comparing the phase transition behavior in water of PZPE (**HP-5** in **Table 4.13**) with the one of PSPE (**HP-1** in **Table 4.3**) from samples, which were made under the same condition and have similar DP_n , it is obvious that PZPE is much less water-soluble than PSPE, although both polymers have a similar chemical structure. PSPE bearing ammoniosulfonate moieties is still soluble in pure water, especially at the high temperature. It seems that the sulfate group in PZPE is the key factor for their low solubility (**Figure 4.24**).

Table 4.13. UCST-type cloud point of 3 g/L aqueous solutions of PZPE homopolymers in H₂O and physiological saline. Temperature measurement between 20 - 75°C (cooling run). Concentration of sodium chloride in physiological saline is 9 g/L or 0.154 M.

Sample	Cloud Point	
	H ₂ O [°C]	Physiological saline [°C]
HP-4	insoluble	47
HP-5	insoluble	60
HP-6	insoluble	> 75

The phase transition behavior of PZPE was also studied in physiological saline solutions. In this case, all three PZPE samples could be dissolved. This means that the salting-in effect is also effective in PZPE. The presence of salt may shield the opposite charges and reduce the electrostatic attraction between the polymer chains, thus increasing the solubility of the polymers. As for PSPE, the cloud point of PZPE was of the UCST-type and increased with

increasing DP_n (**HP-4** < **HP-5** < **HP-6**). In fact, the solution of **HP-6** was turbid in the entire temperature range studied, indicating that the cloud point must be above 75°C.

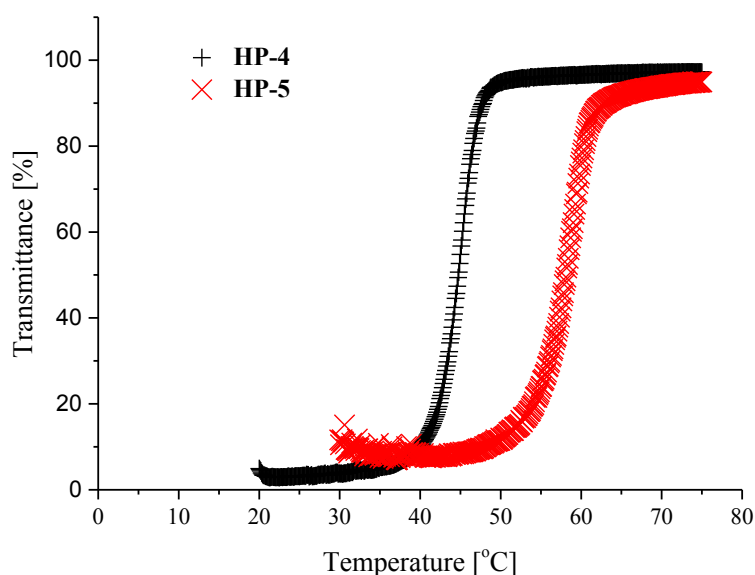


Figure 4.24. Temperature dependent turbidity (cooling run) of 3 g/L aqueous solutions of PZPE homopolymers in physiological saline.

The phase transition behavior of PZPE contrasts with the behavior of PSPE, as PSPE experiences a phase transition in water, but not in physiological saline solution, even for similar DP_n , for instance when comparing **HP-1** and **HP-5**. Despite the fact that they have similar chemical structures and only differ in the anion groups, the effect of sulfonate and sulfate groups in PSPE and PZPE, respectively, on the solubility in aqueous solutions is very strong. This coincides with the work of Vasantha *et al*, which reported that the polysulfobetaines were insoluble in water and only soluble with the addition of salt [74, 76]. This behavior is also similar to the finding that the zwitterionic ammoniosulfate surfactants display higher upper critical temperatures than their ammoniosulfonate analogues with the same alkyl spacer of C3 between the positive and negative charges in their hydrophilic part [78, 113-114].

4.4.2.2. Statistical copolymers of SPE and ZPE

To study the phase transitions behavior of P(SPE-*co*-ZPE) copolymers, like previous turbidity measurements of PZPE polymers, sample solutions with a concentration of 3 g/L were prepared in pure water and physiological saline solution. The results are shown in **Table 4.14**. Cloud points are exhibited in both pure water and physiological saline. The phase transition behavior of P(SPE-*co*-ZPE) copolymers lies between the one of PSPE and PZPE homopolymers. Comparing the phase transition behaviors of **CP-4** and **HP-5** in pure water, which have similar values of DP_n of PZPE, it becomes clear that the presence of SPE units in the copolymer helped to dissolve them and shifted the cloud point to lower values. Compared to the PZPE homopolymer, **HP-5**, which was insoluble in pure water, the water-solubility of the copolymer increases. When adding a more water-soluble co-monomer, such as SPE, a phase transition is observed. Vice versa, the presence of ZPE units in the copolymers increases the cloud point in salt containing solution. In comparison to **HP-1** that was soluble in physiological saline solutions at all temperatures, **CP-3** e.g. still presents a cloud point. The cloud point of the P(SPE-*co*-ZPE) copolymers in pure water evolved as expected, increasing with decreasing SPE portion in the copolymers (phase transition of **CP-2** < **CP-3** < **CP-4**).

Table 4.14. UCST-type cloud point of 3 g/L aqueous solutions of P(SPE-*co*-ZPE)_n copolymers in H₂O and physiological saline. Temperature measurement between 5 - 75°C (cooling run). Concentration of sodium chloride in physiological saline is 9 g/L or 0.154 M.

Sample	Cloud Point	
	H ₂ O [°C]	Physiological saline [°C]
CP-2	20	soluble
CP-3	62	22
CP-4	70	42

Similar results were obtained for the cloud points of the P(SPE-*co*-ZPE) copolymers in physiological saline solutions. By reducing the more water-soluble monomer content, i.e. SPE, within the copolymers, the cloud point rose in the order of **CP-2** < **CP-3** < **CP-4**. Nevertheless, as observed for all the zwitterionic homopolymers, cloud points in physiological saline solutions were much lower than in pure water (**Table 4.14**). The marked salting-in effect seems to be a general phenomenon for polyzwitterions, because the ions of

the added low molar mass salts screen the electrostatic intragroup, intra- and interchain interactions of the P(SPE-*co*-ZPE) copolymers, thus weakening the electrostatic attractions, so that the copolymers are more easily dissolved, and consequently, the cloud points are lower in physiological saline than in pure water.

4.4.2.3. Block copolymers of ZPE

The phase transition behavior of **BC-16** in pure water and physiological saline was also studied. Samples with a concentration of 3 g/L were prepared and their turbidity was measured during cooling the solutions. The results are listed in **Table 4.15**. No phase transition was observed for **BC-16** in pure water. The polymers could be dispersed, but the solution remained turbid in the entire temperature range measured. This finding was not so surprising, since PZPE homopolymer (for instance, **HP-5** with similar DP_n of ZPE) already had a high phase transition temperature (60°C). Considering the phase transitions of mPEG₁₁₄-*b*-PSPE_n block copolymers, in which the incorporation of mPEG resulted in increasing cloud points, it might have been expected that **BC-16** would have a phase transition temperature higher than 60°C.

Table 4.15. Cloud point of 3 g/L aqueous solutions of **BC-16** in H₂O and physiological saline. Temperature measurement between 5 - 75°C (cooling run). Concentration of sodium chloride in physiological saline is 9 g/L or ~ 0.154 M.

Sample	Polymers	Cloud Point	
		H ₂ O [°C]	Physiological saline [°C]
BC-16	mPEG ₁₁₄ - <i>b</i> -PZPE ₅₈	> 75	12 (UCST) & 55 (LCST)

Interestingly, more than one phase transition was observed for **BC-16** in physiological saline solution. As shown on **Figure 4.25**, two types of phase transition behavior, i.e. UCST- and LCST-type, occurred, where the UCST-type cloud point was lower than the LCST-type one (**Table 4.15**). This was similar to the behavior of mPEG₁₁₃-*b*-PSBE_n block copolymers (**BC-14**) in pure water. As in the case of **BC-14**, PZPE is also a poorly water-soluble polymer, and as mentioned before, the mPEG block itself may show LCST-type phase transition

behavior, when attached to the second block. Therefore, it seems that the phase transition behavior of mPEG indeed contributes to the overall phase transition behavior of the block copolymers, which contained poorly water-soluble polymers in the other block, especially, when the length of PZPE blocks is shorter than of mPEG blocks. Nonetheless, as in the case for other zwitterionic polymers, a salting-in effect occurs for **BC-16**, so that added salt increases the solubility of the block copolymers. Presumably, the low molar mass ions screen the intra- and interpolymer electrostatic attraction between the zwitterionic groups, enabling the polymer-water interactions to dissolve the block copolymers easily.

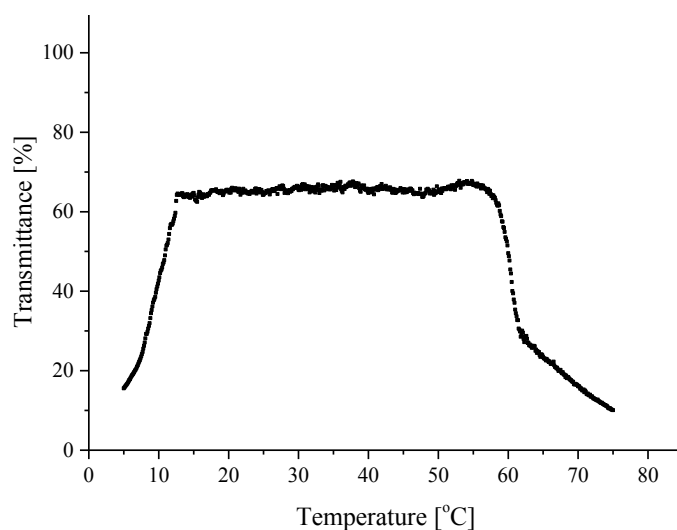


Figure 4.25. Temperature dependent turbidity (cooling run) of 3 g/L aqueous solutions of **BC-16** in physiological saline solution (9 g/L NaCl).

4.4.2.4. Statistical block copolymers with SPE and ZPE

To study the phase transition behavior of **BC-17** and **BC-18**, sample solutions with concentration of 3 g/L in pure water and physiological saline were prepared. The phase transition behavior was followed by turbidity measurements and the results are summarized in **Table 4.16**. It was assumed that block copolymers with well-defined phase transition temperature in physiological saline solution could be prepared, and these block copolymers could be useful for controlled release of model compound.

The cloud point of mPEG₁₁₄-*b*-P(SPE_{*x*}-*co*-ZPE_{*y*}) block copolymers increased with increasing ZPE content in the polyzwitterions blocks. While in pure water, **BC-17** displayed a cloud point of 43°C, **BC-18** that has a higher ZPE content was turbid in the entire temperature range measured, meaning that the cloud point was above 70°C. These results match very well with

4. Poly(sulfobetaine)s and Poly(sulfobetaine) Based Copolymers

the results for the simple statistical copolymers P(SPE-*co*-ZPE)_n (**Table 4.14**). The more ZPE is incorporated in the copolymers, the higher the cloud point will be. Moreover, comparing the transition temperatures of P(SPE-*co*-ZPE)_n and of their analogous block copolymers, it can be seen that the presence of mPEG increased the cloud points, just as found for mPEG₁₁₄-*b*-PSPE_n block copolymers in comparison to the PSPE homopolymers (**Table 4.4**). It is supposed that the permanently hydrophilic block mPEG interacts with the zwitterionic block, enhancing the overall interchain attraction, and stabilizes the micelles.

Table 4.16. UCST-type cloud point of 3 g/L aqueous solutions of mPEG₁₁₄-*b*-P(SPE_x-*co*-ZPE_y) block copolymers in H₂O and physiological saline. Concentration of sodium chloride in physiological saline is 9 g/L or 0.154 M. Temperature measurement between 10 - 75°C (cooling run).

Sample	Polymers	Cloud Point	
		H ₂ O [°C]	Physiological saline [°C]
BC-17	mPEG ₁₁₄ - <i>b</i> -P(SPE ₅₄ - <i>co</i> -ZPE ₁₂)	43	< 10
BC-18	mPEG ₁₁₄ - <i>b</i> -P(SPE ₄₃ - <i>co</i> -ZPE ₃₉)	> 70	45

Importantly, for mPEG₁₁₄-*b*-P(SPE_x-*co*-ZPE_y) block copolymers UCST-type phase transition behavior was also observed in physiological saline solution, but no indication for an additional LCST type transition. Similar to the situation in pure water, the cloud points of the block copolymers rose with increasing ZPE content in the zwitterionic blocks. The cloud point of **BC-17** could not be determined since it appeared below the temperature window measured. The lower cloud points in physiological saline, shows that the salting-in effect happened also for the mPEG₁₁₄-*b*-P(SPE_x-*co*-ZPE_y) block copolymers. Still, by adapting the ZPE content, an UCST-type phase transition can be implemented despite the marked salting-in effect, and enables a cloud point under physiologically relevant conditions. Thus, the cloud point of **BC-18** was in the targeted range that seems useful e.g. for drug delivery applications.

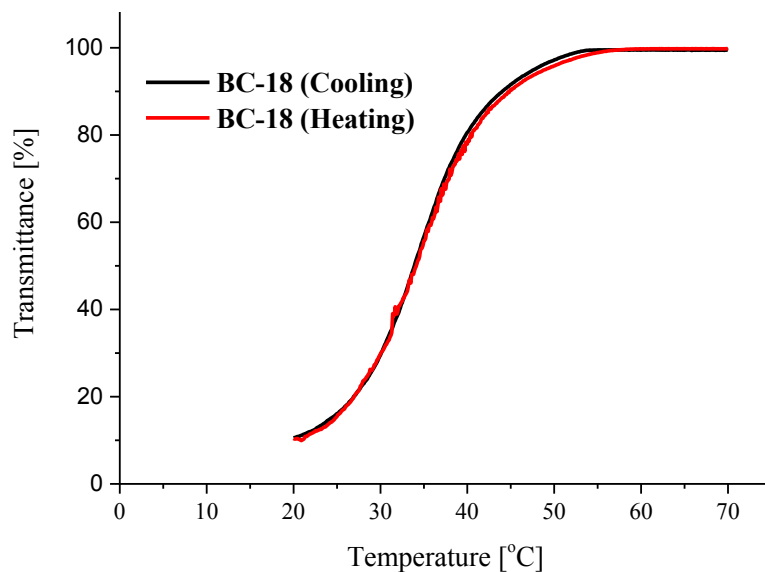


Figure 4.26. Temperature dependent turbidity (cooling and heating run) of 3 g/L aqueous solutions of **BC-18** in physiological saline.

The investigation of the phase transition behavior of **BC-18** was continued to learn whether a hysteresis appeared between cooling and heating curves. As can be seen in **Figure 4.26**, both cooling and heating curves almost overlapped, so that no hysteresis occurs. This result is a good indication that the polymers were trapped not in a metastable state and that phase separation may occur spontaneously.

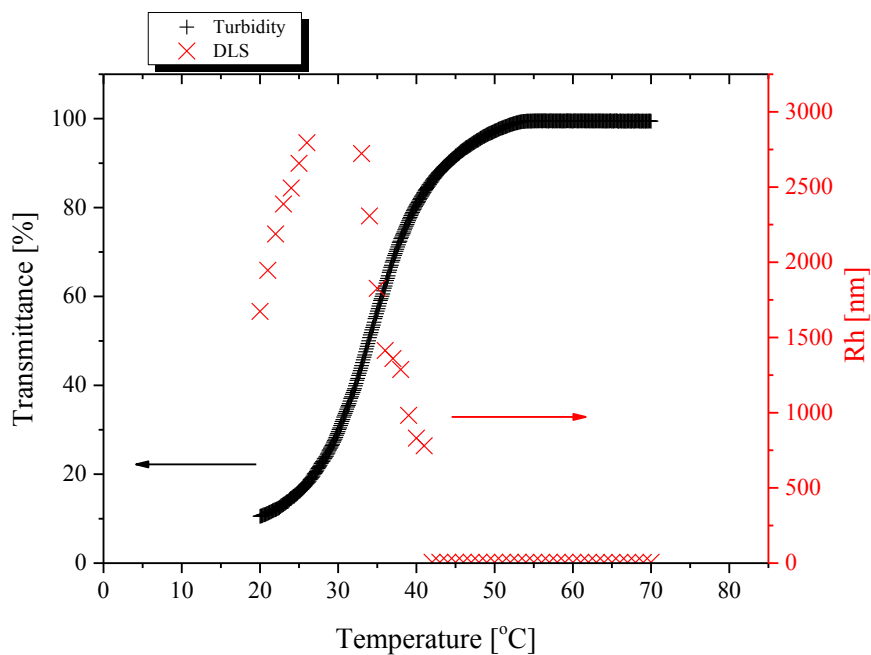


Figure 4.27. Turbidity and DLS measurements (cooling runs) of 3 g/L solutions of **BC-18** in physiological saline.

In order to confirm the cloud point of **BC-18**, dynamic light scattering measurements were performed. **Figure 4.27** tells that phase separation occurred, which is indicated by the formation of aggregates during the cooling. The hydrodynamic radius obtained at high temperature was about 5 nm, suggesting that block copolymers were dissolved individually in the coil conformation. Meanwhile, at low temperature, micellization and aggregation of the micelles occurred, which was indicated by large hydrodynamic radius of about 2500 nm. The cloud point from the DLS measurements was 41°C, which is slightly lower than the value obtained by turbidimetry.

5. Solubilization Studies of Solvatochromic Dyes as Model Active Agents by Block Copolymer BC-18

This chapter describes exploratory studies of the temperature-controlled release of active agents from polymeric micelles upon passing through the UCST-transition. The active agent was expected to be incorporated in the core of micelles when the core-forming block is collapsed at low temperature ($T < T_{cp}$), while the loaded active agent was expected to be released at high temperature ($T > T_{cp}$), at which the micellar core expands and becomes more hydrophilic to form unimers (**Figure 5.1**).

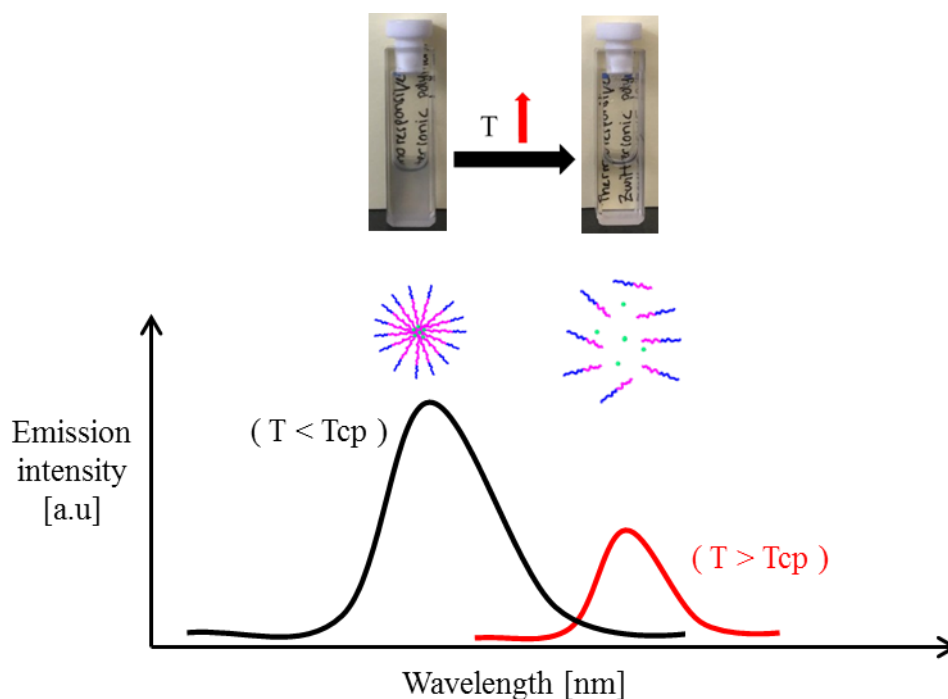


Figure 5.1. Illustration of the temperature-triggered release of active agents from a thermoresponsive polymeric micelle, followed by fluorescence spectroscopy using solvatochromic model cargos.

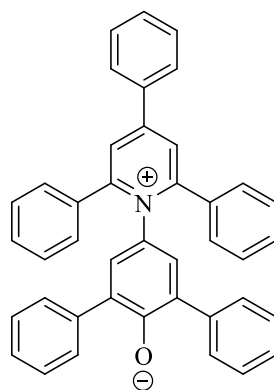
The thermoresponsive block copolymer **BC-18** was chosen for this purpose since it has a UCST-type cloud point of 45°C in physiological saline, which is in the physiological relevant temperature range. Several fluorescent dyes were chosen as model active agents which mimic drugs, to explore whether the localization of these dyes might be detected using absorbance or fluorescence spectroscopy. For that, dyes with different hydrophobicity and charged groups

were investigated, in order to study, which dyes are capable to be encapsulated inside the micelles at low, and to be released at high temperature. Moreover, solvatochromic dyes were used to study the encapsulation and release of the dyes, by following the shift of the emission wavelength at low and high temperature.

This type of studies was necessary because there is little information about the ability of polyzwitterions to incorporate organic materials. There are only a few studies, in which the idea of solubilization organic compound into polyzwitterions, has been described [28, 115]. Some studies have mentioned that non-charged compounds could not be solubilized by poly(sulfobetaine)s [28, 116]. Although it is not obvious, to which extent the solubilization can work, typically, it has been suggested that to achieve incorporation into polyzwitterions, such as polybetaines block copolymers, charged solubilizates are advantageous to make strong interactions [115]. Moreover, the study about solubilization of polysoap reported by Anton and Laschewsky indicates that it is not obvious, whether the solubilization was successful because of the charges in the active agents or it was due to some additional hydrophobic moieties within the polymers [115]. However, it is noteworthy that complementary ionic interactions are helpful. That is why the studies were focused mostly on charged dyes as model active agents.

5.1. Reichardt's dye

The first dye used as for solubilization experiments is Reichardt's dye. It is a well-known strong solvatochromic dye from the class of merocyanines and very hydrophobic. The chemical structure of Reichardt's dye is shown in **Figure 5.2**.



**Reichardt's Dye
(Dye 1)**

Figure 5.2. Chemical structure of Reichardt's dye.

Typically, absorbance and emission fluorescence and can be used to detect solvatochromism. While experience shows that solvatochromism is very sensitive and often more pronounced when using fluorescence emission, the solvatochromic effect of the non-fluorescent Reichardt's dye is followed by absorbance. Therefore, for this experiment, UV-Vis spectroscopy was used.

As explained before, the idea is to observe the difference of λ_{\max} absorbance between Reichardt's dye alone and solubilized by **BC-18** in physiological saline. Samples were prepared by dissolving separately the dye and **BC-18** in physiological saline by heating. After that, these two solutions were mixed, cooled to room temperature, and stirred for about 18 h. Then, the mixture was centrifuged and decanted to separate the undissolved dye, and the absorbance spectra were recorded. As reference, a solution with Reichardt's dye alone in physiological saline was prepared in the identical way.

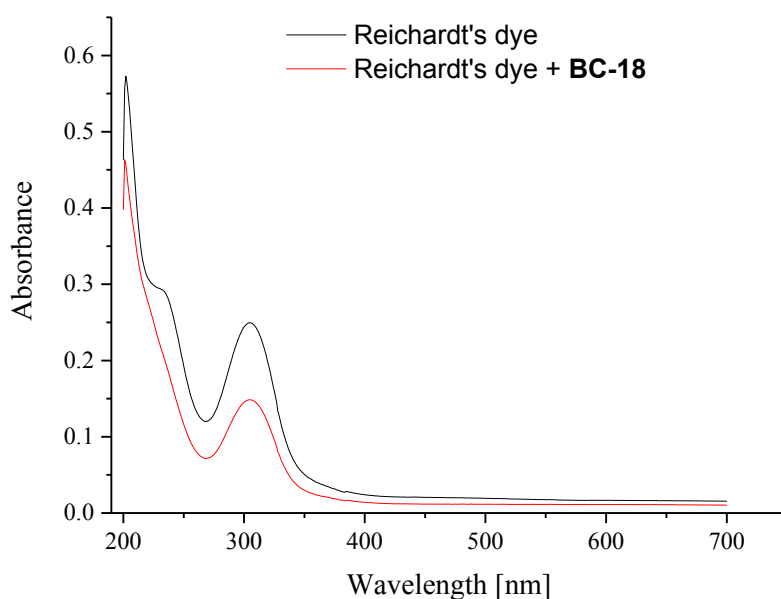


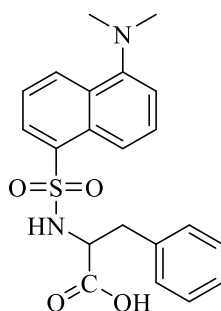
Figure 5.3. Absorbance spectrum of Reichardt's dye and **BC-18** loaded Reichardt's dye in physiological saline at room temperature.

The result of the solubilization experiments is shown in **Figure 5.3**. No shift of the wavelength occurred between samples containing Reichardt's dye alone and in the presence of **BC-18**, since both samples give λ_{\max} absorbance of about 305 nm. This indicates that there was no dye uptake by the polymer, which might be due to the high hydrophobicity of Reichardt's dye. Because of this finding, it was reasoned to continue the solubilization studies with fluorescent dyes which bear charges and are more polar, as thus, the uptake of the dyes

by the polybetaine block might be improved. In addition, fluorescence dyes may show a more pronounced solvatochromism to be followed via fluorescence emission than via absorbance.

5.2. Dansyl L-phenylalanine

The second dye explored is dansyl L-phenylalanine (**Figure 5.4**). The dansyl group is an effective fluorophore and known to be sensitive to the polarity of the medium, in particular to hydrophobic-hydrophilic changes of the environment [117-118].



Dansyl L-phenylalanine (Dye 2)

Figure 5.4. Chemical structure of dansyl L-phenylalanine.

At first, solvatochromism studies were done in several alcohols of decreasing polarity as the solvent, i.e., in methanol, ethanol, propanol, and butanol. Dansyl L-phenylalanine solutions were prepared by dissolving it in the alcohols and also in PBS with a defined concentration, and their fluorescence spectra were recorded. Yellowish solutions were obtained for the dansyl L-phenylalanine.

Figure 5.5 displays the fluorescence spectra of dansyl L-phenylalanine in the homologous series of alcohols and also in PBS (aqueous solution). The $\lambda_{\max}^{\text{emission}}$ shifted to shorter wavelengths (hypsochromic shift) as the solvent became less polar. It is also noted that the less polar the solvent is, the higher the fluorescent intensity of the dansyl L-phenylalanine becomes. It seems that the hydrophobic part of dansyl L-phenylalanine plays the main role in the solubilization. When PBS was used as the solvent for dansyl L-phenylalanine, the fluorescence intensity is much weaker than in the alcohols, although a fluorescence spectrum was still obtained.

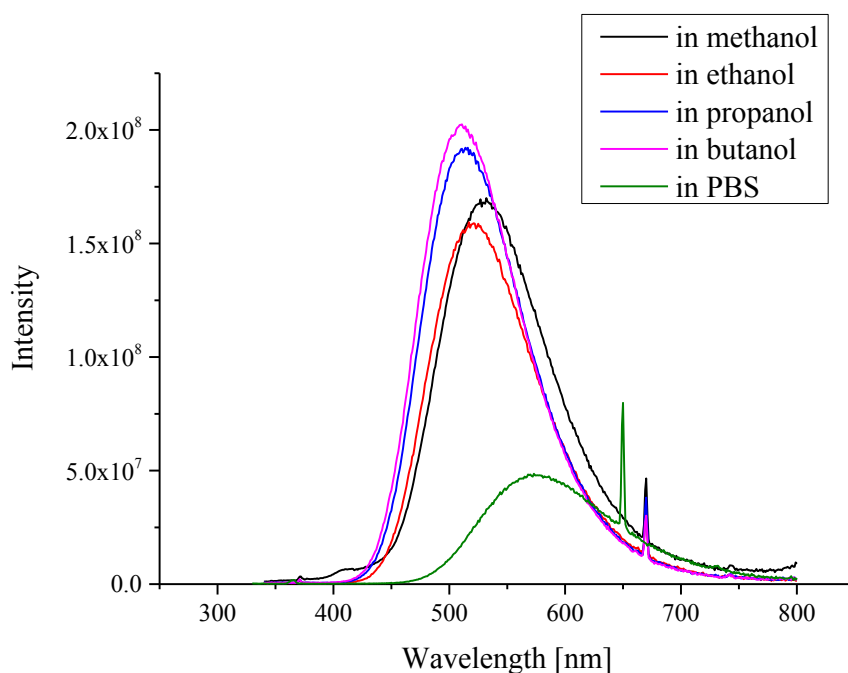


Figure 5.5. Fluorescence spectra of dansyl L-phenylalanine in a homologous series of alcohols and PBS.

In comparison, the fluorescence of dansyl L-phenylalanine in other aqueous solutions, i.e. in pure water and physiological saline, was also studied. As shown in **Figure 5.6**, all three samples exhibit the same $\lambda_{\max}^{\text{emission}}$ of 575 nm. However, the fluorescence intensity of dansyl L-phenylalanine is the highest in PBS solution, while physiological saline gives the lowest intensity. Since the presence of dansyl L-phenylalanine still can be detected in physiological saline, the next step was to explore the possibility to encapsulate and release dansyl L-phenylalanine in/ from block copolymer **BC-18** in physiological saline using the temperature-triggered mechanism.

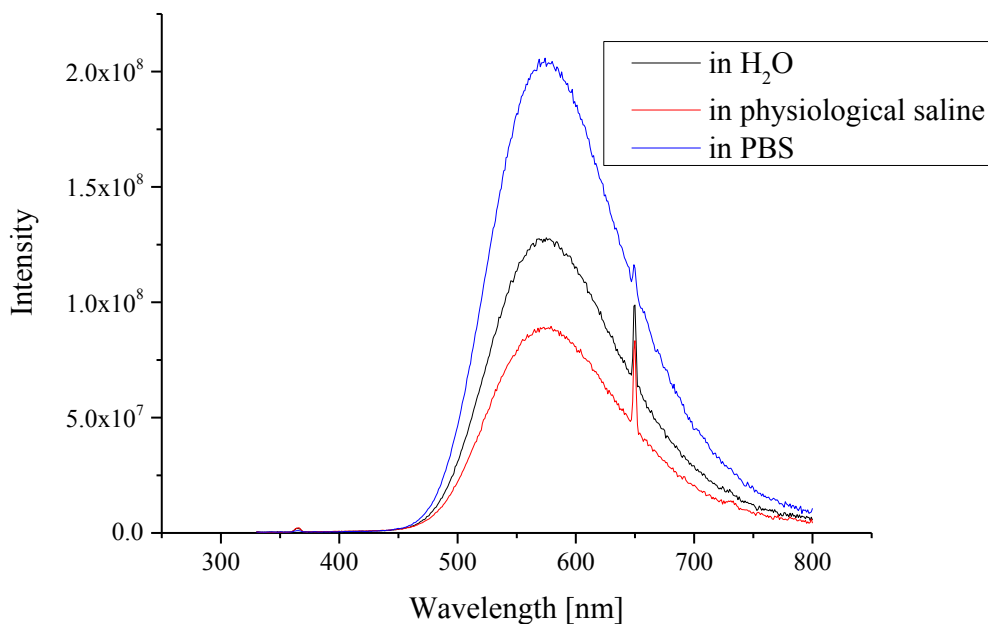


Figure 5.6. Fluorescence spectra of dansyl L-phenylalanine in aqueous solutions.

Samples were prepared by dissolving dansyl L-phenylalanine and **BC-18** in physiological saline with the help of heating. These two solutions were mixed, cooled, and stirred for about 18 h. Then, the mixture was centrifuged and decanted to separate the undissolved dansyl L-phenylalanine. The fluorescence spectrum of the supernatant was recorded at low (25°C) and at high (70°C) temperature, which corresponds to the loaded and released state, respectively. As reference, samples of **BC-18** with dansyl L-phenylalanine in pure water, and of dansyl L-phenylalanine only in physiological saline were also studied.

Figure 5.7 shows the fluorescence spectra of load and release experiments of dansyl L-phenylalanine with **BC-18**. No shift of the $\lambda_{\max}^{\text{emission}}$ could be detected for any of the samples at low and high temperature, except for the one in the pure water at 70°C, which shifted about 5 nm to the shorter wavelength. However, from **Figure 5.5**, it is noted that the shift to the shorter wavelength is indicative for a more hydrophobic environment. Therefore, it is most probable that the dansyl was not released at the higher temperature, but more tightly bound to **BC-18**, also considering that the cloud point of **BC-18** in pure water is still higher than 70°C.

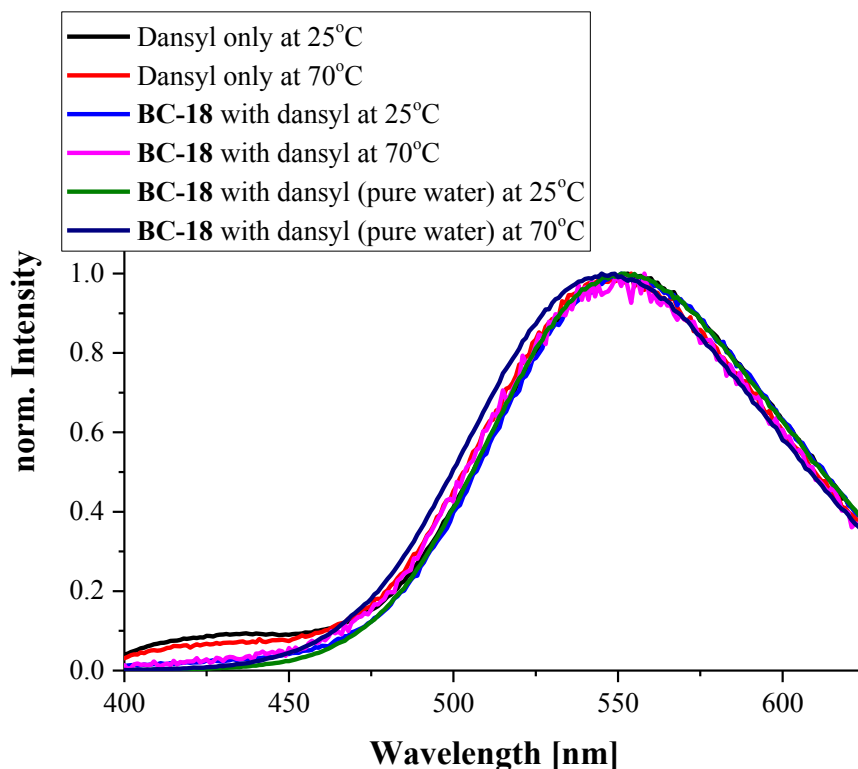


Figure 5.7. Fluorescence spectra of temperature-triggered release experiments of **BC-18** loaded with dansyl L-phenylalanine at 25°C and 70° in physiological saline and pure water.

5.3. Cyanine dyes

Since the loading and release experiment of dansyl L-phenylalanine with **BC-18** was not successful, several other ionic dyes were also investigated. The purpose was to understand more about the possibility of dyes to be encapsulated in the collapsed zwitterionic polymers, about which little information existed. Other dyes used for this experiment are cationic and zwitterionic hemicyanine dyes of increasing hydrophobicity, which show strong solvatochromism and have been studied not only in non-polar solvents, but also in polar solvents and micellar solutions [115, 119-125]. In addition, their solubilization by certain amphiphilic polymeric betaines has also been reported [115, 123]. Finally, a dye from the class of merocyanines, which was reported to exhibit a marked solvatochromic effect [126], was also used. The chemical structure of the dyes used in this experiment is given in **Figure 5.8**.

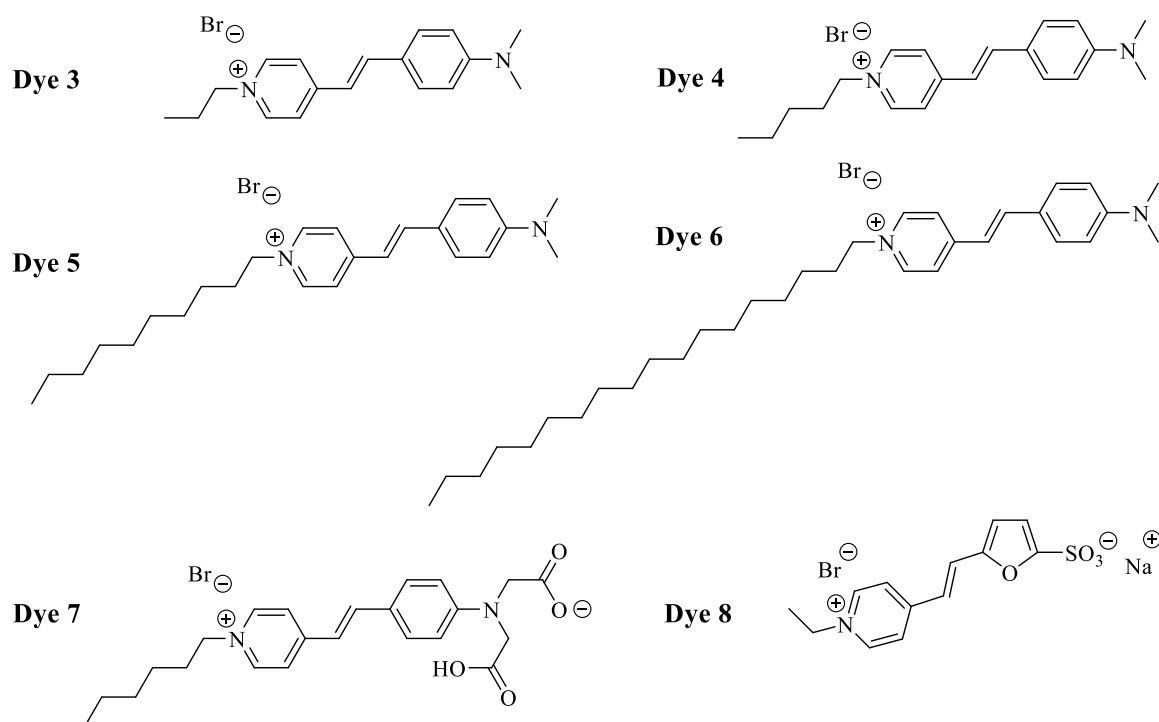


Figure 5.8. Chemical structure of the dyes used for solubilization experiments [121, 125].

Quick screening experiments were performed by investigating the difference of $\lambda_{\max}^{\text{emission}}$ between the dye alone and in the presence of **BC-18** in physiological saline. The purpose was to explore, which dye shows the highest solvatochromic effect and would be useful for release experiments. The preparation of the samples was similar to the one with dansyl L-phenylalanine. For the screening, the fluorescence spectra were recorded only at low temperature (22°C). The results of the screening are displayed in **Figure 5.9**.

As shown in **Figure 5.9**, no fluorescence spectrum could be recorded for very hydrophobic dye 6 since it could not be dissolved properly. **Figure 5.9** also tells that the only sample that shows a shift of $\lambda_{\max}^{\text{emission}}$ contains the ampholytic dye 7, which shifted about 10 nm to shorter wavelengths in the presence of **BC-18**. In addition, the intensity difference between free dye 7 and encapsulated dye 7 is large. Therefore dye 7 was chosen for the next step of loading and release experiments.

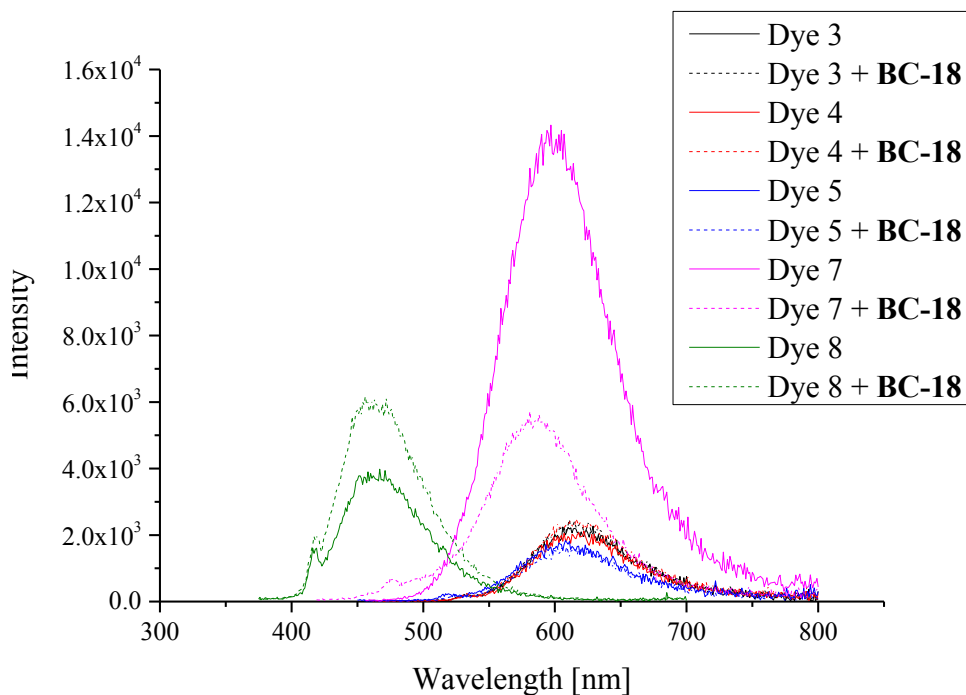


Figure 5.9. Fluorescence spectra of solubilization experiment of free dyes at 22°C and in the presence of **BC-18** in physiological saline.

Figure 5.10 shows the fluorescence spectra of **BC-18** mixed with dye 7 at low and high temperature, and dye 7 alone as the reference. Apparently, there is no shift of $\lambda_{\max}^{\text{emission}}$ between low and high temperature for dye 7 in the presence of **BC-18**. This suggests two possible scenarios: either the dye could not be encapsulated in the zwitterionic block, or the release mechanism of the on/ off micelles did not work as it was expected. The former one seems to be the most probable case, since most of the dyes used in this experiment did not show a shift of $\lambda_{\max}^{\text{emission}}$. This suggests a general difficulty of dye encapsulation that applies not only to hydrophobic dyes, as in the case of Reichardt's dye and dansyl L-phenylalanine, but also to polar charged dyes. Thus, it cannot be concluded whether the release mechanism via switching on/ off micelles upon increasing temperature may be realized as expected.

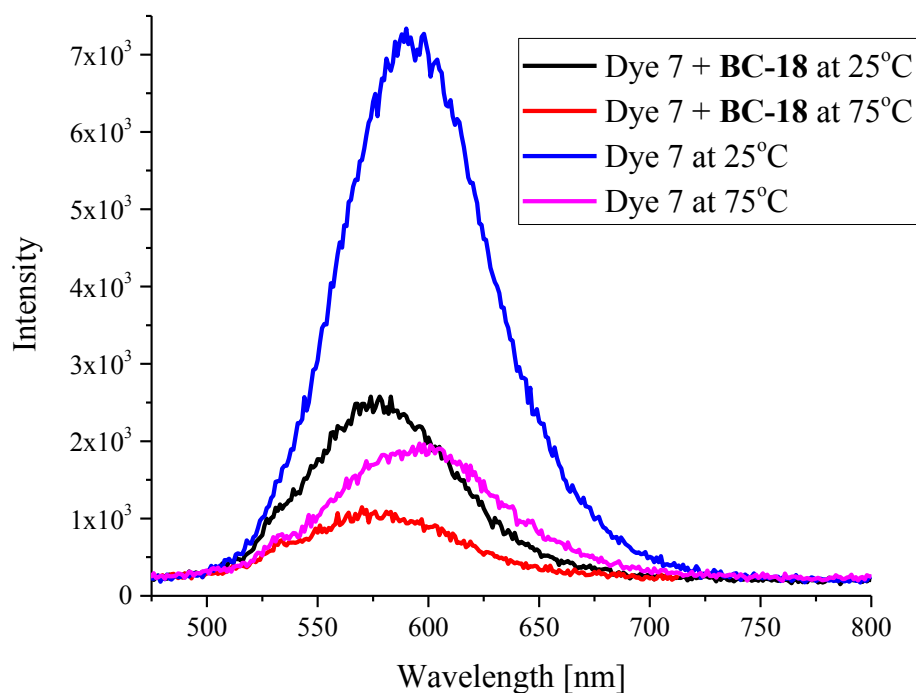


Figure 5.10. Fluorescence spectra of temperature-triggered experiment of **BC-18** loaded dyes 7 at 25°C and 70° in physiological saline.

Although the UCST-type transition as such works out, and even if the polybetaines switch correctly, their structure might be not good for the uptake and release of typical organic active agents. Therefore, when polybetaines are used as the switching block, particular systems need to be identified to allow the solubilization of active agents, before a temperature-triggered release mechanism can be implemented. It is important to make sure that the polybetaine block, in its collapsed state, is able to accommodate or favorably partition the active agents out of the aqueous into the micellar phase. Only after incorporation is obtained, the controlled release feature can be achieved. It is supposed that the present system did not work, because, as mentioned before, the polybetaines are very polar, whereas the active agents are much less polar.

Some suggestions to deal with this problem in the polybetaine systems are in the future to use inorganic active agents, in which the affinity between the polybetaines and the active agents might be high. Another plausible attempt is to add hydrophobic moieties in the switching polybetaine block [115], as synthesized in the case of $m\text{PEG}_{114}\text{-}b\text{-P}(\text{SPE}_x\text{-}b\text{-BzMA}_y)$. However, one has to pay attention to the synthesis method in order to have decent copolymerization, and that the hydrophobicity is not too high to make the polymers insoluble at all. Thus, an optimization of the reaction conditions seems crucial.

6. Conclusions

The aim of this work was to prepare biocompatible block copolymers exhibiting UCST-type phase behavior under physiologically relevant conditions, i.e. in physiological saline solution (9 g/L) within the physiologically interesting window of 30-50°C. Because polymers featuring UCST-type phase behavior in aqueous solution are exceptional, several series of homopolymers, simple copolymers, and block copolymers featuring UCST-type phase behavior were synthesized, and their phase transition behavior was investigated. The synthesis of block copolymers was achieved by atom transfer radical polymerization via a macroinitiator approach, in which mPEG (methoxy poly[ethylene glycol]) was used as the permanently hydrophilic block to stabilize the colloids formed, and thermoresponsive polymers as the second block to promote temperature-triggered assembly-disassembly of the micelles formed at low temperature, and eventually, controlled release.

The initial attempt of making such biocompatible block copolymers was based on PHEMA, which had been postulated to exhibit UCST-type phase behavior. Thus, a series of PHEMA-based block copolymers containing OEGMA₄₇₅ was prepared to tune the phase transition temperature, for which the PHEMA itself was reported to exhibit an UCST-type transition. It turned out that the block copolymers obtained exhibited an LCST-type transition, but no UCST-type one as claimed in the literature. Therefore, the studies were continued using poly(sulfobetaine)s, which had been known to show UCST-type transitions.

Further, the possibility of using such block copolymers as smart carriers for the controlled release of active agents was explored. Because for typical physiological conditions, stimulation may be achieved by an increase of temperature, for instance due to fever or inflammation, the use of UCST-based systems seems to be particularly relevant. In this scenario, the drug is released at elevated temperature, at which the responsive block forming the micellar core experiences a globule-to-coil transition upon heating.

Several series of poly(sulfobetaine)s-based (co)polymers were prepared, which indeed exhibited UCST-type phase behavior in aqueous solution. First, PSPE-based block copolymers of mPEG₁₁₄-*b*-PSPE_n were synthesized, resulting in UCST-type phase transitions only in water, but not in physiological saline. This corresponds to the well-known high

sensitivity of polyzwitterions phase transition to salt concentration. Consequently, statistical block copolymers containing a poorly water-soluble co-monomer, namely benzyl methacrylate, in the thermoresponsive block ($m\text{PEG}_{114}\text{-}b\text{-P}[\text{SPE}_x\text{-}b\text{-coM}_y]$) were also prepared in order to tune the phase transition temperature in aqueous phase, especially in physiological saline, expecting that the presence of poorly water-soluble may increase the phase transition temperature in physiological saline. In general, all (co)polymers had higher UCST-type cloud point with increasing degree of polymerization in pure water. An interesting observation was that the block copolymers containing benzyl methacrylate as co-monomer, $m\text{PEG}_{114}\text{-}b\text{-P}(\text{SPE}_x\text{-}b\text{-BzMA}_y)$, exhibits apparently two UCST-type cloud points. The major transition was affected by the increasing of benzyl methacrylate content in the polysulfobetaine block, while the minor one stayed in similar range of cloud point of about 40°C. This is possibly due to the gradient structure that $m\text{PEG}_{114}\text{-}b\text{-P}(\text{SPE}_x\text{-}b\text{-BzMA}_y)$ might have, considering benzyl methacrylate was apparently more reactive in the copolymerization than SPE.

Because of the simple block of $m\text{PEG}_{114}\text{-}b\text{-PSPE}$ and statistical block copolymer of $m\text{PEG}_{114}\text{-}b\text{-P}(\text{SPE}_x\text{-}b\text{-BzMA}_y)$ did not exhibit a phase transition in physiological saline, another alternative of betaine monomer was introduced, namely SBE. This monomer has a longer alkyl spacer between the ammonium and sulfonate groups (C4 instead of C3). Its homopolymer is known to show UCST-type phase transition at higher temperatures than PSPE. Thus, it was explored whether its block copolymer could exhibit phase transition in physiological saline. While the interesting phenomenon occurred for its block copolymer, that two types of phase behavior (UCST- and LCST-type) were observed for block copolymer of $m\text{PEG}_{114}\text{-}b\text{-PSBE}_{70}$ in pure water, the UCST-type transition vanished in physiological saline.

As described, no UCST-type phase transition was observed for poly(sulfobetaine)s-based (co)polymers in physiological saline. Thus, another system with sulfobetaine monomer (ZPE), which is difficult to dissolve in pure water, but a priori better soluble at high salinity, was investigated. Although it differs only by the sulfate group (instead of sulfonate group in PSPE), PZPE has indeed a very low water solubility. Because homopolymer PSPE did not show a phase transition in physiological saline, but homopolymer PZPE did, the copolymerization of both monomers was also undertaken. The incorporation of monomer ZPE could enable the presence of a phase transition in physiological saline. In addition, as the statistical block copolymer was synthesized, it seems that unlike copolymerizing SPE with BzMA, copolymerization of two betaines with a similar chemical structure did not cause a

problem. Indeed, both the simple copolymers of $P(\text{SPE-co-ZPE})_n$ and the block copolymers of $m\text{PEG}_{114}\text{-}b\text{-}P(\text{SPE}_x\text{-}b\text{-}\text{ZPE}_y)$ exhibit UCST-type phase transition in pure water and also in physiological saline, in which the cloud points increased with increasing ZPE content in the copolymers. In fact, statistical block copolymers could be prepared that feature a UCST-type cloud point in the interesting temperature range of 45°C , and showed no hysteresis between heating and cooling curves. This result was corroborated by DLS measurements, demonstrating induced aggregation/ disassembly at the cloud point. The best behaving statistical block copolymer was then used for explorative solubilization and release experiments.

Showing a phase transition under physiological interesting conditions, i.e. physiological saline solution (9 g/L) within the physiologically interesting window of $30\text{-}50^\circ\text{C}$, the block copolymer $m\text{PEG}_{114}\text{-}b\text{-}P(\text{SPE}_{43}\text{-}co\text{-}\text{ZPE}_{39})$ seemed well-suited to establish such “smart” carriers. Several solvatochromic dyes were used as model active agents to be encapsulated for the solubilization-and-release studies. The dyes were chosen with respect to their hydrophobicity and charges. It seems, however, that the polybetaines have only a low affinity to dyes, since no difference of $\lambda_{\text{max}}^{\text{emission}}$ could be observed between the dye in the presence and in the absence of the thermoresponsive polymer. The only dye for which a spectral shift was observed, was the ampholytic Dye 7. However, when the release experiment was performed at high temperature, the $\lambda_{\text{max}}^{\text{emission}}$ stayed at the same wavelength as at low temperature. It looks like when using polyzwitterions, such as poly(sulfobetaine)s, as the switching block, particular systems need to be identified, to enable the solubilization of active agents, before such block copolymer can work with a triggered release mechanism. Therefore, in the future, it seems interesting to incorporate additional hydrophobic moieties into the switching block; this will require optimization work to get well-defined copolymer compositions on the one hand, and to achieve an UCST-type switch at physiological relevant condition on the other hand. This could be done either by making the backbone more hydrophobic or by copolymerizing hydrophobic co-monomers. In addition, it might be interesting also to explore whether inorganic active agents might bind stronger to polyzwitterions, and thus, might allow their uptake by the polyzwitterions.

7. Experimental Part

7.1. Materials

Table 7.1. Chemicals used in the experiments.

Chemical	formula	CAS	purity	supplier
L-ascorbic acid 6-palmitate	C ₂₂ H ₃₈ O ₇	137-66-6	95 %	Alfa Aesar
acetonitrile	C ₂ H ₃ N	75-05-8	99.8 %	Aldrich
benzyl methacrylate	C ₁₁ H ₁₂ O ₂	2495-37-6	96 % ^a	Sigma- Aldrich
2,2'-bipyridyl	C ₁₀ H ₈ N ₂	366-18-7	-	Fluka
α- bromo isobutyryl bromide	C ₄ H ₆ Br ₂	20769-85-1	98 %	Acros
1,4-butane sultone	C ₄ H ₈ O ₃ S	1633-83-6	99+ %	Acros
chloroform-d	CDCl ₃	865-49-6	99.8atom%D	Armar
copper bromide	CuBr	7787-70-4	- ^b	Sigma- Aldrich
dansyl-L-phenylalanine	C ₂₁ H ₂₂ N ₂ O ₄ S	1104-36-5	98 %	TCI
deuterium oxide	D ₂ O	7789-20-2	99.9atom%D	VWR
dichloromethane	CH ₂ Cl ₂	75-09-2	99.8 %	J. T. Baker
diethyl ether	C ₄ H ₁₀ O	60-29-7	99.8 %	ChemSolute
2-(dimethylamino)ethyl methacrylate	C ₈ H ₁₅ NO ₂	2867-47-2	98 % ^c	Aldrich
ethanol	C ₂ H ₆ O	64-17-5	99.5 %	ChemSolute
ethyl α- bromo isobutyrate	C ₆ H ₁₁ BrO ₂	600-00-0	98 %	Fluka
hexafluoroisopropanol (HFIP)	C ₃ H ₂ F ₆ O	920-66-1	99 %	ABCR
hexamethyltriethylenetetramine (HMTETA)	C ₁₂ H ₃₀ N ₄	3083-10-1	97 %	Sigma- Aldrich
2- hydroxyethyl methacrylate	C ₆ H ₁₀ O ₃	868-77-9	96 % ^d	Acros
magnesium sulfate	MgSO ₄	7487-88-9	99.5 %	Alfa Aesar
3-((2-(methacryloyloxy)- ethyl)dimethylammonio)- propane-1-sulfonate (SPE)	C ₁₁ H ₂₁ NO ₅ S	3637-26-1	97 %	Sigma- Aldrich
methanol	CH ₄ O	67-56-1	99.5 %	Avantor

Chemical	formula	CAS	purity	supplier
oligo(ethylene glycol)	C ₅ H ₈ O ₂ -	26915-72-0	- ^e	Sigma-
methylether methacrylate (M _n = 475 g/mol) (OEGMA ₄₇₅)	(C ₂ H ₄ O) _n			Aldrich
molecular sieve 3 Å	-	-	-	Roth
pentamethyldiethylenetriamine (PMDETA)	C ₉ H ₂₃ N ₃	3030-47-5	99%	Sigma- Aldrich
phosphate buffered saline (PBS)	-	P4417	- ^f	Aldrich
poly(ethylene glycol) monomethyl ether (M _n = 5000 g/mol) (mPEG-OH)	-	9004-74-4	- ^g	Fluka
Reichardt's dye	C ₄₁ H ₂₉ NO	10081-39-7	90 %	Sigma- Aldrich
sodium chloride	NaCl	7647-14-5	99 %	ChemSolute
toluene	C ₇ H ₈	108-88-3	99.8 %	Merck
triethylamine	C ₆ H ₁₅ N	121-44-8	99 %	Acros
trifluoroethanol (TFE)	C ₂ H ₃ F ₃ O	75-89-8	99.8 %	Roth

^a contains 50-100 ppm MEHQ as inhibitor

^b LOT# K21X001

^c contains 2000 ppm MEHQ as inhibitor

^d contains 200-400 ppm MEHQ as inhibitor

^e contains 300 ppm BHT and 100 ppm MEHQ as inhibitor

^f LOT# BCBF6911

^g LOT# 1128575 31205058

Poly(ethylene glycol) methyl ether (mPEG-OH) was dried over toluene by azeotropic distillation prior to use. Typically, mPEG-OH was dissolved in toluene and distilled between 90-110°C under nitrogen to remove excess water.

Benzyl methacrylate was passed through a column filled with “inhibitor remover” from Aldrich (Batch# 08527BH) in order to remove inhibitors prior to use. Deionized water was provided and purified by a Millipore Milli-Q Plus water purification system (resistivity

18 M Ω ·cm⁻¹). Phosphate buffered saline (PBS) solution was prepared according to the instruction provided by Aldrich. Dialysis membrane from cellulose was provided from ZelluTrans/Roth by Carl Roth company with nominal cut-off MW 3500. The synthesis of Dye 3 – Dye 8 was described elsewhere. All other chemicals were used as received.

7.2. Methods and calculations

Proton nuclear magnetic resonance (¹H-NMR) spectroscopy

The apparatus Bruker Avance 300 MHz Spectrometer (Bruker, USA) was used. Samples were prepared by dissolving the product into a suitable deuterated solvent. The minimum sample concentration for ¹H-NMR was 0.01 mol/L.

Monomer conversions were determined via ¹H-NMR spectra of the crude mixtures at the end of polymerization and were counter-checked by the yields from weighing the isolated polymers. Theoretically expected number average molar masses $M_{n(theo)}$ are calculated according to equation 6.1.

$$M_{n(theo)} = \frac{[Monomer]_0 \cdot M_{Monomer}}{[Initiator]_0} \cdot conversion + M_{Initiator} \quad (6.1)$$

$[Monomer]_0$	= initial molar concentration of the monomer
$[Initiator]_0$	= initial molar concentration of the initiator
$M_{Monomer}$	= molar mass of the monomer repeat unit
$M_{Initiator}$	= molar mass of ATRP (macro)initiator

Turbidimetry

Cloud point measurements were performed using a Varian Cary 50 Scan UV-Vis spectrophotometer (Agilent, Germany) equipped with a thermoelectric Peltier element for temperature control. In a glass cuvette of 1 cm inner path length, a polymer solution with a defined concentration was prepared in Millipore water, in physiological saline, or in PBS. The transmittance of the sample was monitored at 500 nm as a function of temperature with a cooling rate of 1°C/min, and when needed, a heating rate of 1°C/min.

Dynamic light scattering (DLS)

Measurements of dynamic light scattering were done with an instrument High Performance Particle Sizer (HPPS-5001, Malvern Instrument, UK) using a He-Ne laser beam, and a thermoelectric Peltier element to control the temperature of the sample cell. The backscattering mode was used at a scattering angle of $\theta = 173^\circ$. Samples were prepared by diluting with Millipore water or in physiological saline to a defined concentration.

Gel permeation chromatography (GPC)

Gel permeation chromatography was performed to estimate the molar mass and the molar mass distribution of the polymers. According to the eluent, two types of GPC equipment were used. GPC with DMF as eluent (with addition of 0.1% LiBr, flow rate of 1 mL/min) uses a refractive index and UV detector (SEC-3010 from WGE Dr. Bures), PSS GRAMM gel as column. GPC measurements were calibrated with linear polystyrene standards with the molar masses range from 265 – 2,570,000 Da (PSS, Germany). The other equipment uses HFIP-gel, PL HFIP gel as column and 0.05 mol CF₃COONa in hexafluoroisopropanol (HFIP) as eluent, and a flow rate of 1 mL/min, and RI detector (SEC-3010, WGE Dr. Bures, $\lambda = 620$ nm). Narrowly distributed poly(methyl methacrylate) standards covering the range from 100 to 520,000 Da (PSS, Germany) were used for calibration. Calibration was always made prior to measurement as the columns are endangered by aging effects due to the aggressiveness of the eluent. This implies also that the individual uncalibrated elugrams cannot be directly compared, because the measurements were performed over an extended period of time.

Micro-differential scanning calorimetry (μ -DSC)

Micro-differential scanning calorimetry was carried out to investigate phenomena in phase transition. The measurement was performed using μ -DSC III (Setaram Instrumentation) in the temperature range between 0°C and 80°C in a closed steel cell. The heating-cooling cycle was repeated three times with heating rate at 1°C.

Ultraviolet-Visible (UV-Vis) spectroscopy

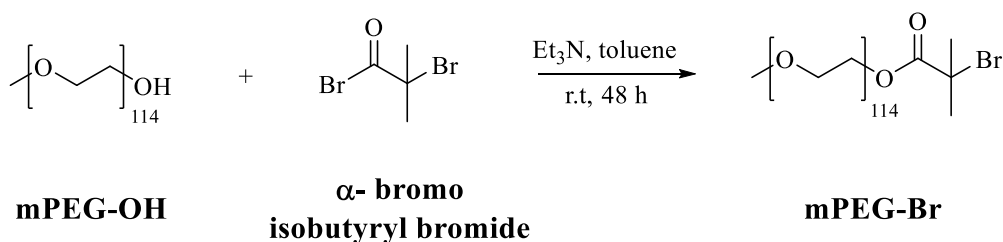
UV-Vis measurement was performed using Perkin Elmer UV/Vis/NIR Spectrometer Lambda 19 and absorption spectra were recorded. Quartz cuvettes with an optical path length of 1 cm were utilized.

Fluorescence spectroscopy

Fluorescence spectroscopy measurement was done using FLS920-stm fluorescence spectrometer (Edinburgh Instruments) and a FluoroMax-4 Horiba Jobin Yvon. Quartz cuvettes with an optical path length of 1 cm were used. Different excitation wavelength was used. FLS920-stm fluorescence spectrometer (Edinburgh Instruments) has the excitation and emission slits to 1 nm. The FluoroMax-4 apparatus has slit width of 2 nm and is equipped with a thermostated cell holder.

7.3. Synthesis of mPEG-Br initiator

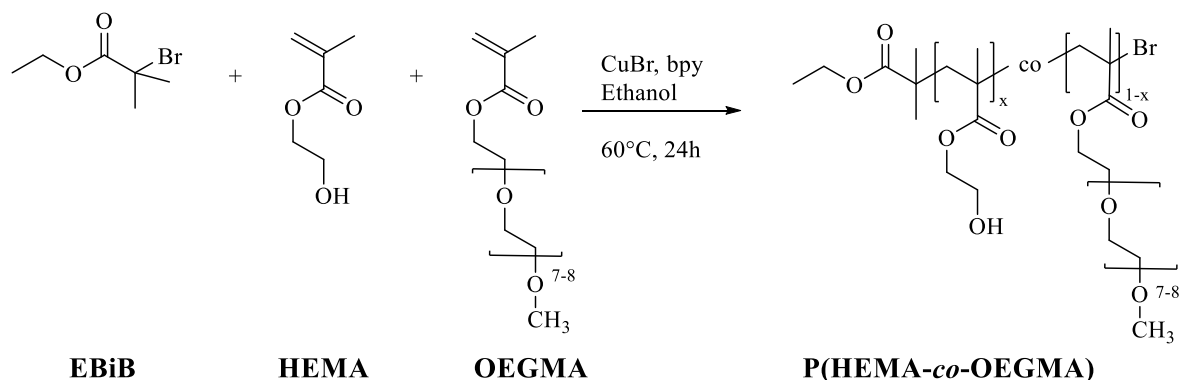
Synthesis of macroinitiator poly(ethylene glycol) mono methyl ether 2-bromoisobutyrate (mPEG-Br)



The synthesis of the mPEG-Br macroinitiator was adapted from the work of Ranger *et al* [86]. 10.0 g (2.00 mmol) of dried poly(ethylene glycol) methyl ether ($M_n = \sim 5000$ g/mol) were dissolved in 200 g of toluene in a three-neck flask equipped with a septum, and stirred with a magnetic stirrer. The solution was purged by nitrogen for 20 min to remove the oxygen inside. After that, 0.4 g (4 mmol) of triethylamine were added dropwise for 30 min. Then, still at room temperature, 0.912 g (4.00 mmol) of α -bromoisobutyryl bromide were added continuously dropwise over 1 h. The reaction was stirred at room temperature for 48 h. Next, the solution was extracted with water. The aqueous phase was re-extracted with 50 mL of dichloromethane three times. The organic phases were collected, washed with water of pH 5-7, dried with MgSO_4 , and filtered through a filter paper. The majority of the solvent was removed by evaporation until the crude extract was obtained. Finally, the crude extract was precipitated into diethyl ether. The white solid formed was isolated by filtration by filter paper, and dried in *vacuo* overnight. Yield: 50%, colorless hygroscopic solid. $^1\text{H-NMR}$ (δ , ppm, D_2O): 1.94 ppm (6H, $-\text{C}(\text{CH}_3)_2\text{Br}$), 3.48 ppm (3H, $-\text{O}-\text{CH}_3$), 3.5 - 4 ppm (4H, $-\text{CH}_2-\text{CH}_2-\text{O}-$), and 4.4 ppm (2H, $-\text{COOCH}_2-$).

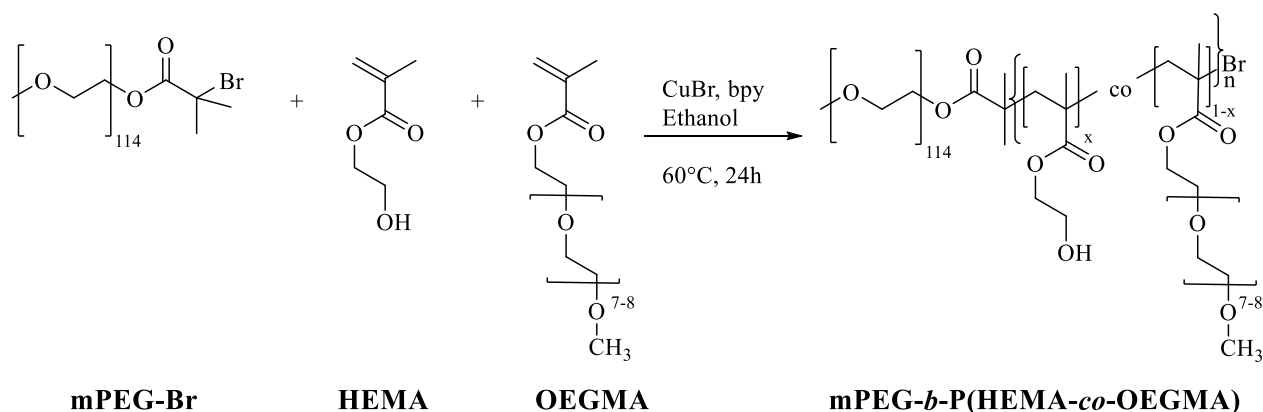
7.4. Synthesis of PHEMA based (co)polymers

7.4.1. Synthesis of non-ionic copolymers



In a 50 mL flask, 0.053 g (0.37 mmol) of copper (I) bromide, 0.115 g (0.740 mmol) of 2,2'-bipyridyl, 0.077 g (0.185 mmol) of L-ascorbic acid 6-palmitate, and 0.072 g (0.37 mmol) of EBiB were weighed, and dissolved in 6 mL of ethanol. Then, 4.574 g (35.15 mmol; 95 mol%) of HEMA and 0.878 g (1.85 mmol; 5 mol%) of OEGMA₄₇₅ were added into the flask and deoxygenated. The ratio of [monomer]₀: [initiator]₀: [catalyst]₀: [ligand]₀ was 100: 1: 1: 2. The mixture was stirred using a magnetic stirrer and bubbled with nitrogen for 30 min. After that, the flask was heated in an oil bath to 60°C for 24 h. After 24 h, the reaction was stopped by cooling and exposing the solution to the air. The purification was done by dialysis against distilled water for 5 d with a membrane with a nominal cut-off of MW 3500. Last, the mixture was lyophilized overnight to give solid polymer.

7.4.2. Synthesis of non-ionic block copolymers



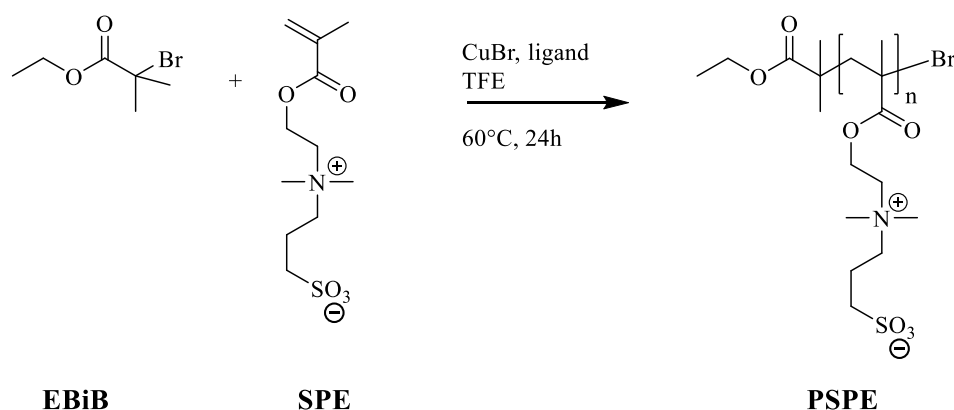
In a typical procedure, 10.6 mg (0.074 mmol) of copper (I) bromide, 23.2 mg (0.148 mmol) of 2,2'-bipyridyl, 15.4 mg (0.037 mmol) of L-ascorbic acid 6-palmitate (reducing agent), and 0.370 g (0.074 mmol) of mPEG-Br were weighed in a 25 mL flask, and dissolved in 6 mL of ethanol. Then, 0.915 g (7.03 mmol; 95 mol%) of HEMA and 0.176 g (0.370 mmol; 5 mol%) of OEGMA₄₇₅ were added into the flask, and the reaction mixture was deoxygenated by seven cycles of vacuum-flushing nitrogen. The ratio of [monomer]₀: [initiator]₀: [catalyst]₀: [ligand]₀ was 100: 1: 1: 2. The mixture was stirred by a magnetic stirrer and bubbled with nitrogen for 30 min. After that, the flask was heated in an oil bath to 60°C for 24 h. After 24 h the reaction was stopped by cooling and exposing the solution to the air. The purification was done by dialysis against distilled water for 5 d with a membrane with a nominal cut-off of MW 3500. Last, the mixture was lyophilized overnight to get solid polymers.

Table 7.2. Reaction recipes for HEMA-based block copolymerization (24 h, 60°C in 6 mL of ethanol using 2,2'-bipyridyl as ligand).

Sample	co-M	M:co-M	m _M [g]	m _{co-M} [g]	m _I [g]	m _{CuBr} [mg]	m _{Lig} [mg]	m _{Red} [mg]
BC-1	-	100:0	0.963	-	0.370	10.6	23.2	15.4
BC-2	OEGMA	98:2	0.944	0.070	0.370	10.6	23.2	15.4
BC-3	OEGMA	95:5	0.915	0.176	0.370	10.6	23.2	15.4
BC-4	OEGMA	85:15	0.819	0.527	0.370	10.6	23.2	15.4

7.5. Synthesis of sulfobetaine and sulfobetaine based (co)polymers

7.5.1. Synthesis of zwitterionic homopolymers

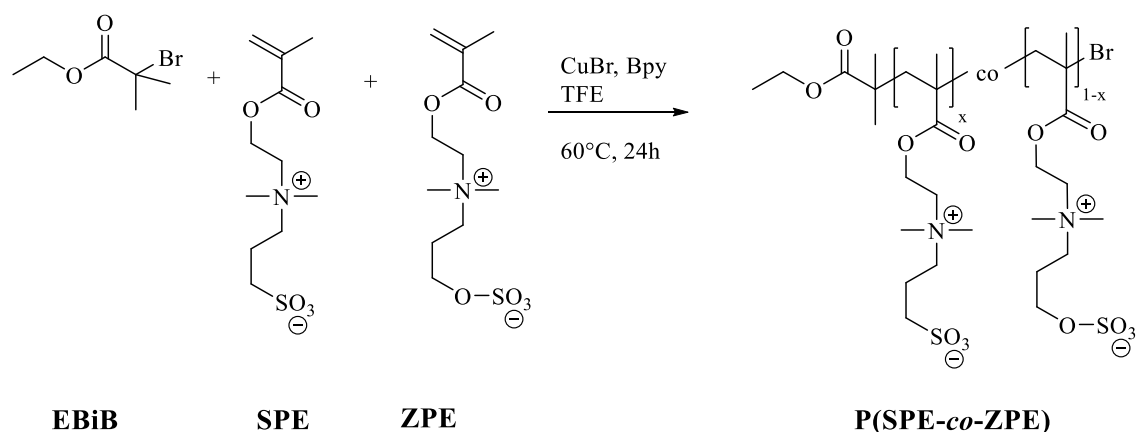


In a typical procedure, 2.067 g (7.400 mmol) of monomer SPE were weighed in a 50 mL Schlenk flask, dissolved in 6 mL of TFE under stirring, and deoxygenated by seven cycles of vacuum-flushing nitrogen. In a 25 mL Schlenk flask, 14.4 mg (0.074 mmol) of EBiB were diluted by 6 mL of TFE and degassed. In another 25 mL Schlenk flask, 10.6 mg (0.074 mmol) of copper (I) bromide, 23.2 mg (0.148 mmol) of 2,2'-bipyridyl, and 15.4 mg (0.037 mmol) of L-ascorbic acid 6-palmitate were weighed, dissolved in TFE, and deoxygenated. The diluted initiator was transferred into catalyst solution under stirring and protection by nitrogen. The initiator-catalyst solution was then transferred into the monomer solution under protection by nitrogen. The mixture was stirred by a magnetic stirrer, and bubbled with nitrogen for 30 min. After that, the flask was placed in an oil bath at 60°C for 24 h. After 24 h the reaction was stopped by cooling and exposing the solution to the air. The purification was done by dialysis against distilled water for 5 d with a membrane with a nominal cut-off of MW 3500. Finally, the mixture was lyophilized overnight to get solid polymers.

Table 7.3. Reaction recipes for homopolymerization of sulfobetaine (SPE) and sulfabetaine (ZPE) in TFE.

Sample	Monomer	Ligand	molar ratio M:I:CuBr:Lig	m_M	m_I	m_{CuBr}	m_{Lig}	m_{Red}
				[g]	[mg]	[mg]	[mg]	[mg]
HP-1	SPE	bpy	100:1:1:2	2.067	14.4	10.6	23.2	15.4
HP-2	SPE	PMDETA	100:1:1:2	2.067	14.4	10.6	25.7	15.4
HP-3	SPE	HMTETA	100:1:1:2	2.067	14.4	10.6	34.2	15.4
HP-4	ZPE	bpy	50:1:1:2	1.092	14.4	10.6	23.2	15.4
HP-5	ZPE	bpy	100:1:1:2	2.183	14.4	10.6	23.2	15.4
HP-6	ZPE	bpy	200:1:1:2	4.366	14.4	10.6	23.2	15.4

7.5.2. Synthesis of zwitterionic copolymers



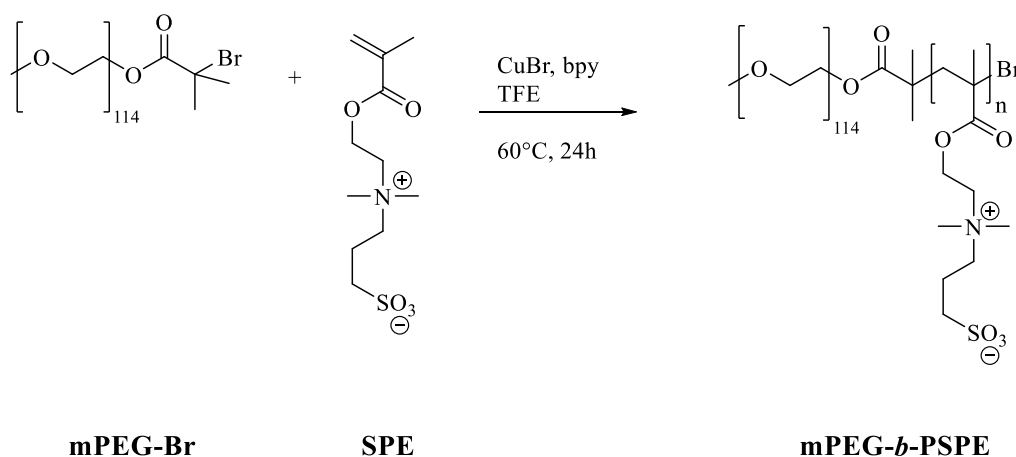
In a typical procedure, 1.652 g (5.920 mmol; 80 mol%) of monomer SPE and 0.437 g (1.48 mmol; 20 mol%) of sulfabetaine monomer (ZPE) were weighed in a 50 mL Schlenk flask, dissolved in 6 mL TFE under stirring, and deoxygenated by seven cycles of vacuum-flushing nitrogen. In 25 mL Schlenk flask, 14.4 mg (0.074 mmol) of EBiB was diluted in 3 mL of TFE and degassed. In another 25 mL Schlenk flask, 10.6 mg (0.074 mmol) of copper (I) bromide, 23.2 mg (0.148 mmol) of 2,2'-bipyridyl, and 15.4 mg (0.037 mmol) of L-ascorbic acid 6-palmitate were weighed, dissolved in 4 mL of TFE, and deoxygenated. The diluted initiator was transferred into the catalyst solution under stirring and protection by nitrogen. This initiator-catalyst solution was transferred into the monomer solution under protection by nitrogen. The ratio of $[\text{monomer}]_0$: $[\text{initiator}]_0$: $[\text{catalyst}]_0$: $[\text{ligand}]_0$ was 100: 1: 1: 2. The mixture was stirred by a magnetic stirrer and bubbled with nitrogen for 30 min. After that, the flask was placed into an oil bath at 60°C for 24 h. After 24 h, the reaction was stopped by

cooling and exposing the solution to the air. The purification was done by dialysis against distilled water for 5 d with a membrane with a nominal cut-off of MW 3500. Finally, the mixture was lyophilized overnight to give solid polymer.

Table 7.4. Reaction recipes for copolymerization of sulfobetaine (SPE) with co-monomers ZPE in TFE.

Sample	co-M	M:co-M	m_M [g]	m_{co-M} [g]	m_I [mg]	m_{CuBr} [mg]	m_{Lig} [mg]	m_{Red} [mg]
CP-2	ZPE	80:20	1.652	0.437	14.4	10.6	23.2	15.4
CP-3	ZPE	50:50	1.032	1.092	14.4	10.6	23.2	15.4
CP-4	ZPE	20:80	0.413	1.746	14.4	10.6	23.2	15.4

7.5.3. Synthesis of zwitterionic block copolymers



In a typical procedure, 2.065 g (7.400 mmol) of monomer SPE were weighed in a 50 mL flask, dissolved in 6 mL TFE under stirring, and deoxygenated by seven cycles of vacuum-flushing nitrogen. Then, in another 50 mL Schlenk flask, 0.370 g (0.074 mmol) of mPEG-Br, 10.6 mg (0.074 mmol) of copper (I) bromide, 23.2 mg (0.148 mmol) of 2,2'-bipyridyl, and 15.4 mg (0.037 mmol) of L-ascorbic acid 6-palmitate were weighed, dissolved in 6 mL TFE, and degassed. The initiator-catalyst solution was then transferred into the monomer solution under protection by nitrogen. The ratio of $[\text{monomer}]_0$: $[\text{initiator}]_0$: $[\text{catalyst}]_0$: $[\text{ligand}]_0$ was 100: 1: 1: 2. The mixture was stirred by a magnetic stirrer, and bubbled with nitrogen for 30 min. After that, the flask was placed in an oil bath at 60°C for 24 h. After 24 h, the reaction was stopped by cooling and exposing the solution to the air. The purification was done by dialysis against distilled water for 5 days with a membrane with a

7. Experimental Part

nominal cut-off of MW 3500. Finally, the mixture was lyophilized overnight to give solid polymers.

Table 7.5. Reaction recipes for sulfobetaine (SPE and SBE) based block copolymers in TFE.

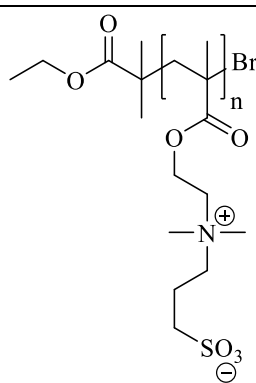
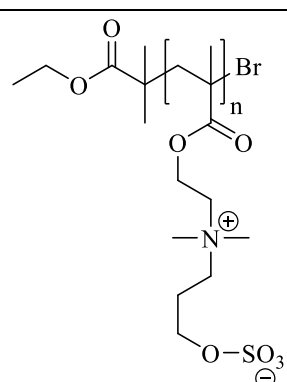
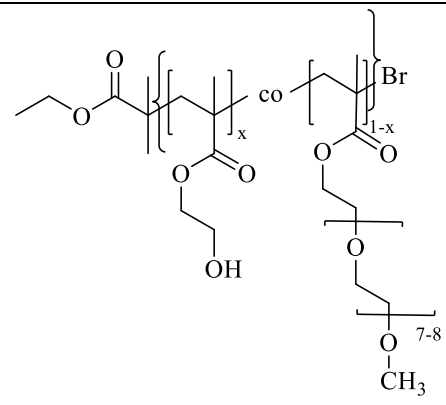
Sample	co-M	M:co-M	molar ratio M:I:CuBr:Lig	m _M [g]	m _{co-M} [g]	m _I [g]	m _{CuBr} [mg]	m _{Lig} [mg]
BC-5	-	100:0	100:1:1:2	2.067	-	0.370	10.6	23.2
BC-6 ^a	-	100:0	100:1:1:2	2.067	-	0.370	10.6	34.2
BC-7 ^b	-	100:0	30:1:1:2	0.840	-	0.5	17	15.6
BC-8 ^b	-	100:0	50:1:1:2	1.400	-	0.5	17	15.6
BC-9 ^b	-	100:0	100:1:1:2	2.790	-	0.5	17	15.6
BC-10 ^b	-	100:0	200:1:1:2	2.790	-	0.25	8.5	7.8
BC-11	BzMA	98:2	100:1:1:2	2.026	0.026	0.37	10.6	23.2
BC-12	BzMA	95:5	100:1:1:2	1.962	0.065	0.37	10.6	23.2
BC-13	BzMA	90:10	100:1:1:2	1.858	0.130	0.37	10.6	23.2
BC-14 ^c	-	100:0	100:1:1:2	1.086	-	0.185	5.3	11.6
BC-15 ^c	-	100:0	200:1:1:2	2.168	-	0.185	5.3	11.6
BC-16	ZPE	100:0	100:1:1:2	2.183	-	0.37	10.6	23.2
BC-17 ^b	ZPE	80:20	100:1:1.2:1	2.232	0.500	0.5	17	15.6
BC-18 ^b	ZPE	50:50	100:1:1.2:1	1.392	1.475	0.5	17	15.6

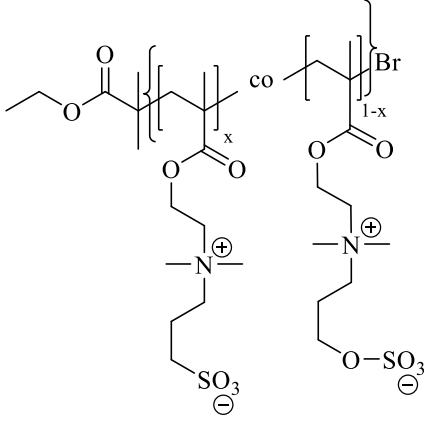
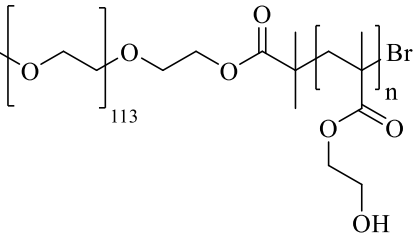
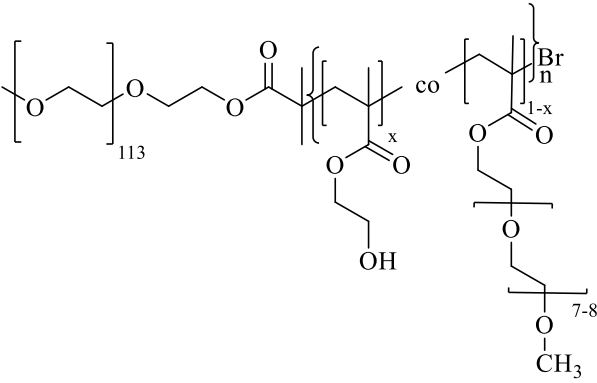
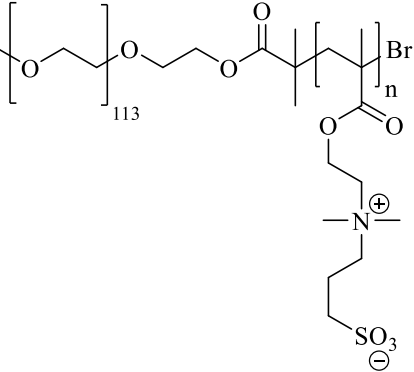
^a using HMTETA as ligand

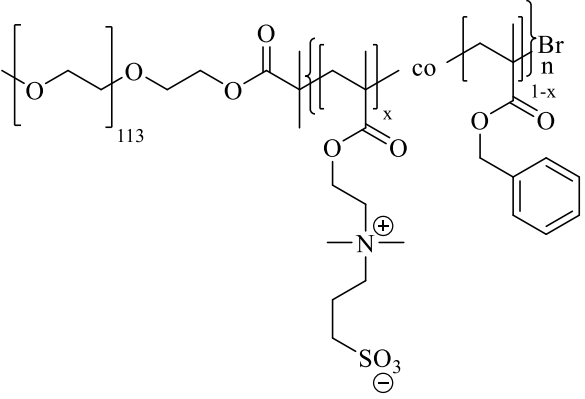
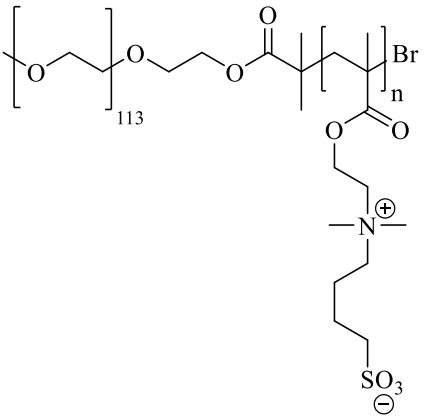
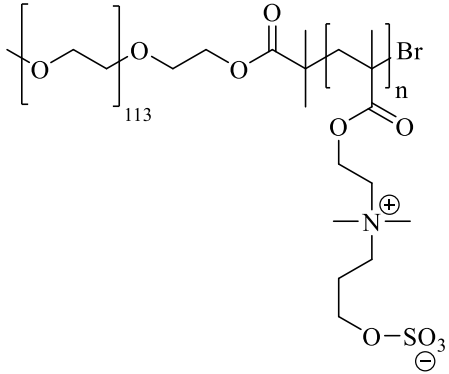
^b using H₂O/MeOH (3/2 v/v) as solvent at room temperature for 5 h

^c using SBE as monomer

Table 7.6. Chemical structures of the polymers produced.

Sample	Polymers	Structure
HP-1	homopolymer of polyzwitterions (poly[sulfobetaine]s)	 <p style="text-align: center;">PSPE</p>
HP-2		
HP-3		
HP-4	homopolymer of polyzwitterions (poly[sulfabetaine]s)	 <p style="text-align: center;">PZPE</p>
HP-5		
HP-6		
CP-1	nonionic copolymers	 <p style="text-align: center;">P(HEMA-<i>co</i>-OEGMA)</p>

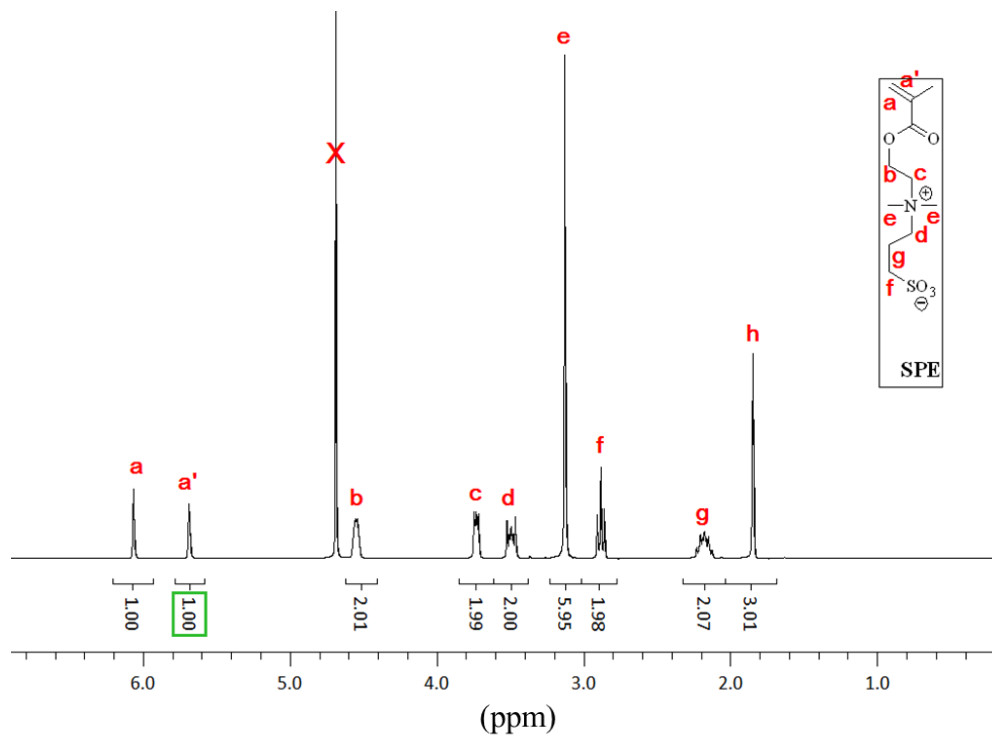
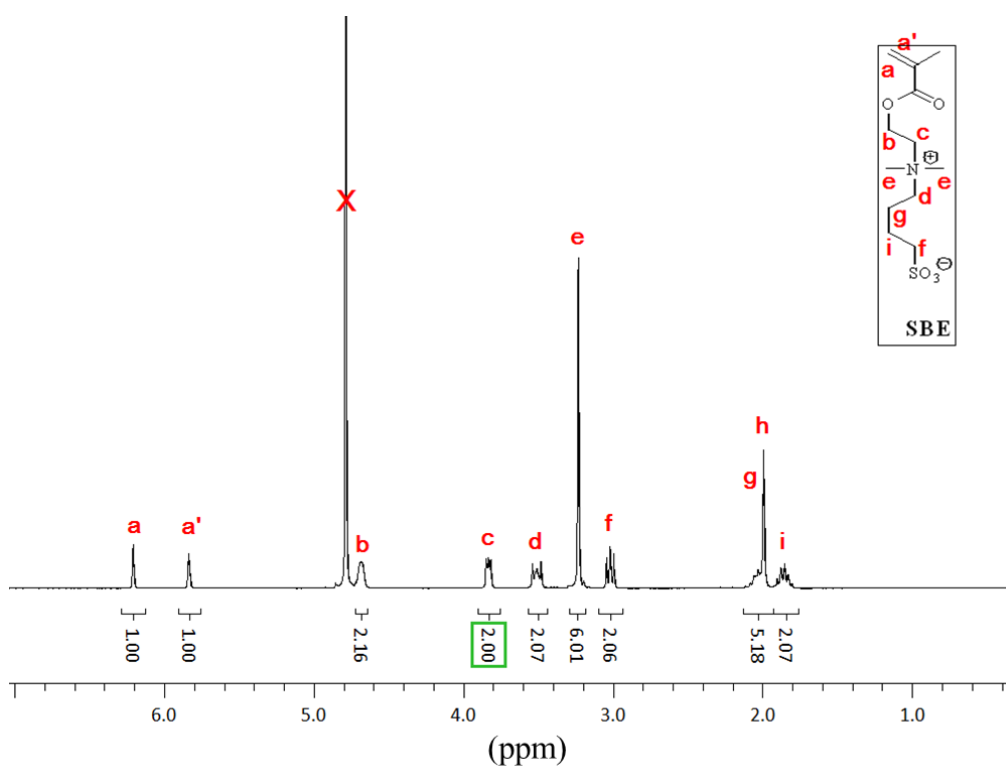
CP-2	zwitterionic copolymers	 <p style="text-align: center;">P(SPE-<i>co</i>-ZPE)</p>
CP-3		
CP-4		
BC-1	nonionic block copolymers	 <p style="text-align: center;">mPEG-<i>b</i>-PHEMA</p>
BC-2	nonionic block copolymers with co-monomer	 <p style="text-align: center;">mPEG-<i>b</i>-P(HEMA-<i>co</i>-OEGMA)</p>
BC-3		
BC-4		
BC-5	PSPE based zwitterionic block copolymers	 <p style="text-align: center;">mPEG-<i>b</i>-PSPE</p>
BC-6		
BC-7		
BC-8		
BC-9		
BC-10		

BC-11		
BC-12		
BC-13	zwitterionic block copolymers with hydrophobic moieties	 <p style="text-align: center;">mPEG-<i>b</i>-P(SPE-<i>co</i>-BzMA)</p>
BC-14		
BC-15	PSBE based zwitterionic block copolymers	 <p style="text-align: center;">mPEG-<i>b</i>-PSBE</p>
BC-16	PZPE based zwitterionic block copolymers	 <p style="text-align: center;">mPEG-<i>b</i>-PZPE</p>

BC-17		
BC-18	zwitterionic based block copolymers	<p>The chemical structure shows a block copolymer consisting of three main segments. On the left is a poly(ethylene glycol) (PEG) block with a degree of polymerization of 113, represented as $[-OCH_2CH_2-]_{113}$. This is connected via an ester linkage to a central block copolymer segment. This central segment consists of two copolymerized units: a styrene-<i>tert</i>-butyl acrylate (SPE) unit with a degree of polymerization of x, and a zwitterionic poly(ethylene methacrylate) (ZPE) unit with a degree of polymerization of $1-x$. The SPE unit has a methyl group and a <i>tert</i>-butyl group. The ZPE unit has a methacrylate backbone with a quaternary ammonium cation (N^+) and a sulfonate anion (SO_3^-) attached to the side chain. The entire structure is terminated with a bromine atom (Br) on the right.</p> <p>mPEG-<i>b</i>-P(SPE-<i>co</i>-ZPE)</p>

Appendix

NMR Spectra

Figure A.1. $^1\text{H-NMR}$ spectrum of SPE in D_2O Figure A.2. $^1\text{H-NMR}$ spectrum of SBE in D_2O

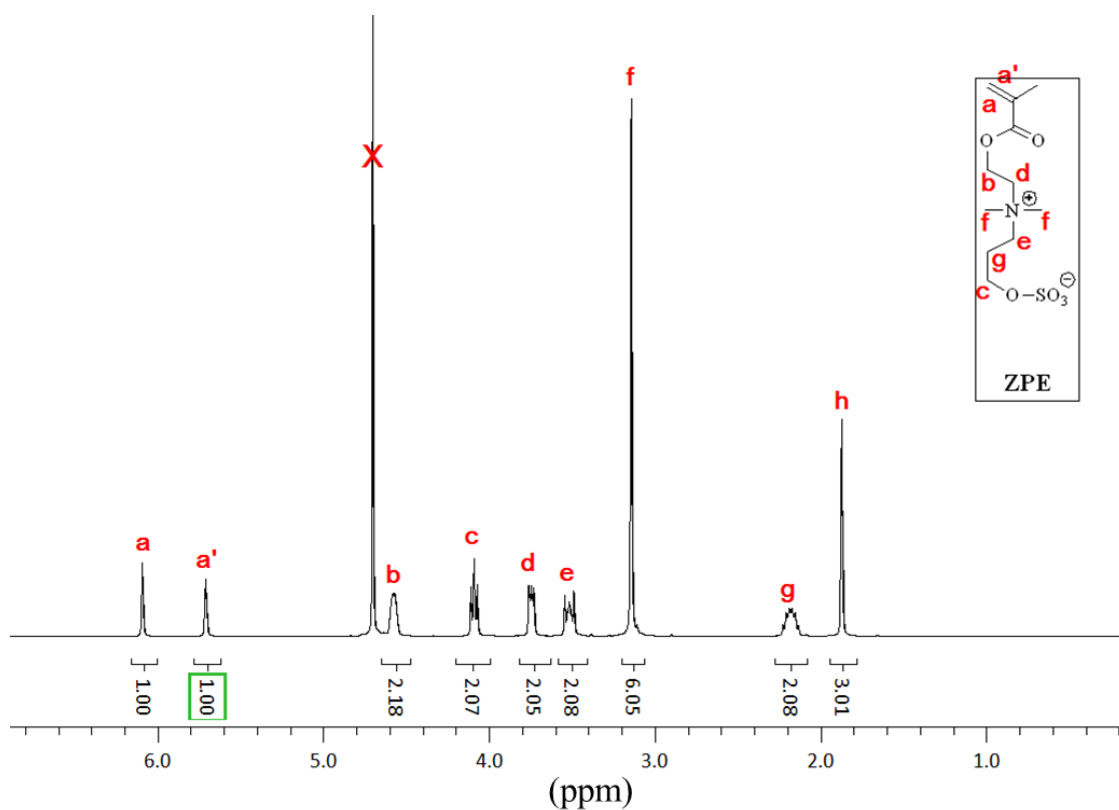


Figure A.3. $^1\text{H-NMR}$ spectrum of ZPE in D_2O

GPC Elugram

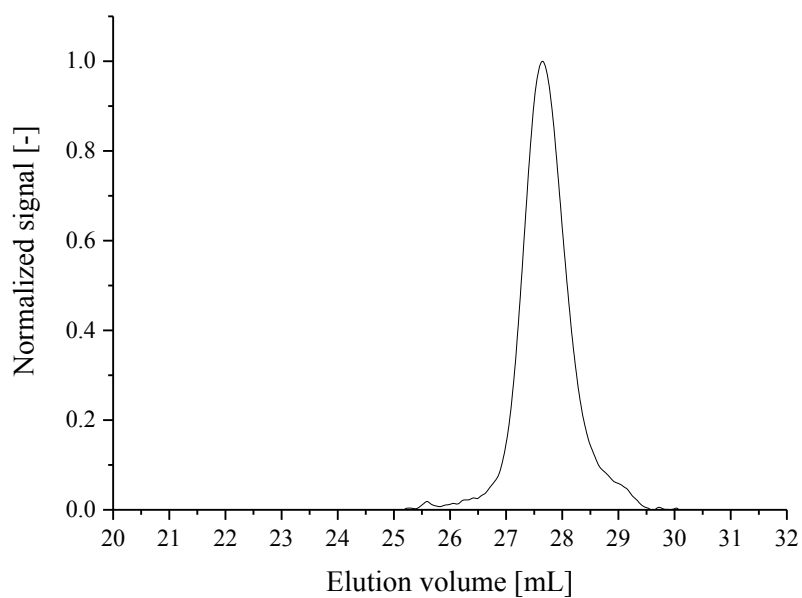


Figure A.4. GPC elugram of mPEG-Br macroinitiator using DMF as eluent

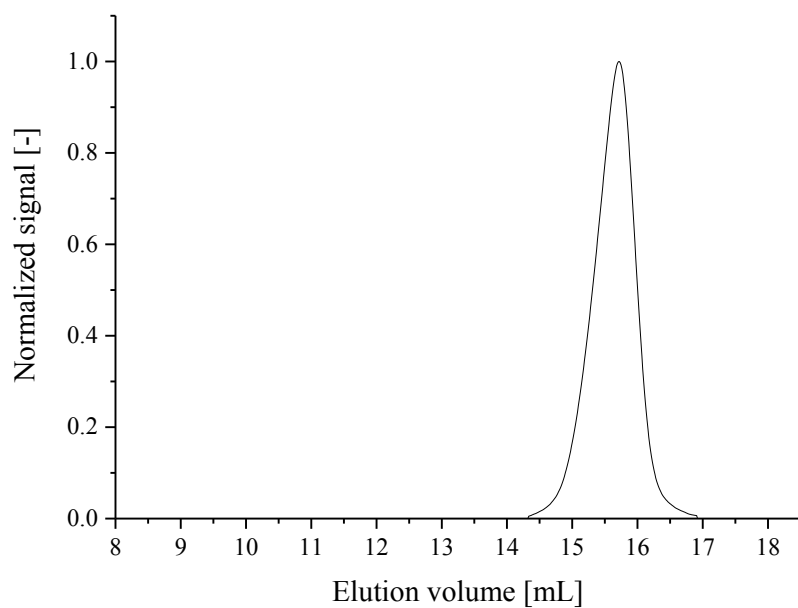


Figure A.5. GPC elugram of mPEG-Br macroinitiator using HFIP as eluent

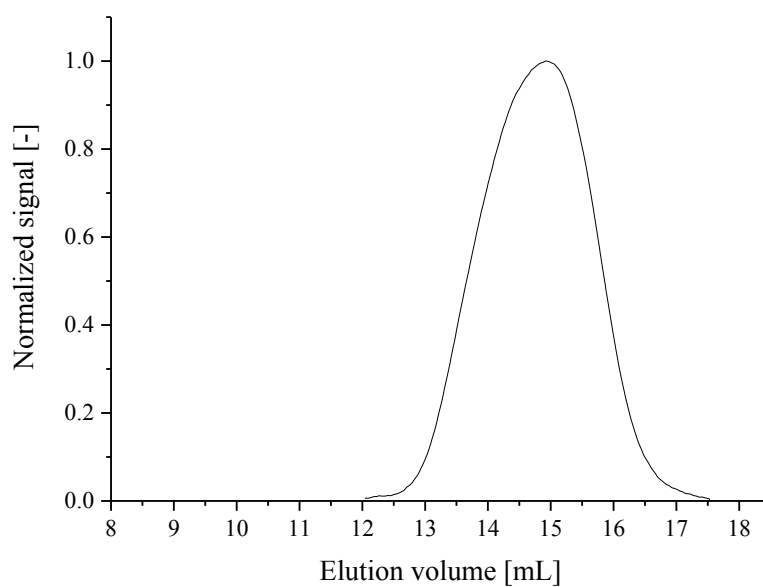


Figure A.6. GPC elugram of PSPE homopolymer (**HP-1**) using HFIP as eluent

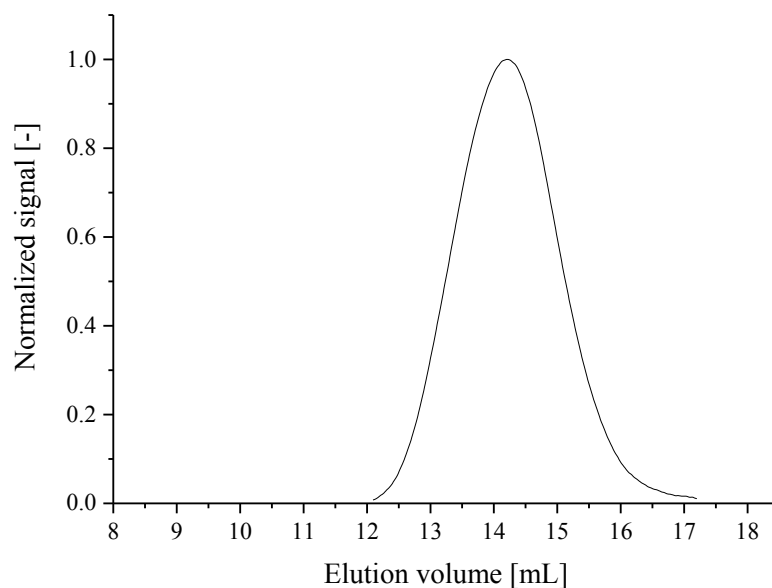


Figure A.7. GPC elugram of PSPE homopolymer (**HP-2**) using HFIP as eluent

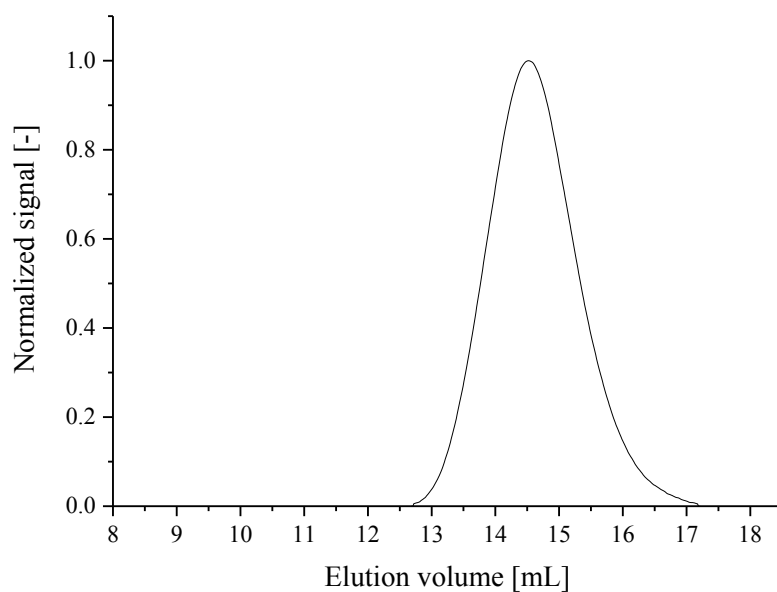


Figure A.8. GPC elugram of PSPE homopolymer (**HP-3**) using HFIP as eluent

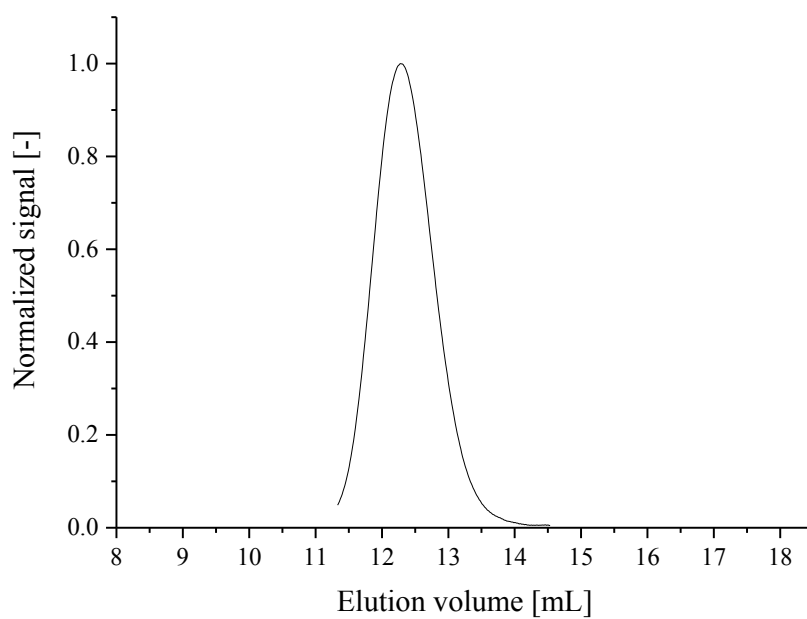


Figure A.9. GPC elugram of PZPE homopolymer (**HP-4**) using HFIP as eluent

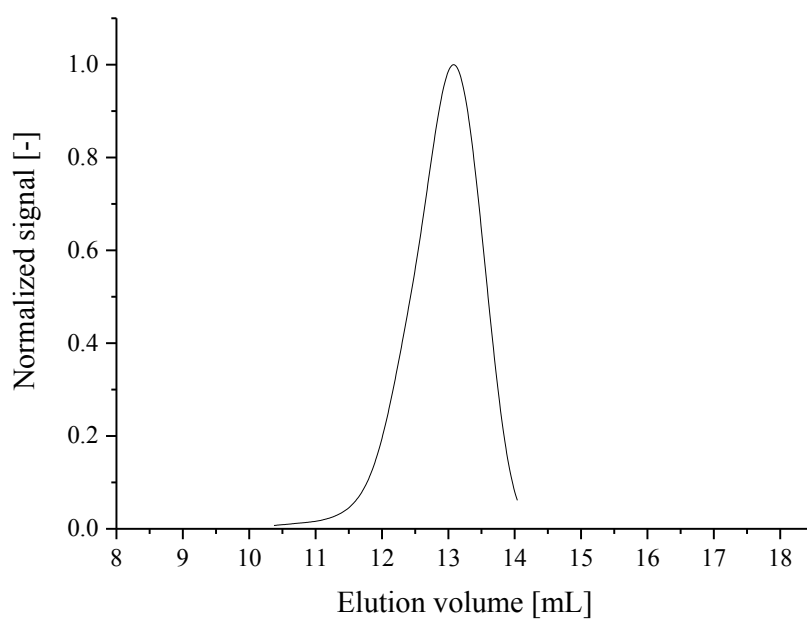


Figure A.10. GPC elugram of PZPE homopolymer (**HP-5**) using HFIP as eluent

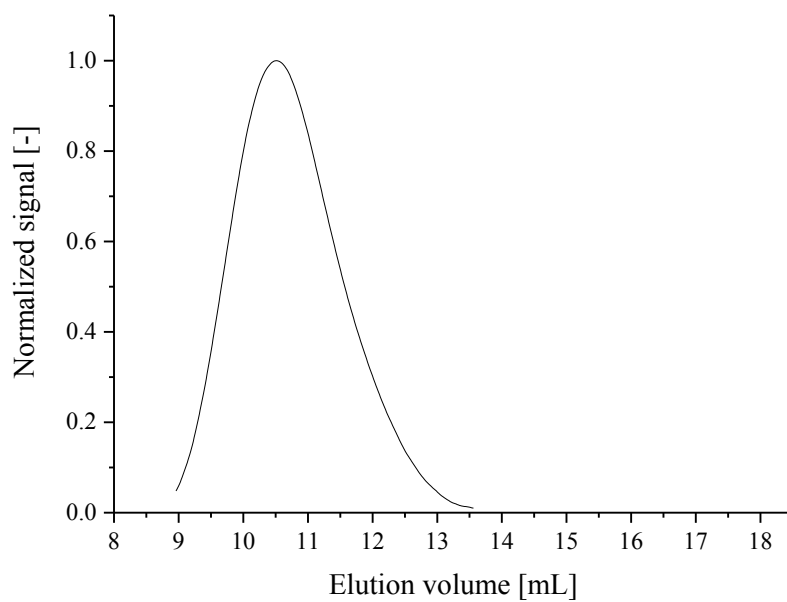


Figure A.11. GPC elugram of PZPE homopolymer (**HP-6**) using HFIP as eluent

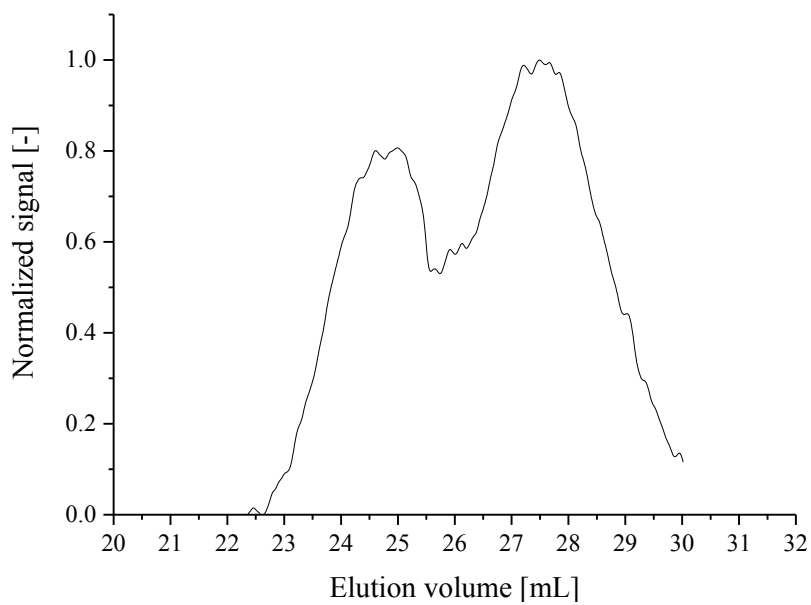


Figure A.12. GPC elugram of P(HEMA-co-OEGMA₄₇₅) copolymer (**CP-1**) using DMF as eluent

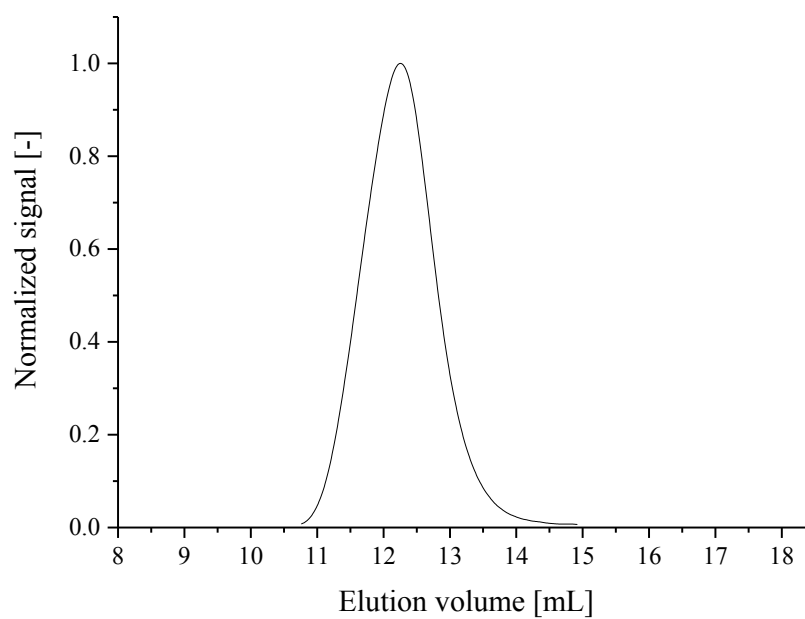


Figure A.13. GPC elugram of P(SPE-*co*-ZPE) copolymer (**CP-2**) using HFIP as eluent

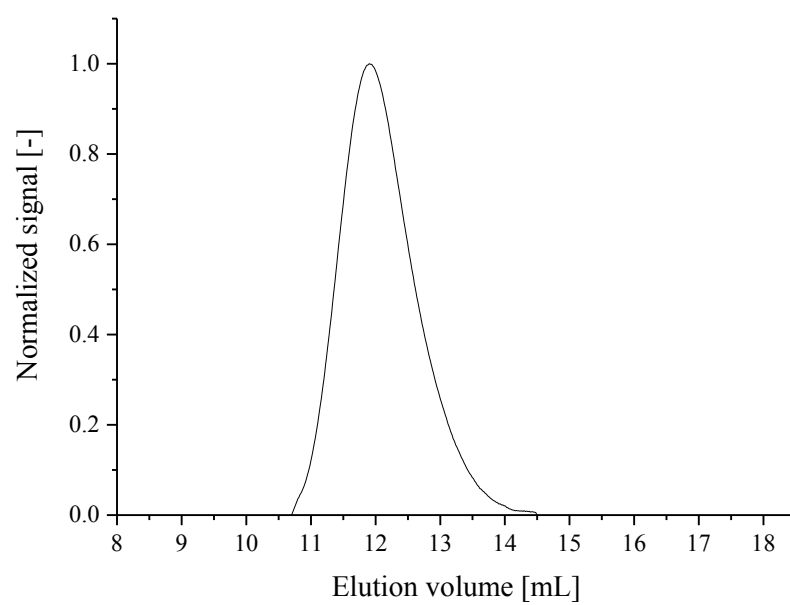


Figure A.14. GPC elugram of P(SPE-*co*-ZPE) copolymer (**CP-3**) using HFIP as eluent

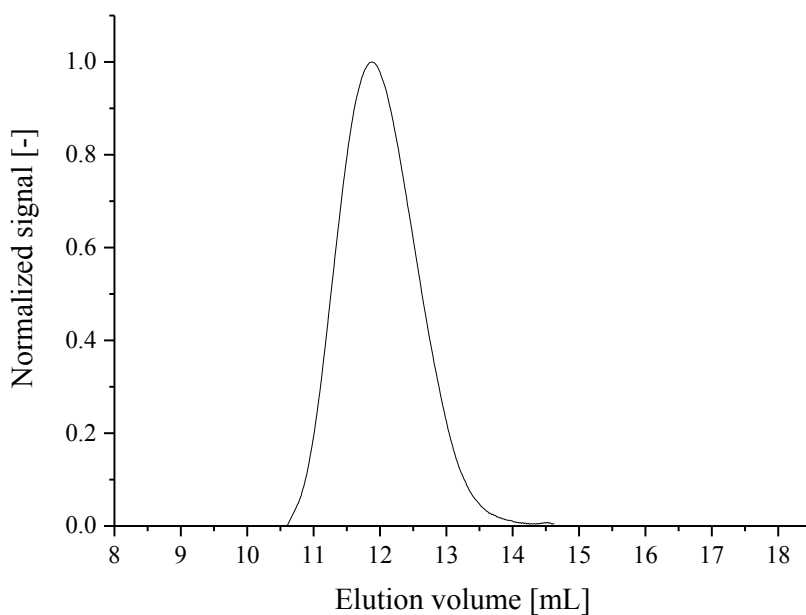


Figure A.15. GPC elugram of P(SPE-*co*-ZPE) copolymer (**CP-4**) using HFIP as eluent

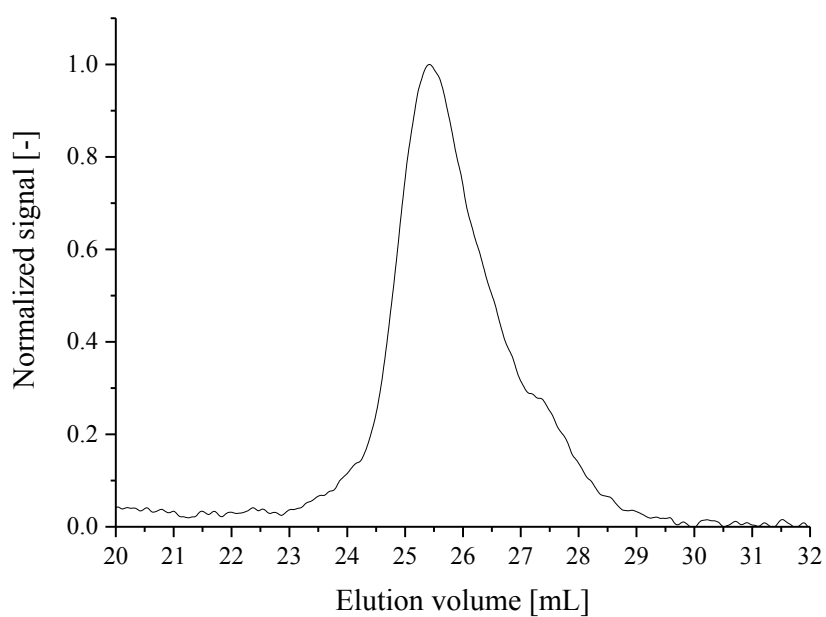


Figure A.16. GPC elugram of mPEG-*b*- P(HEMA-*co*-OEGMA₄₇₅) block copolymer (**BC-1**) using DMF as eluent

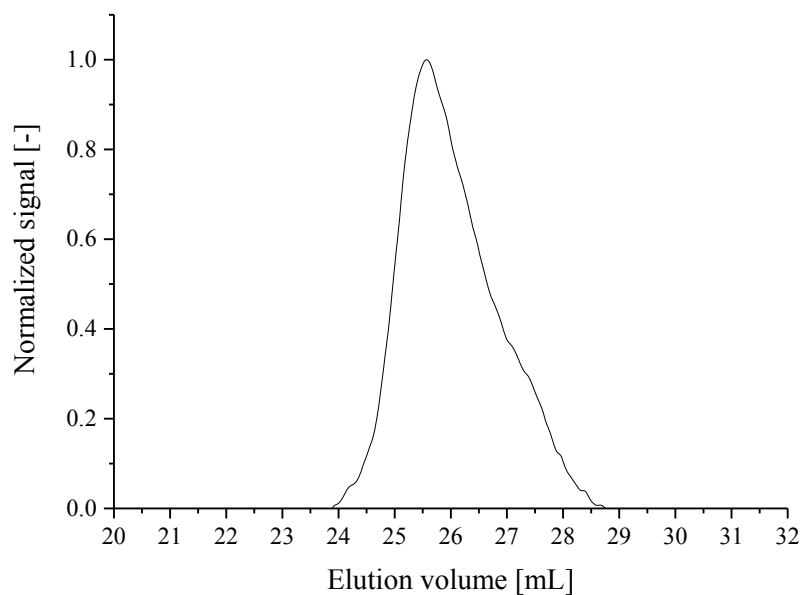


Figure A.17. GPC elugram of mPEG-*b*- P(HEMA-*co*-OEGMA₄₇₅) block copolymer (**BC-2**) using DMF as eluent

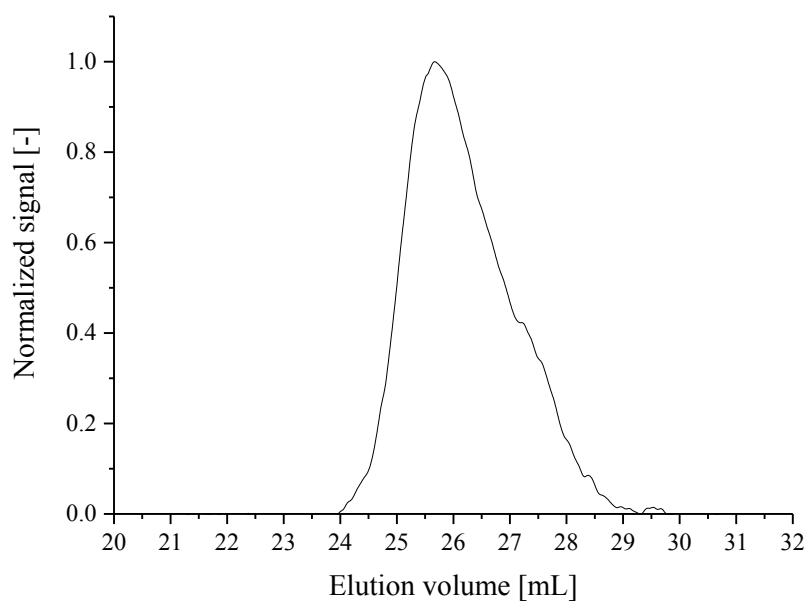


Figure A.18. GPC elugram of mPEG-*b*- P(HEMA-*co*-OEGMA₄₇₅) block copolymer (**BC-3**) using DMF as eluent

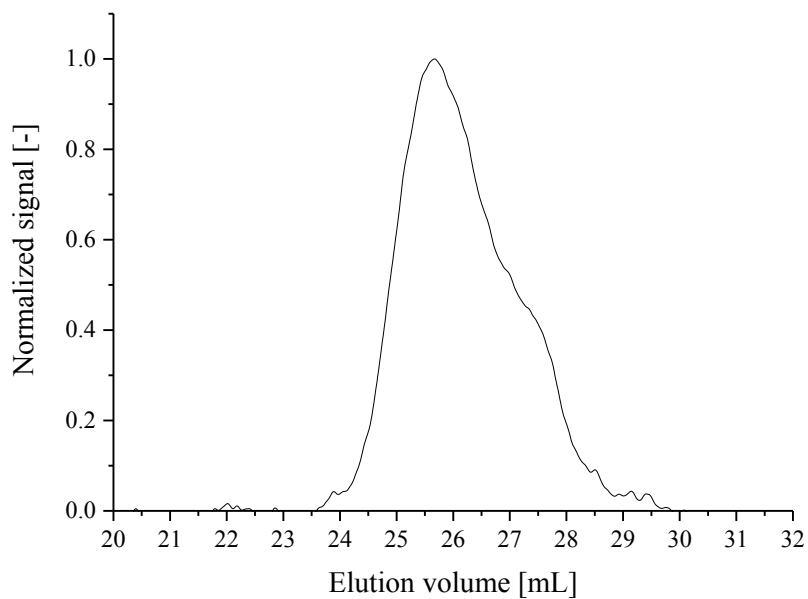


Figure A.19. GPC elugram of mPEG-*b*-P(HEMA-*co*-OEGMA₄₇₅) block copolymer (**BC-4**) using DMF as eluent

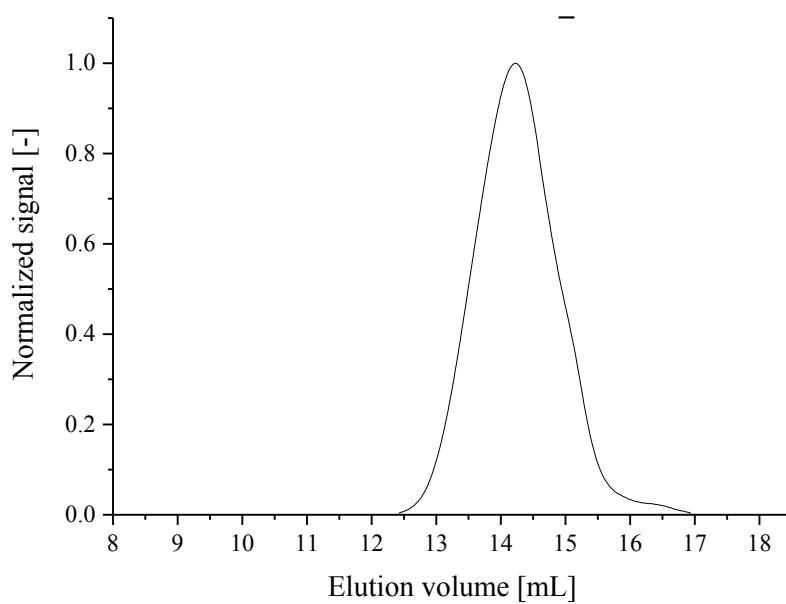


Figure A.20. GPC elugram of mPEG-*b*-PSPE block copolymer (**BC-5**) using HFIP as eluent

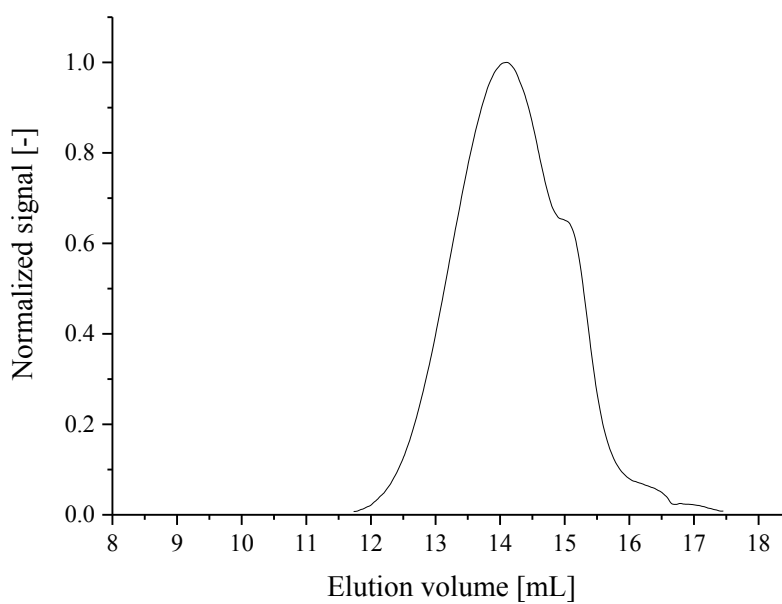


Figure A.21. GPC elugram of mPEG-*b*-PSPE block copolymer (**BC-6**) using HFIP as eluent

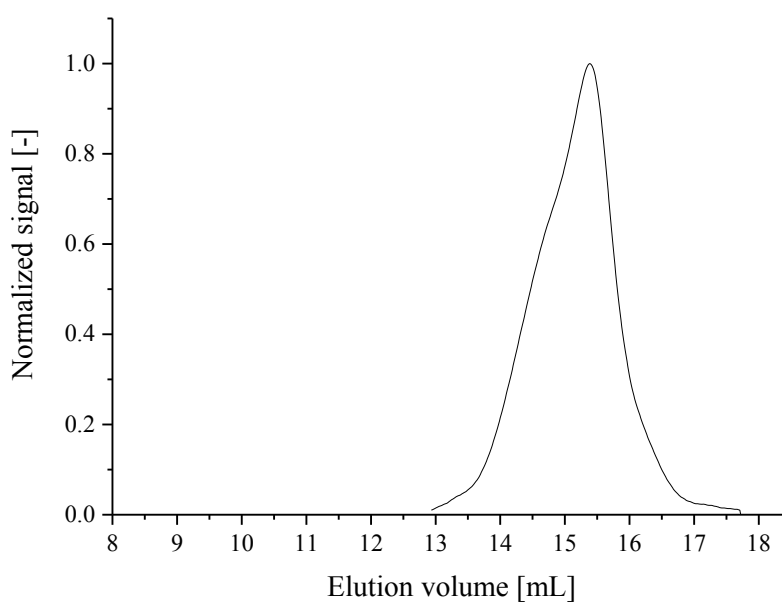


Figure A.22. GPC elugram of mPEG-*b*-PSPE block copolymer (**BC-7**) using HFIP as eluent

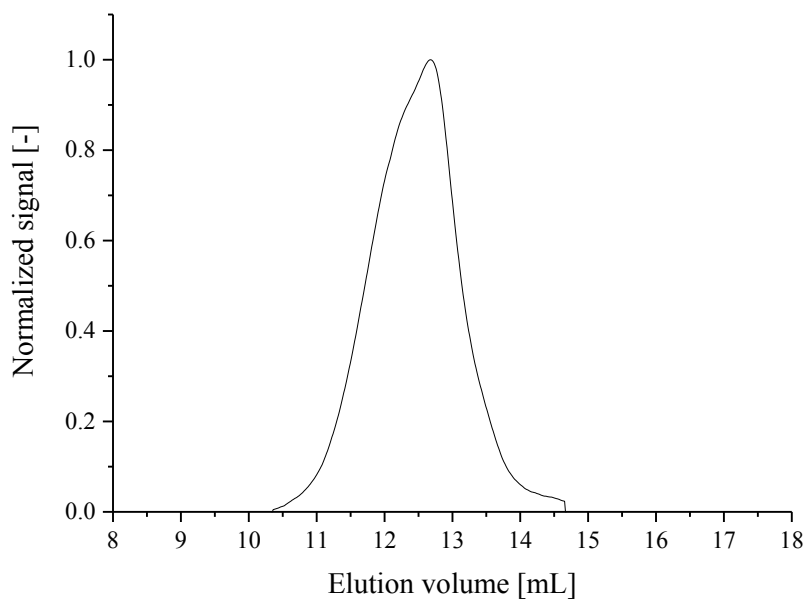


Figure A.23. GPC elugram of mPEG-*b*-PSPE block copolymer (**BC-8**) using HFIP as eluent

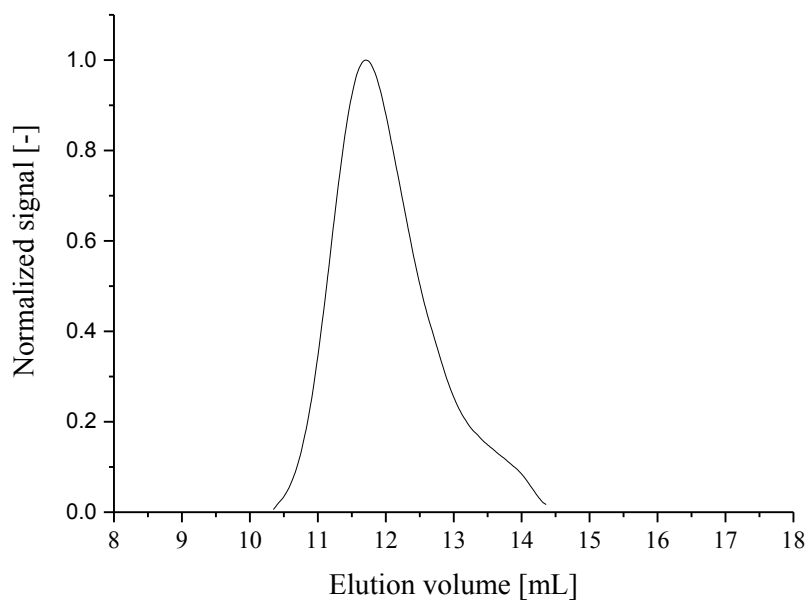


Figure A.24. GPC elugram of mPEG-*b*-PSPE block copolymer (**BC-9**) using HFIP as eluent

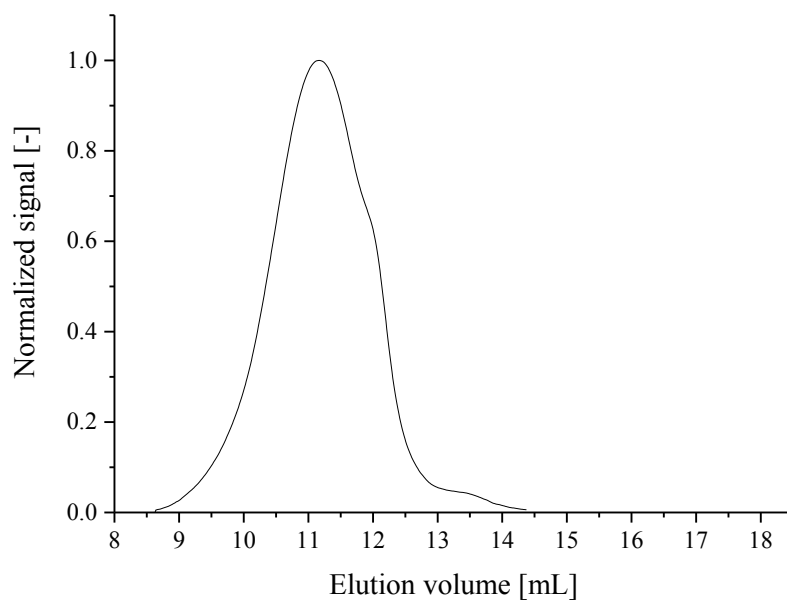


Figure A.25. GPC elugram of mPEG-*b*-PSPE block copolymer (**BC-10**) using HFIP as eluent

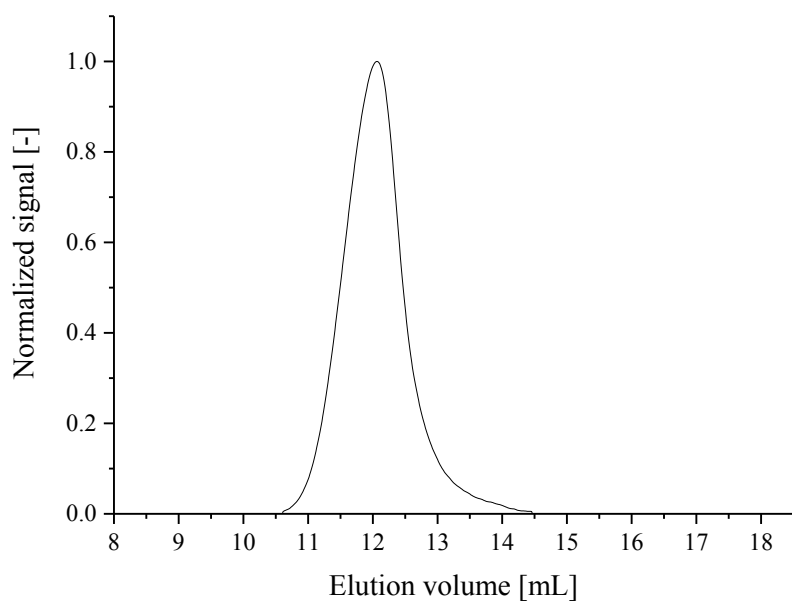


Figure A.26. GPC elugram of mPEG-*b*-P(SPE-*co*-BzMA) block copolymer (**BC-11**) using HFIP as eluent

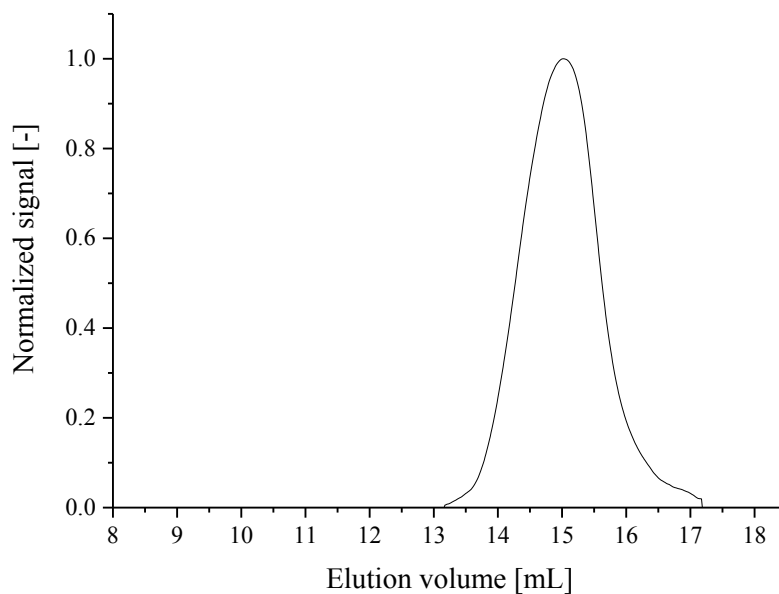


Figure A.27. GPC elugram of mPEG-*b*-P(SPE-*co*-BzMA) block copolymer (**BC-12**) using HFIP as eluent

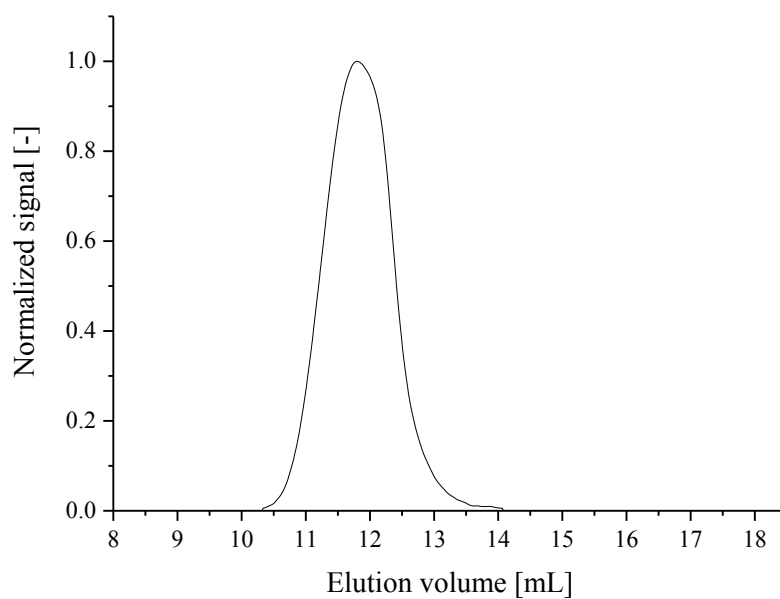


Figure A.28. GPC elugram of mPEG-*b*-P(SPE-*co*-BzMA) block copolymer (**BC-13**) using HFIP as eluent

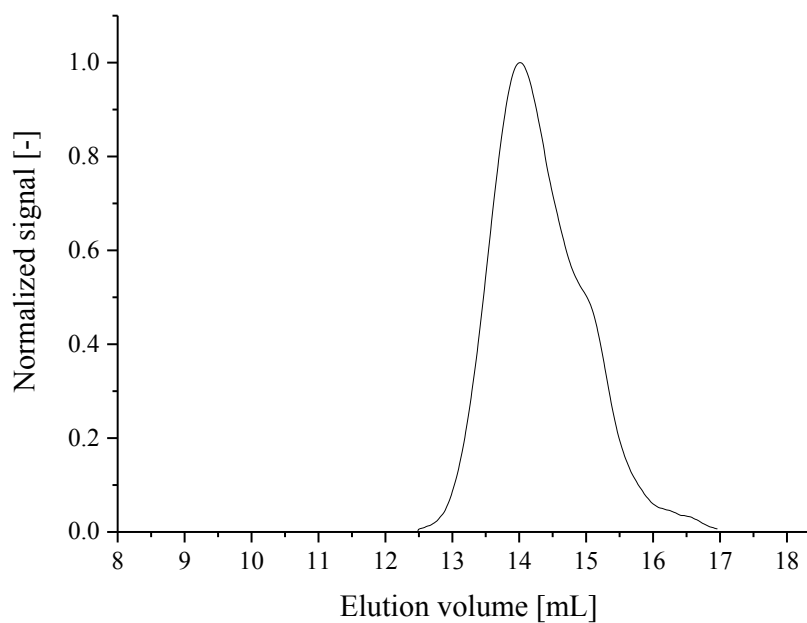


Figure A.29. GPC elugram of mPEG-*b*-PSBE block copolymer (**BC-14**) using HFIP as eluent

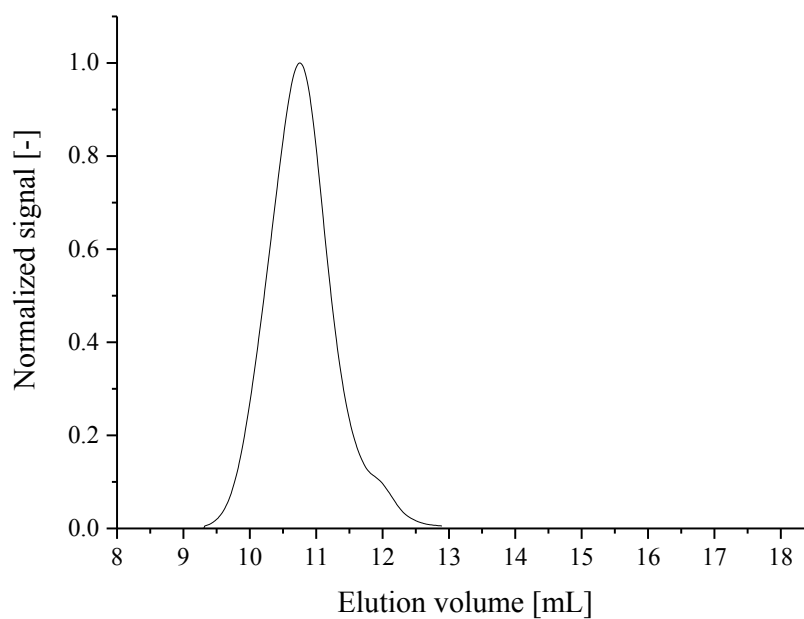


Figure A.30. GPC elugram of mPEG-*b*-PSBE block copolymer (**BC-15**) using HFIP as eluent

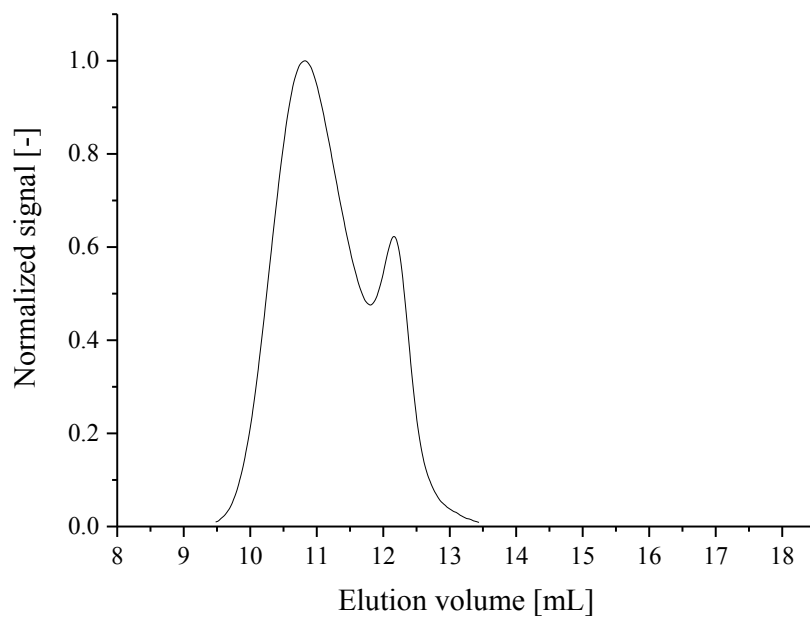


Figure A.31. GPC elugram of mPEG-*b*-PZPE block copolymer (**BC-16**) using HFIP as eluent

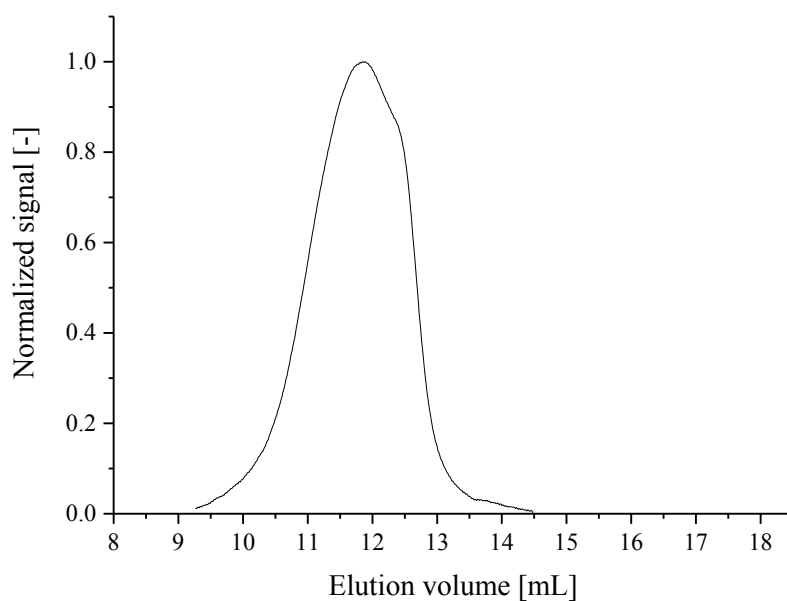


Figure A.32. GPC elugram of mPEG-*b*-P(SPE-*co*-ZPE) block copolymer (**BC-17**) using HFIP as eluent

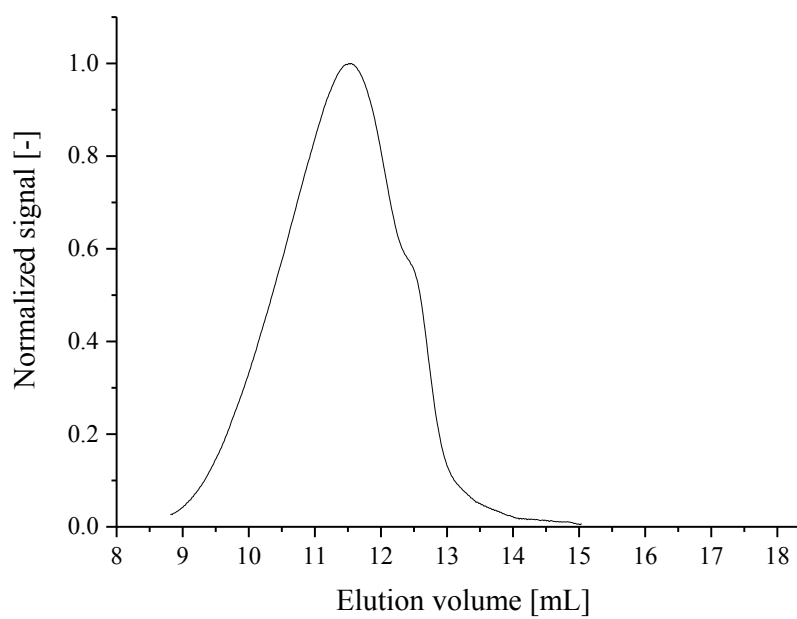


Figure A.33. GPC elugram of mPEG-*b*-P(SPE-*co*-ZPE) block copolymer (**BC-18**) using HFIP as eluent

List of Figures

Figure 1.1. Scheme of micelle formation and disassembly of block copolymers containing an UCST-type polymer block for the controlled release of poorly water-soluble active agents (e.g., drugs) at elevated temperature.	2
Figure 1.2. Schematic phase diagrams of polymers bearing a) LCST and b) UCST behavior (temperature v. mole fraction of polymers).....	4
Figure 1.3. Model of the temperature triggered coil-to-globule transition of hydrated polymer chains.....	5
Figure 1.4. Schematic illustration of a) intra- and b) intermolecular electrostatic interactions within zwitterionic polymers causing UCST behavior.....	9
Figure 1.5. The general chemical structure of phosphatidyl choline lipids (lecithins).	9
Figure 1.6. Exemplary chemical structures of a) poly(phosphobetaine)s, b) poly(carboxybetaine)s, and c) poly(sulfobetaine)s derived from poly(methacrylate)s.	10
Figure 1.7. The reaction scheme of the typical sulfobetaine monomer synthesis (mostly $n=3$ or 4).	11
Figure 1.8. General reaction mechanism as one major principle of reversible-deactivation radical polymerization (RDRP).....	12
Figure 1.9. General mechanism of atom transfer radical polymerization (ATRP) [13].....	13
Figure 1.10. Schematic illustration of active agents release via polymer micelle formation-disassembly using a globule-to-coil phase transition in a physiological relevant temperature range.	17
Figure 2.1. Reaction scheme of macroinitiator, mPEG-Br, synthesis.....	18
Figure 2.2. $^1\text{H-NMR}$ spectra of poly[(ethylene glycol) methyl ether 2-bromoisobutyrate] (mPEG-Br) macroinitiator in D_2O	20
Figure 3.1. $^1\text{H-NMR}$ spectrum of P(HEMA- <i>co</i> -OEGMA ₄₇₅) copolymer (CP-1) in D_2O	22
Figure 3.2. $^1\text{H-NMR}$ spectrum of mPEG- <i>b</i> -PHEMA copolymer (BC-1) in D_2O	24
Figure 3.3. $^1\text{H-NMR}$ spectrum of mPEG- <i>b</i> -P(HEMA- <i>co</i> -OEGMA ₄₇₅) copolymer (BC-3) in D_2O	24

Figure 3.4. Temperature dependent turbidity (heating run) of 3 g/L aqueous solutions of CP-1 in H ₂ O.....	26
Figure 3.5. Temperature dependent turbidity (heating run) of 3 g/L aqueous solutions of mPEG- <i>b</i> -P(HEMA- <i>co</i> -OEGMA ₄₇₅) block copolymers.....	28
Figure 4.1. Chemical structure of monomer SPE.....	29
Figure 4.2. ¹ H-NMR spectrum of PSPE homopolymer (HP-2) in D ₂ O with 0.5 M NaCl.	31
Figure 4.3. ¹ H-NMR spectrum of mPEG- <i>b</i> -PSPE block copolymer (BC-10) in D ₂ O with 0.5 M NaCl.	33
Figure 4.4. Temperature dependent turbidity (cooling run) of 30 g/L aqueous solutions of PSPE homopolymers synthesized using different ligands in H ₂ O: bpy (black squares), PMDETA (red circles), HMTETA (blue triangles).	35
Figure 4.5. Cloud points versus degree of polymerization (DP _n) of mPEG ₁₁₄ - <i>b</i> -PSPE _n in H ₂ O: polymers synthesized in TFE (black squares), and in H ₂ O/MeOH 3/2 v/v (red triangles).	39
Figure 4.6. Temperature dependent turbidity (cooling run) of 30 g/L aqueous solutions of mPEG ₁₁₄ - <i>b</i> -PSPE _n with different degrees of polymerization in H ₂ O.....	40
Figure 4.7. Temperature dependent turbidity of 30 g/L aqueous solutions of physical mixing of mPEG-Br with PSPE in H ₂ O.....	41
Figure 4.8. ¹ H-NMR spectrum of mPEG- <i>b</i> -P(SPE- <i>co</i> -BzMA) block copolymer (BC-12) in TFA-d.....	43
Figure 4.9. Temperature dependent turbidity (cooling run) of 30 g/L aqueous solutions of mPEG ₁₁₄ - <i>b</i> -P(SPE _x - <i>co</i> -BzMA _y) block copolymers in H ₂ O.	45
Figure 4.10. Temperature dependent DLS measurement (cooling run) of 30 g/L aqueous solutions of BC-13 in H ₂ O.	46
Figure 4.11. Temperature dependent turbidity (cooling run) of 30 g/L aqueous solutions of mPEG ₁₁₄ - <i>b</i> -P(SPE _x - <i>co</i> -BzMA _y) block copolymers in physiological saline.	46
Figure 4.12. Temperature dependent turbidity (cooling run) of 30 g/L aqueous solutions of BC-12 with different salt concentration.	47

Figure 4.13. Temperature dependent DLS measurement (cooling run) of 30 g/L aqueous solutions of BC-12 in H ₂ O a) from 10 to 60°C and b) zoom-in from 25 to 60°C.....	48
Figure 4.14. Turbidity (cooling runs) and micro DSC measurements (heating run) of 30 g/L solutions of BC-12 in H ₂ O.....	49
Figure 4.15. Chemical structure difference between SPE and SBE.....	50
Figure 4.16. ¹ H-NMR spectrum of mPEG- <i>b</i> -PSBE block copolymer (BC-15) in D ₂ O with 0.5 M NaCl.....	51
Figure 4.17. Temperature dependent turbidity (cooling run) of 30 g/L aqueous solutions of mPEG ₁₁₄ - <i>b</i> -PSBE _n block copolymers in a) H ₂ O, b) physiological saline solution (9 g/L NaCl). Black is BC-14 , red is BC-15	54
Figure 4.18. Temperature dependent ¹ H-NMR (heating run) of 30 g/L aqueous solutions of BC-14 in D ₂ O.....	55
Figure 4.19. Chemical structure difference of SPE and ZPE.....	56
Figure 4.20. ¹ H-NMR spectrum of PZPE homopolymer (HP-4) in D ₂ O with 0.5 M of NaCl.....	57
Figure 4.21. ¹ H-NMR spectrum of P(SPE- <i>co</i> -ZPE) copolymer (CP-2) in D ₂ O with 0.5 M NaCl.....	59
Figure 4.22. ¹ H-NMR spectrum of mPEG- <i>b</i> -PZPE block copolymer (BC-16) in D ₂ O with 0.5 M NaCl.....	61
Figure 4.23. ¹ H-NMR spectrum of mPEG- <i>b</i> -P(SPE- <i>co</i> -ZPE) block copolymer (BC-18) in D ₂ O with 0.5 M NaCl.....	63
Figure 4.24. Temperature dependent turbidity (cooling run) of 3 g/L aqueous solutions of PZPE homopolymers in physiological saline.....	66
Figure 4.25. Temperature dependent turbidity (cooling run) of 3 g/L aqueous solutions of BC-16 in physiological saline solution (9 g/L NaCl).....	69
Figure 4.26. Temperature dependent turbidity (cooling and heating run) of 3 g/L aqueous solutions of BC-18 in physiological saline.....	71
Figure 4.27. Turbidity and DLS measurements (cooling runs) of 3 g/L solutions of BC-18 in physiological saline.....	71
Figure 5.1. Illustration of the temperature-triggered release of active agents from a thermoresponsive polymeric micelle, followed by fluorescence spectroscopy using solvatochromic model cargos.....	73

Figure 5.2. Chemical structure of Reichardt's dye.....	74
Figure 5.3. Absorbance spectrum of Reichardt's dye and BC-18 loaded Reichardt's dye in physiological saline at room temperature.....	75
Figure 5.4. Chemical structure of dansyl L-phenylalanine.	76
Figure 5.5. Fluorescence spectra of dansyl L-phenylalanine in a homologous series of alcohols and PBS.....	77
Figure 5.6. Fluorescence spectra of dansyl L-phenylalanine in aqueous solutions.....	78
Figure 5.7. Fluorescence spectra of temperature-triggered release experiments of BC-18 loaded with dansyl L-phenylalanine at 25°C and 70° in physiological saline and pure water.....	79
Figure 5.8. Chemical structure of the dyes used for solubilization experiments [120, 124].....	80
Figure 5.9. Fluorescence spectra of solubilization experiment of free dyes at 22°C and in the presence of BC-18 in physiological saline.	81
Figure 5.10. Fluorescence spectra of temperature-triggered experiment of BC-18 loaded dyes 7 at 25°C and 70° in physiological saline.....	82

List of Tables

Table 1.1. Examples of polymers with LCST behavior.	6
Table 1.2. Examples of polymers with UCST behavior.	8
Table 1.3. Examples of ligands for copper catalyst in ATRP.	14
Table 3.1. Analytical data of the P(HEMA- <i>co</i> -OEGMA ₄₇₅) copolymer.	23
Table 3.2. Analytical data of the mPEG- <i>b</i> -P(HEMA- <i>co</i> -OEGMA ₄₇₅) block copolymers.	25
Table 3.3. LCST-type phase transition temperature of 3 g/L aqueous solutions of the P(HEMA- <i>co</i> -OEGMA ₄₇₅) copolymer in H ₂ O. Temperature measurement between 25 – 60°C (heating run).	26
Table 3.4. LCST-type cloud point of 3 g/L aqueous solutions of mPEG- <i>b</i> -P(HEMA- <i>co</i> -OEGMA ₄₇₅) block copolymers in H ₂ O. Temperature measurement between 40 – 95°C (heating run).	27
Table 4.1. Analytical data of the PSPE homopolymers made by ATRP using EBiB as initiator and CuBr as catalyst precursor in TFE at 60°C for 24 h.	32
Table 4.2. Analytical data of the mPEG ₁₁₄ - <i>b</i> -PSPE _n block copolymers. Unless indicated, the ratio of [M] : [I] was 100 : 1.	34
Table 4.3. UCST-type cloud point of 30 g/L aqueous solutions of PSPE homopolymers in H ₂ O and physiological saline. Temperature measurement between 10 - 40°C (cooling run). Concentration of sodium chloride in physiological saline is 9 g/L or 0.154 M.	36
Table 4.4. UCST-type cloud point of 30 g/L aqueous solutions of mPEG ₁₁₄ - <i>b</i> -PSPE _n block copolymers in H ₂ O and physiological saline. Temperature measurement between 5 - 75°C (cooling run). Concentration of sodium chloride in physiological saline is 9 g/L or 0.154 M.	38
Table 4.5. Analytical data of the mPEG ₁₁₄ - <i>b</i> -P(SPE _x - <i>co</i> -BzMA _y) block copolymers.	44
Table 4.6. UCST-type cloud point of 30 g/L aqueous solutions of mPEG ₁₁₄ - <i>b</i> -P(SPE _x - <i>co</i> -BzMA _y) block copolymers in H ₂ O and physiological saline.	45
Table 4.7. Analytical data of the mPEG ₁₁₄ - <i>b</i> -PSBE _n block copolymers made by ATRP using mPEG-Br as macroinitiator, CuBr/ bipyridyl as complex catalyst in TFE at 60°C for 24 h.	52
Table 4.8. Cloud point of 30 g/L aqueous solutions of mPEG ₁₁₄ - <i>b</i> -PSBE _n block copolymers in H ₂ O and physiological saline. Temperature measurement between 5 - 75°C	

(cooling run). Concentration of sodium chloride in physiological saline is 9 g/L or 0.154 M.....	53
Table 4.9. Analytical data of the PZPE homopolymers made by ATRP using EBiB as initiator, CuBr/ bipyridyl as complex catalyst in TFE at 60°C for 24 h.	58
Table 4.10. Analytical data of the P(SPE- <i>co</i> -ZPE) _n copolymers made by ATRP using EBiB as initiator, CuBr/ bipyridyl as complex catalyst in TFE at 60°C for 24 h.....	60
Table 4.11. Analytical data of the mPEG ₁₁₄ - <i>b</i> -PZPE _n block copolymers made by ATRP using mPEG-Br as macroinitiator, CuBr/ bipyridyl as complex catalyst in TFE at 60°C for 24 h.....	62
Table 4.12. Analytical data of the mPEG ₁₁₄ - <i>b</i> -P(SPE _x - <i>co</i> -ZPE _y) block copolymers made by ATRP using mPEG-Br as macroinitiator, CuBr/ bipyridyl as complex catalyst in H ₂ O/MeOH (3/2 v/v) at r.t for 5 h.	63
Table 4.13. UCST-type cloud point of 3 g/L aqueous solutions of PZPE homopolymers in H ₂ O and physiological saline. Temperature measurement between 20 - 75°C (cooling run). Concentration of sodium chloride in physiological saline is 9 g/L or 0.154 M.....	65
Table 4.14. UCST-type cloud point of 3 g/L aqueous solutions of P(SPE- <i>co</i> -ZPE) _n copolymers in H ₂ O and physiological saline. Temperature measurement between 5 - 75°C (cooling run). Concentration of sodium chloride in physiological saline is 9 g/L or 0.154 M.....	67
Table 4.15. Cloud point of 3 g/L aqueous solutions of BC-16 in H ₂ O and physiological saline. Temperature measurement between 5 - 75°C (cooling run). Concentration of sodium chloride in physiological saline is 9 g/L or ~ 0.154 M.	68
Table 4.16. UCST-type cloud point of 3 g/L aqueous solutions of mPEG ₁₁₄ - <i>b</i> -P(SPE _x - <i>co</i> -ZPE _y) block copolymers in H ₂ O and physiological saline. Concentration of sodium chloride in physiological saline is 9 g/L or 0.154 M. Temperature measurement between 15 - 75°C (cooling run).	70
Table 7.1. Chemicals used in the experiments.	86
Table 7.2. Reaction recipes for HEMA-based block copolymerization (24 h, 60°C in 6 mL of ethanol using 2,2'-bipyridyl as ligand).	92
Table 7.3. Reaction recipes for homopolymerization of sulfobetaine (SPE) and sulfobetaine (ZPE) in TFE.....	94
Table 7.4. Reaction recipes for copolymerization of sulfobetaine (SPE) with co-monomers ZPE in TFE.	95
Table 7.5. Reaction recipes for sulfobetaine (SPE and SBE) based block copolymers in TFE.	96

Table 7.6. Chemical structures of the polymers produced. 97

Declaration

I hereby declare that I have made this work independently using only the referenced literatures and sources. This work has not been submitted to any other university.

Hiermit erkläre ich, dass ich die vorliegende Arbeit selbstständig und mit der angegebenen Literatur, sowie Hilfsmittel angefertigt habe. Diese Arbeit wurde an keiner anderen Hochschule eingereicht.

Potsdam, 22 February 2018

Noverra Mardhatillah Nizado

Bibliography

- [1.] Aseyev, V.; Tenhu, H.; Winnik, F., Non-ionic Thermoresponsive Polymers in Water. *Adv. Polym. Sci.* **2011**, *242*, 29-89.
- [2.] Schattling, P.; Jochum, F. D.; Theato, P., Multi-stimuli responsive polymers – the all-in-one talents. *Polym. Chem.* **2014**, *5*, 25-36.
- [3.] Akdemir, Ö.; Badi, N.; Pfeifer, S.; Zarafshani, Z.; Laschewsky, A.; Wischerhoff, E.; Lutz, J.-F., Design of Thermoresponsive Materials by ATRP of Oligo(ethylene glycol)-based (Macro)monomers. *ACS Symp. Ser.* **2009**, *1023*, 189-202.
- [4.] Zhu, Y.; Batchelor, R.; Lowe, A. B.; Roth, P. J., Design of Thermoresponsive Polymers with Aqueous LCST, UCST, or Both: Modification of a Reactive Poly(2-vinyl-4,4-dimethylazlactone) Scaffold. *Macromolecules* **2016**, *49*, 672-680.
- [5.] Seuring, J.; Agarwal, S., Polymers with Upper Critical Solution Temperature in Aqueous Solution. *Macromol. Rapid. Commun.* **2012**, *33*, 1898-1920.
- [6.] Asadujjaman, A.; Kent, B.; Bertin, A., Phase transition and aggregation behaviour of an UCST-type copolymer poly(acrylamide-co-acrylonitrile) in water: effect of acrylonitrile content, concentration in solution, copolymer chain length and presence of electrolyte. *Soft Matter* **2017**, *13*, 658-669.
- [7.] Zhang, Q.; Tang, X.; Wang, T.; Yu, F.; Guo, W.; Pei, M., Thermo-sensitive zwitterionic block copolymers via ATRP. *RSC Adv.* **2014**, *4*, 24240-24247.
- [8.] Jenkins, A. D.; Jones, R. G.; Moad, G., Terminology for reversible-deactivation radical polymerization previously called "controlled" or "living" radical polymerization. *Pure Appl. Chem.* **2010**, *82*, 483-491.
- [9.] Shipp, D. A., Reversible-Deactivation Radical Polymerizations. *Polym. Rev.* **2011**, *51*, 99-103.
- [10.] Matyjaszewski, K.; Müller, A. H. E.; eds., *Controlled and Living Polymerizations. From Mechanisms to Applications*. Wiley-VCH: Weinheim (Germany), 2009.
- [11.] Chiefari, J.; Chong, Y. K.; Ercole, F.; Krstina, J.; Jeffery, J.; Le, P. T. T.; Mayadunne, R. T. A.; Meijs, G. F.; Moad, C. L.; Moad, G.; Rizzardo, E.; Thang, S. H., Living Free-Radical Polymerization by Reversible Addition-Fragmentation Chain Transfer: The RAFT Process. *Macromolecules* **1998**, *31*, 5559-5562.
- [12.] Moad, G.; Rizzardo, E.; Thang, S. H., Radical addition-fragmentation chemistry in polymer synthesis. *Polymer* **2008**, *49*, 1079-1131.
- [13.] Krzysztof, M.; Jianhui, X., Atom Transfer Radical Polymerization. *Chem. Rev.* **2001**, *101*, 2921-2990.
- [14.] Kamigaito, M.; Ando, T.; Sawamoto, M., Metal-Catalyzed Living Radical Polymerization. *Chem. Rev.* **2001**, *101*, 3689-3745.
- [15.] Matyjaszewski, K., Atom Transfer Radical Polymerization (ATRP): Current Status and Future Perspectives. *Macromolecules* **2012**, *45*, 4015-4039.
- [16.] Jakubowski, W.; Matyjaszewski, K., Activators Regenerated by Electron Transfer for Atom-Transfer Radical Polymerization of (Meth)acrylates and Related Block Copolymers. *Angew. Chem. Int. Ed.* **2006**, *45*, 4482-4486.

-
- [17.] Gupta, M. K.; Martin, J. R.; Werfel, T. A.; Shen, T.; Page, J. M.; Duvall, C. L., Cell Protective, ABC Triblock Polymer-Based Thermoresponsive Hydrogels with ROS-Triggered Degradation and Drug Release. *J. Am. Chem. Soc.* **2014**, *136*, 14896-14902.
- [18.] Li, W.; Huang, L.; Ying, X.; Jian, Y.; Hong, Y.; Hu, F.; Du, Y., Antitumor Drug Delivery Modulated by A Polymeric Micelle with an Upper Critical Solution Temperature. *Angew. Chem. Int. Ed.* **2015**, *54*, 3126-3131.
- [19.] Klouda, L.; Perkins, K. R.; Watson, B. M.; Hacker, M. C.; Bryant, S. J.; Raphael, R. M.; Kurtis Kasper, F.; Mikos, A. G., Thermoresponsive, in situ cross-linkable hydrogels based on N-isopropylacrylamide: Fabrication, characterization and mesenchymal stem cell encapsulation. *Acta Biomater.* **2011**, *7*, 1460-1467.
- [20.] Tan, H.; Ramirez, C. M.; Miljkovic, N.; Li, H.; Rubin, J. P.; Marra, K. G., Thermosensitive injectable hyaluronic acid hydrogel for adipose tissue engineering. *Biomaterials* **2009**, *30*, 6844-6853.
- [21.] Hoffman, A. S.; Chen, J. P., Polymer-protein conjugate II. Affinity precipitation separation of human immunoglobulin by a poly(N-isopropylacrylamide-) protein A conjugate. *Biomaterials* **1990**, *11*, 631-634.
- [22.] Kondo, A.; Kaneko, T.; Higashitani, K., Development and application of thermo-sensitive immunomicrospheres for antibody purification. *Biotechnol. Bioeng.* **1994**, *44*, 1-6.
- [23.] Zhu, H.; Li, Y.; Qiu, R.; Shi, L.; Wu, W.; Zhou, S., Responsive fluorescent Bi₂O₃@PVA hybrid nanogels for temperature-sensing, dual-modal imaging, and drug delivery. *Biomaterials* **2012**, *33*, 3058-3069.
- [24.] Taylor, M.; Tomlins, P.; Sahota, T., Thermoresponsive Gels. *Gels* **2017**, *3*, 4.
- [25.] Kotsuchibashi, Y.; Ebara, M.; Aoyagi, T.; Narain, R., Recent Advances in Dual Temperature Responsive Block Copolymers and Their Potential as Biomedical Applications. *Polymers* **2016**, *8*, [380] 1-25.
- [26.] Lau, A. C. W.; Wu, C., Thermally Sensitive and Biocompatible Poly(N-vinylcaprolactam): Synthesis and Characterization of High Molar Mass Linear Chains. *Macromolecules* **1999**, *32*, 581-584.
- [27.] Klouda, L.; Mikos, A. G., Thermoresponsive hydrogels in biomedical applications. *Eur. J. Pharm. Biopharm.* **2008**, *68*, 34-45.
- [28.] Arotçaréna, M.; Heise, B.; Ishaya, S.; Laschewsky, A., Switching the Inside and the Outside of Aggregates of Water-Soluble Block Copolymers with Double Thermoresponsivity. *J. Am. Chem. Soc.* **2002**, *124*, 3787-3793.
- [29.] Glatzel, S.; Laschewsky, A.; Lutz, J.-F., Well-Defined Uncharged Polymers with a Sharp UCST in Water and in Physiological Milieu. *Macromolecules* **2011**, *44*, 413-415.
- [30.] Fujihara, A.; Shimada, N.; Maruyama, A.; Ishihara, K.; Nakai, K.; Yusa, S.-i., Preparation of upper critical solution temperature (UCST) responsive diblock copolymers bearing pendant ureido groups and their micelle formation behavior in water. *Soft Matter* **2015**, *11*, 5204-5213.
- [31.] Halperin, A.; Kröger, M.; Winnik, F. M., Poly(N-isopropylacrylamide) Phase Diagrams: Fifty Years of Research. *Angew. Chem. Int. Ed.* **2015**, *54*, 15342-15367.
-

- [32.] de las Heras Alarcon, C.; Pennadam, S.; Alexander, C., Stimuli responsive polymers for biomedical applications. *Chem. Soc. Rev.* **2005**, *34*, 276-285.
- [33.] Bajpai, A. K.; Shukla, S. K.; Bhanu, S.; Kankane, S., Responsive polymers in controlled drug delivery. *Prog. Polym. Sci.* **2008**, *33*, 1088-1118.
- [34.] Roth, P. J.; Jochum, F. D.; Forst, F. R.; Zentel, R.; Theato, P., Influence of End Groups on the Stimulus-Responsive Behavior of Poly[oligo(ethylene glycol) methacrylate] in Water. *Macromolecules* **2010**, *43*, 4638-4645.
- [35.] Wischerhoff, E.; Uhlig, K.; Lanckenau, A.; Börner, H. G.; Laschewsky, A.; Duschl, C.; Lutz, J.-F., Controlled Cell Adhesion on PEG-based Switchable Surfaces. *Angew. Chem. Int. Ed.* **2008**, *47*, 5666-5668.
- [36.] Lutz, J.-F.; Hoth, A., Preparation of Ideal PEG Analogues with a Tunable Thermosensitivity by Controlled Radical Copolymerization of 2-(2-Methoxyethoxy)ethyl Methacrylate and Oligo(ethylene glycol) Methacrylate. *Macromolecules* **2006**, *39*, 893-896.
- [37.] Lutz, J.-F., Polymerization of Oligo(Ethylene Glycol) (Meth)Acrylates: Toward a New Generation of Smart Biocompatible Materials. *J. Polym. Sci., Part A: Polym. Chem.* **2008**, *46*, 3459-3470.
- [38.] Maeda, Y.; Yamauchi, H.; Fujisawa, M.; Sugihara, S.; Ikeda, I.; Aoshima, S., Infrared Spectroscopic Investigation of Poly(2-methoxyethyl vinyl ether) during Thermosensitive Phase Separation in Water. *Langmuir* **2007**, *23*, 6561-6566.
- [39.] Fujishige, S.; Kubota, K.; Ando, I., Phase Transition of Aqueous Solutions of Poly(N-isopropylacrylamide) and Poly(N-isopropylmethacrylamide). *J. Phys. Chem.* **1989**, *93*, 3311-3313.
- [40.] Han, S.; Hagiwara, M.; Ishizone, T., Synthesis of Thermally Sensitive Water-Soluble Polymethacrylates by Living Anionic Polymerizations of Oligo(ethylene glycol) Methyl Ether Methacrylates. *Macromolecules* **2003**, *36*, 8312-8319.
- [41.] Meeussen, F.; Nies, E.; Berghmans, H.; Verbrugghe, S.; Goethals, E.; Du Prez, F., Phase behaviour of poly(N-vinyl caprolactam) in water. *Polymer* **2000**, *41*, 8597-8602.
- [42.] Cortez-Lemus, N. A.; Licea-Claverie, A., Poly(N-vinylcaprolactam), a comprehensive review on a thermoresponsive polymer becoming popular. *Prog. Polym. Sci.* **2016**, *53*, 1-51.
- [43.] Schäfer-Soenen, H.; Moerkerke, R.; Berghmans, H.; Koningsveld, R.; Dušek, K.; Šolc, K., Zero and Off-Zero Critical Concentrations in Systems Containing Polydisperse Polymers with Very High Molar Masses. 2. The System Water–Poly(vinyl methyl ether). *Macromolecules* **1997**, *30*, 410-416.
- [44.] Meeussen, F.; Bauwens, Y.; Moerkerke, R.; Nies, E.; Berghmans, H., Molecular complex formation in the system poly(vinyl methyl ether)/water. *Polymer* **2000**, *41*, 3737-3743.
- [45.] Liu, F.; Seuring, J.; Agarwal, S., Controlled radical polymerization of N-acryloylglycinamide and UCST-type phase transition of the polymers. *J. Polym. Sci., Part A: Polym. Chem.* **2012**, *50*, 4920-4928.
- [46.] Chua, G. B. H.; Roth, P. J.; Duong, H. T. T.; Davis, T. P.; Lowe, A. B., Synthesis and Thermoresponsive Solution Properties of Poly[oligo(ethylene glycol)]

- (meth)acrylamide]s: Biocompatible PEG Analogues. *Macromolecules* **2012**, *45*, 1362-1374.
- [47.] Seuring, J.; Bayer, F. M.; Huber, K.; Agarwal, S., Upper Critical Solution Temperature of Poly(N-acryloyl glycinamide) in Water: A Concealed Property. *Macromolecules* **2012**, *45*, 374-384.
- [48.] Nagaoka, H.; Ohnishi, N.; Eguchi, M., Thermoresponsive polymer and production method thereof. US20070203313 A1: 2007; Vol. US20070203313 A1.
- [49.] Shimada, N.; Ino, H.; Maie, K.; Nakayama, M.; Kano, A.; Maruyama, A., Ureido-Derivatized Polymers Based on Both Poly(allylurea) and Poly(l-citrulline) Exhibit UCST-Type Phase Transition Behavior under Physiologically Relevant Conditions. *Biomacromolecules* **2011**, *12*, 3418-3422.
- [50.] Shimada, N.; Nakayama, M.; Kano, A.; Maruyama, A., Design of UCST Polymers for Chilling Capture of Proteins. *Biomacromolecules* **2013**, *14*, 1452-1457.
- [51.] Seuring, J.; Agarwal, S., First Example of a Universal and Cost-Effective Approach: Polymers with Tunable Upper Critical Solution Temperature in Water and Electrolyte Solution. *Macromolecules* **2012**, *45*, 3910-3918.
- [52.] Käfer, F.; Liu, F.; Stahlschmidt, U.; Jérôme, V.; Freitag, R.; Karg, M.; Agarwal, S., LCST and UCST in One: Double Thermoresponsive Behavior of Block Copolymers of Poly(ethylene glycol) and Poly(acrylamide-co-acrylonitrile). *Langmuir* **2015**, *31*, 8940-8946.
- [53.] Longenecker, R.; Mu, T.; Hanna, M.; Burke, N. A. D.; Stöver, H. D. H., Thermally Responsive 2-Hydroxyethyl Methacrylate Polymers: Soluble–Insoluble and Soluble–Insoluble–Soluble Transitions. *Macromolecules* **2011**, *44*, 8962-8971.
- [54.] Zhu, Y.; Noy, J.-M.; Lowe, A. B.; Roth, P. J., The synthesis and aqueous solution properties of sulfobutylbetaine (co)polymers: comparison of synthetic routes and tuneable upper critical solution temperatures. *Polym. Chem.* **2015**, *6*, 5705-5718.
- [55.] Hildebrand, V.; Laschewsky, A.; Wischerhoff, E., Modulating the solubility of zwitterionic poly((3-methacrylamidopropyl)ammonioalkane sulfonate)s in water and aqueous salt solutions via the spacer group separating the cationic and the anionic moieties. *Polym. Chem.* **2016**, *7*, 731-740.
- [56.] Hildebrand, V.; Laschewsky, A.; Päch, M.; Müller-Buschbaum, P.; Papadakis, C. M., Effect of the Zwitterion Structure on the Thermo-responsive Behaviour of Poly(Sulfobetaine Methacrylate)s. *Polym. Chem.* **2017**, *8*, 310-322.
- [57.] Hildebrand, V.; Laschewsky, A.; Zehm, D., On the hydrophilicity of polyzwitterion poly (N,N-dimethyl-N-(3-(methacrylamido)propyl)ammonio propane sulfonate) in water, deuterated water, and aqueous salt solutions. *J. Biomater. Sci., Polym. Ed.* **2014**, *25*, 1602-1618.
- [58.] Galin, J.-C., Polyzwitterions. In *Polymer Materials Encyclopedia*, Salamone, J. C., Ed. CRC Press: Boca Raton (Florida), 1996; Vol. 9, pp 7189-7201.
- [59.] Lowe, A. B.; McCormick, C. L., Synthesis and solution properties of zwitterionic polymers. *Chem. Rev.* **2002**, *102*, 4177-4189.
- [60.] Kudaibergenov, S.; Jaeger, W.; Laschewsky, A., Polymeric betaines: synthesis, characterization and application. *Adv. Polym. Sci.* **2006**, *201*, 157-224.

- [61.] Laschewsky, A., Structures And Synthesis Of Zwitterionic Polymers. *Polymers* **2014**, *6*, 1544-1601.
- [62.] Xiang, T.; Lu, T.; Xie, Y.; Zhao, W.-F.; Sun, S.-D.; Zhao, C.-S., Zwitterionic polymer functionalization of polysulfone membrane with improved antifouling property and blood compatibility by combination of ATRP and click chemistry. *Acta Biomater.* **2016**, *40*, 162-171.
- [63.] Zhao, Y.; Bai, T.; Shao, Q.; Jiang, S.; Shen, A. Q., Thermoresponsive self-assembled NiPAm-zwitterion copolymers. *Polym. Chem.* **2015**, *6*, 1066-1077.
- [64.] Nakai, S.; Nakaya, T.; Imoto, M., Polymeric phospholipid analog, 10. Synthesis and polymerization of 2-(methacryloyloxy)ethyl 2-aminoethyl hydrogen phosphate. *Makromol. Chem.* **1977**, *178*, 2963-2967.
- [65.] Ladenheim, H.; Morawetz, H., A new type of polyampholyte: Poly(4-vinyl pyridine betaine). *J. Polym. Sci.* **1957**, *26*, 251-254.
- [66.] Hart, R.; Timmermann, M., New Polyampholytes: The Polysulfobetaines. *J. Polym. Sci., Part A: Polym. Chem.* **1958**, *28*, 638-640.
- [67.] Jin, Q.; Chen, Y.; Wang, Y.; Ji, J., Zwitterionic drug nanocarriers: A biomimetic strategy for drug delivery. *Coll. Surf. B* **2014**, *124*, 80-86.
- [68.] Huang, K.-T.; Fang, Y.-L.; Hsieh, P.-S.; Li, C.-C.; Dai, N.-T.; Huang, C.-J., Zwitterionic nanocomposite hydrogels as effective wound dressings. *J. Mater. Chem. B* **2016**, *4*, 4206-4215.
- [69.] Doncom, K. E. B.; Willcock, H.; O'Reilly, R. K., The direct synthesis of sulfobetaine-containing amphiphilic block copolymers and their self-assembly behavior. *Eur. Polym. J.* **2017**, *87*, 497-507.
- [70.] Jiang, S.; Cao, Z., Ultralow-Fouling, Functionalizable, and Hydrolyzable Zwitterionic Materials and Their Derivatives for Biological Applications. *Adv. Mater.* **2010**, *22*, 920-932.
- [71.] Schlenoff, J. B., Zwitteration: Coating Surfaces with Zwitterionic Functionality to Reduce Nonspecific Adsorption. *Langmuir* **2014**, *30*, 9625-9636.
- [72.] Köberle, P.; Laschewsky, A.; Lomax, T. D., Interactions of a zwitterionic polysoap and its cationic analog with inorganic salts. *Makromol. Chem., Rapid Commun.* **1991**, *12*, 427- 433.
- [73.] Woodfield, P. A.; Zhu, Y.; Pei, Y.; Roth, P. J., Hydrophobically Modified Sulfobetaine Copolymers with Tunable Aqueous UCST through Postpolymerization Modification of Poly(pentafluorophenyl acrylate). *Macromolecules* **2014**, *47*, 750-762.
- [74.] Vasantha, V. A.; Jana, S.; Parthiban, A.; Vancso, J. G., Halophilic polysulfobetaines - synthesis and study of gelation and thermoresponsive behavior. *RSC Advances* **2014**, *4*, 22596-22600.
- [75.] Vasantha, V. A.; Jana, S.; Lee, S. S.-C.; Lim, C.-S.; Teo, S. L.-M.; Parthiban, A.; Vancso, J. G., Dual hydrophilic and salt responsive schizophrenic block copolymers - synthesis and study of self-assembly behavior. *Polym. Chem.* **2015**, *6*, 599-606.
- [76.] Arjunan Vasantha, V.; Junhui, C.; Ying, T. B.; Parthiban, A., Salt-Responsive Polysulfobetaines from Acrylate and Acrylamide Precursors: Robust Stabilization of Metal Nanoparticles in Hyposalinity and Hypersalinity. *Langmuir* **2015**, *31*, 11124-11134.

- [77.] Vasantha, V. A.; Zainul Rahim, S. Z.; Jayaraman, S.; Junyuan, G. H.; Puniredd, S. R.; Ramakrishna, S.; Teo, S. L.-M.; Parthiban, A., Antibacterial, electrospun nanofibers of novel poly(sulfobetaine) and poly(sulfobetaine)s. *J. Mater. Chem. B* **2016**, *4*, 2731-2738.
- [78.] Shao, Q.; Jiang, S., Influence of Charged Groups on the Properties of Zwitterionic Moieties: A Molecular Simulation Study. *J. Phys. Chem. B* **2014**, *118*, 7630-7637.
- [79.] Terayama, Y.; Kikuchi, M.; Kobayashi, M.; Takahara, A., Well-Defined Poly(sulfobetaine) Brushes Prepared by Surface-Initiated ATRP Using a Fluoroalcohol and Ionic Liquids as the Solvents. *Macromolecules* **2011**, *44*, 104-111.
- [80.] Shih, Y.-J.; Chang, Y.; Deratani, A.; Quemener, D., "Schizophrenic" Hemocompatible Copolymers via Switchable Thermoresponsive Transition of Nonionic/Zwitterionic Block Self-Assembly in Human Blood. *Biomacromolecules* **2012**, *13*, 2849-2858.
- [81.] Wang, Y.; Li, L.; Li, J.; Yang, B.; Wang, C.; Fang, W.; Ji, F.; Wen, Y.; Yao, F., Stable and pH-responsive polyamidoamine based unimolecular micelles capped with a zwitterionic polymer shell for anticancer drug delivery. *RSC Adv.* **2016**, *6*, 17728-17739.
- [82.] Qiu, J.; Matyjaszewski, K., Metal complexes in controlled radical polymerization. *Acta Polym.* **1997**, *48*, 169-180.
- [83.] Coessens, V.; Pintauer, T.; Matyjaszewski, K., Functional polymers by atom transfer radical polymerization. *Prog. Polym. Sci.* **2001**, *26*, 337-377.
- [84.] Matyjaszewski, K.; Tsarevsky, N. V., Macromolecular Engineering by Atom Transfer Radical Polymerization. *J. Am. Chem. Soc.* **2014**, *136*, 6513-6533.
- [85.] Siegwart, D. J.; Oh, J. K.; Matyjaszewski, K., ATRP in the design of functional materials for biomedical applications. *Prog. Polym. Sci.* **2012**, *37*, 18-37.
- [86.] Ranger, M.; Jones, M.-C.; Yessine, M.-A.; Leroux, J.-C., From well-defined diblock copolymers prepared by a versatile atom transfer radical polymerization method to supramolecular assemblies. *J. Polym. Sci., Part A: Polym. Chem.* **2001**, *39*, 3861-3874.
- [87.] Li, Y.; Armes, S. P.; Jin, X.; Zhu, S., Direct Synthesis of Well-Defined Quaternized Homopolymers and Diblock Copolymers via ATRP in Protic Media. *Macromolecules* **2003**, *36*, 8268-8275.
- [88.] Kobayashi, M.; Terada, M.; Terayama, Y.; Kikuchi, M.; Takahara, A., Direct Synthesis of Well-Defined Poly[2-(methacryloyloxy)ethyl]trimethylammonium chloride] Brush via Surface-Initiated Atom Transfer Radical Polymerization in Fluoroalcohol. *Macromolecules* **2010**, *43*, 8409-8415.
- [89.] He, W.; Jiang, H.; Zhang, L.; Cheng, Z.; Zhu, X., Atom transfer radical polymerization of hydrophilic monomers and its applications. *Polym. Chem.* **2013**, *4*, 2919-2938.
- [90.] Kobayashi, M.; Terada, M.; Terayama, Y.; Kikuchi, M.; Takahara, A., Direct Controlled Polymerization of Ionic Monomers by Surface-Initiated ATRP Using a Fluoroalcohol and Ionic Liquids. *Isr. J. Chem.* **2012**, *52*, 364-374.
- [91.] Liu, P.; Domingue, E.; Ayers, D. C.; Song, J., Modification of Ti₆Al₄V substrates with well-defined zwitterionic polysulfobetaine brushes for improved surface mineralization. *ACS Appl. Mater. Interfaces* **2014**, *6*, 7141-52.

- [92.] Morimoto, N.; Muramatsu, K.; Wazawa, T.; Inoue, Y.; Suzuki, M., Self-Assembled Microspheres Driven by Dipole-Dipole Interactions: UCST-Type Transition in Water. *Macromol. Rapid Commun.* **2014**, *35*, 103-108.
- [93.] Palanisamy, A.; Albright, V.; Sukhishvili, S. A., Upper Critical Solution Temperature Layer-by-Layer Films of Polyamino acid-Based Micelles with Rapid, On-Demand Release Capability. *Chem. Mater.* **2017**, *29*, 9084-9094.
- [94.] Doncom, K. E. B.; Blackman, L. D.; Wright, D. B.; Gibson, M. I.; O'Reilly, R. K., Dispersity effects in polymer self-assemblies: a matter of hierarchical control. *Chem. Soc. Rev.* **2017**, *46*, 4119-4134.
- [95.] Wolf, T.; Rheinberger, T.; Simon, J.; Wurm, F. R., Reversible Self-Assembly of Degradable Polymersomes with Upper Critical Solution Temperature in Water. *J. Am. Chem. Soc.* **2017**, *139*, 11064-11072.
- [96.] Zhang, Y.; Chu, D.; Zheng, M.; Kissel, T.; Agarwal, S., Biocompatible and degradable poly(2-hydroxyethyl methacrylate) based polymers for biomedical applications. *Polym. Chem.* **2012**, *3*, 2752-2759.
- [97.] West, S. L.; Salvage, J. P.; Lobb, E. J.; Armes, S. P.; Billingham, N. C.; Lewis, A. L.; Hanlon, G. W.; Lloyd, A. W., The biocompatibility of crosslinkable copolymer coatings containing sulfobetaines and phosphobetaines. *Biomaterials* **2004**, *25*, 1195-1204.
- [98.] Zheng, L.; Sundaram, H. S.; Wei, Z.; Li, C.; Yuan, Z., Applications of zwitterionic polymers. *React. Funct. Polym.* **2017**, *118*, 51-61.
- [99.] Duncan, R., The dawning era of polymer therapeutics. *Nat Rev Drug Discov* **2003**, *2*, 347-360.
- [100.] Knop, K.; Hoogenboom, R.; Fischer, D.; Schubert, U. S., Poly(ethylene glycol) in Drug Delivery: Pros and Cons as Well as Potential Alternatives. *Angew. Chem. Int. Ed.* **2010**, *49*, 6288-6308.
- [101.] Kolb, H. C.; Finn, M. G.; Sharpless, K. B., Click Chemistry: Diverse Chemical Function from a Few Good Reactions. *Angew. Chem. Int. Ed.* **2001**, *40*, 2004-2021.
- [102.] Connell, L. S.; Jones, J. R.; Weaver, J. V. M., Transesterification of functional methacrylate monomers during alcoholic copper-catalyzed atom transfer radical polymerization: formation of compositional and architectural side products. *Polym. Chem.* **2012**, *3*, 2735-2738.
- [103.] Xu, F.-J.; Li, H.; Li, J.; Zhang, Z.; Kang, E.-T.; Neoh, K.-G., Pentablock copolymers of poly(ethylene glycol), poly((2-dimethyl amino)ethyl methacrylate) and poly(2-hydroxyethyl methacrylate) from consecutive atom transfer radical polymerizations for non-viral gene delivery. *Biomaterials* **2008**, *29*, 3023-3033.
- [104.] Isobe, Y.; Yamada, K.; Nakano, T.; Okamoto, Y., Stereospecific Free-Radical Polymerization of Methacrylates Using Fluoroalcohols as Solvents. *Macromolecules* **1999**, *32*, 5979-5981.
- [105.] Willcock, H.; Lu, A.; Hansell, C. F.; Chapman, E.; Collins, I. R.; O'Reilly, R. K., One-pot synthesis of responsive sulfobetaine nanoparticles by RAFT polymerisation: the effect of branching on the UCST cloud point. *Polym. Chem.* **2014**, *5*, 1023-1030.

- [106.] Strehmel, V.; Wetzel, H.; Laschewsky, A., Homopolymerization of a Highly Polar Zwitterionic Methacrylate in Ionic Liquids and Its Copolymerization with a Non-polar Methacrylate. *e-Polymers* **2006**, *6*, 131-140.
- [107.] Gao, J.; Zhai, G.; Song, Y.; Jiang, B., Multidimensionally stimuli-responsive phase transition of aqueous solutions of poly((N,N-dimethylamino)ethyl methacrylate) and poly((N,N-dimethyl-N-(methacryloyl)ethyl ammonium butane sulfonate). *J. Appl. Polym. Sci.* **2008**, *107*, 3548-3556.
- [108.] Weber, C.; Hoogenboom, R.; Schubert, U. S., Temperature responsive bio-compatible polymers based on poly(ethylene oxide) and poly(2-oxazoline)s. *Prog. Polym. Sci.* **2012**, *37*, 686-714.
- [109.] Dormidontova, E. E., Influence of End Groups on Phase Behavior and Properties of PEO in Aqueous Solutions. *Macromolecules* **2004**, *37*, 7747-7761.
- [110.] Vishnevetskaya, N. S.; Hildebrand, V.; Niebuur, B.-J.; Grillo, I.; Filippov, S. K.; Laschewsky, A.; Müller-Buschbaum, P.; Papadakis, C. M., "Schizophrenic" Micelles from Doubly Thermoresponsive Polysulfobetaine-b-poly(N-isopropylmethacrylamide) Diblock Copolymers. *Macromolecules* **2017**, *50*, 3985-3999.
- [111.] Bütün, V.; Armes, S. P.; Billingham, N. C., Unusual aggregation behavior of a novel tertiary amine methacrylate-based diblock copolymer: Formation of micelles and reverse micelles in aqueous solution *J. Am. Chem. Soc.* **1998**, *120*, 11818-11819.
- [112.] Bütün, V.; Liu, S.; Weaver, J. V. M.; Bories-Azeau, X.; Cai, Y.; Armes, S. P., A brief review of 'schizophrenic' block copolymers. *React. Funct. Polym.* **2006**, *66*, 157-165.
- [113.] Nilsson, P. G.; Lindman, B.; Laughlin, R. G., The upper consolute boundary in zwitterionic surfactant-water systems. *J. Phys. Chem.* **1984**, *88*, 6357-6362.
- [114.] Laughlin, R. G., Fundamentals of the zwitterionic hydrophilic group. *Langmuir* **1991**, *7*, 842-847.
- [115.] Anton, P.; Laschewsky, A., Solubilization by Polysoaps. *Colloid Polym. Sci.* **1994**, *272*, 1118-1128.
- [116.] Hildebrand, V.; Heydenreich, M.; Laschewsky, A.; Möller, H. M.; Müller-Buschbaum, P.; Papadakis, C. M.; Schanzenbach, D.; Wischerhoff, E., "Schizophrenic" self-assembly of dual thermoresponsive block copolymers bearing a zwitterionic and a non-ionic hydrophilic block. *Polymer* **2017**, *122*, 347-357.
- [117.] Corradini, R.; Dossena, A.; Galaverna, G.; Marchelli, R.; Panagia, A.; Sartor, G., Fluorescent Chemosensor for Organic Guests and Copper(II) Ion Based on Dansyldiethylenetriamine-Modified β -Cyclodextrin. *J. Org. Chem.* **1997**, *62*, 6283-6289.
- [118.] Zhang, L.; Jin, Q.; Lv, K.; Qin, L.; Liu, M., Enantioselective recognition of a fluorescence-labeled phenylalanine by self-assembled chiral nanostructures. *ChemCommun.* **2015**, *51*, 4234-4236.
- [119.] Papoutsis, D.; Bekiari, V.; Stathatos, E.; Lianos, P.; Laschewsky, A., Molecular Diffusion and Fluorescence Energy-Transfer Studies in Thin Surfactant Films. *Langmuir* **1995**, *11*, 4355-4360.
- [120.] Laschewsky, A.; Paulus, W.; Ringsdorf, H.; Schuster, A.; Frick, G.; Mathy, A., Mixed polymeric monolayers and Langmuir-Blodgett multilayers with functional low molecular weight guest compounds. *Thin Solid Films* **1992**, *210-211*, 191-194.

- [121.] Stathatos, E.; Lianos, P.; Laschewsky, A.; Ouari, O.; Van Cleuvenbergen, P., Synthesis of a Hemicyanine Dye Bearing Two Carboxylic Groups and Its Use as a Photosensitizer in Dye-Sensitized Photoelectrochemical Cells. *Chemistry of Materials* **2001**, *13* (11), 3888-3892.
- [122.] Stathatos, E.; Lianos, P.; Laschewsky, A., Photophysical Properties of an Amphiphilic Cationic Hemicyanine Dye in Solution and Adsorbed on a TiO₂ Mesoporous Film. *Langmuir* **1997**, *13*, 259-263.
- [123.] Bonte, N.; Laschewsky, A.; Vermeylen, V., Hybrid materials made from polymeric betaines and low molar mass salts. *Macromol. Symp.* **1997**, *117*, 195-206.
- [124.] Hof, M.; Lianos, P.; Laschewsky, A., An Amphiphilic Hemicyanine Dye Employed as a Sensitive Probe of Water in Reverse AOT Micelles. *Langmuir* **1997**, *13*, 2181-2183.
- [125.] Lunkenheimer, K.; Laschewsky, A.; Warszynski, P.; Hirte, R., On the Adsorption Behavior of Soluble, Surface-Chemically Pure Hemicyanine Dyes at the Air/Water Interface. *J. Colloid Interface Sci.* **2002**, *248*, 260-267.
- [126.] Brooker, L. G. S.; Keyes, G. H.; Heseltine, D. W., Color and Constitution. XI.1 Anhydronium Bases of p-Hydroxystyryl Dyes as Solvent Polarity Indicators. *J. Am. Chem. Soc.* **1951**, *73*, 5350-5356.